ISSN: 2153-1196 Volume 14, Number 4, March 2023

Scientific Research Publishing

Journal of Modern Physics

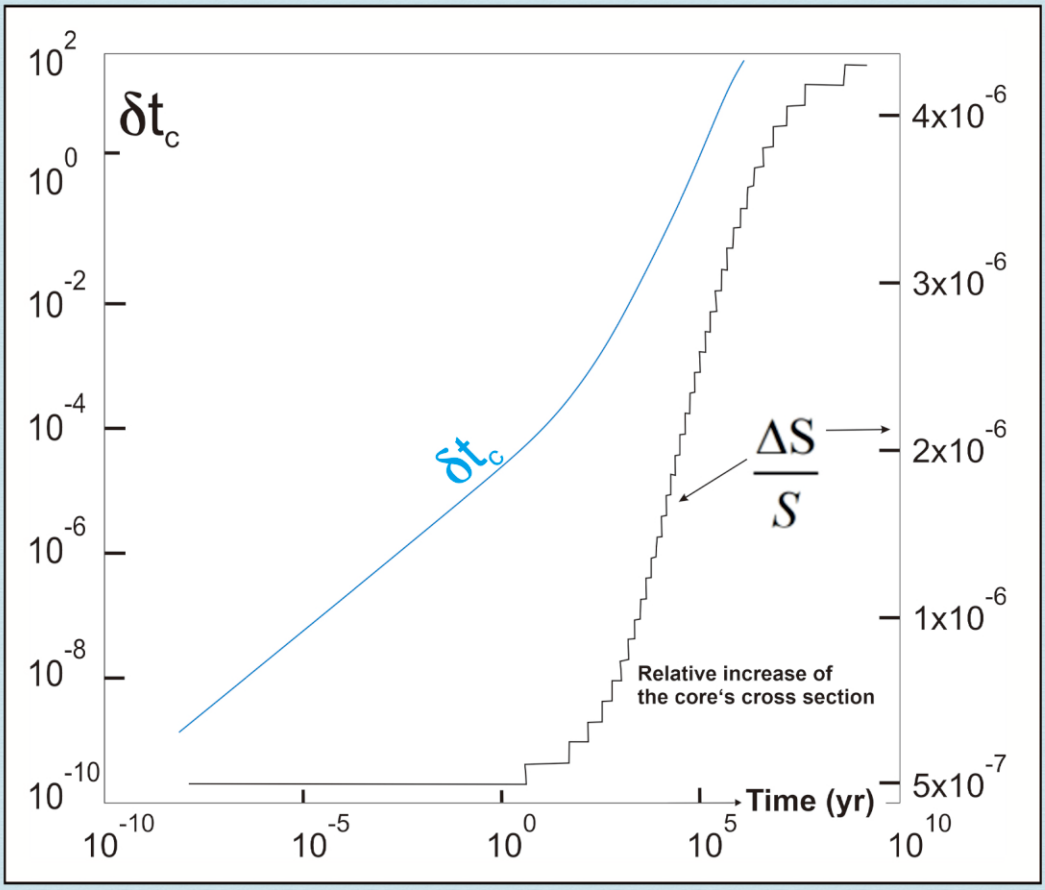

ISSN: 2153-1196

https://www.scirp.org/journal/jmp

Journal Editorial Board

ISSN: 2153-1196 (Print) ISSN: 2153-120X (Online)
https://www.scirp.org/journal/jmp

Editorial Board

Scientific Research Publishing

Journal of Modern Physics, 2023, 14, 415-551
https://www.scirp.org/journal/jmp
ISSN Online: 2153-120X
ISSN Print: 2153-1196

Table of Contents

Volume 14 Number 4 March 2023

The figure on the front cover is from the article published in Journal of Modern Physics, 2023, Vol. 14, No. 4, pp. 415-431 by Ahmad A. Hujeirat.

Journal of Modern Physics (JMP)
Journal Information

SUBSCRIPTIONS

The *Journal of Modern Physics* (Online at Scientific Research Publishing, https://www.scirp.org/) is published monthly by Scientific Research Publishing, Inc., USA.

Subscription rates:
Print: $89 per issue.
To subscribe, please contact Journals Subscriptions Department, E-mail: sub@scirp.org

SERVICES

Advertisements
Advertisement Sales Department, E-mail: service@scirp.org

Reprints (minimum quantity 100 copies)
Reprints Co-ordinator, Scientific Research Publishing, Inc., USA.
E-mail: sub@scirp.org

COPYRIGHT

PRODUCTION INFORMATION

For manuscripts that have been accepted for publication, please contact:
E-mail: jmp@scirp.org

Journal of Modern Physics, 2023, 14, 415-431
https://www.scirp.org/journal/jmp
ISSN Online: 2153-120X
ISSN Print: 2153-1196

Foundation of the Unicentric Model of the Observable Universe—UNIMOUN

Ahmad A. Hujeirat

IWR, University of Heidelberg, Heidelberg, Germany
Email: AHujeirat@uni-heidelberg.de

How to cite this paper: Hujeirat, A.A. (2023) Foundation of the Unicentric Model of the Observable Universe—UNIMOUN. *Journal of Modern Physics*, **14**, 415-431.
https://doi.org/10.4236/jmp.2023.144023

Received: February 6, 2023
Accepted: March 12, 2023
Published: March 15, 2023

Abstract

In view of the growing difficulties of ΛCDM-cosmologies to compete with recent highly accurate cosmological observations, I propose the alternative model: the Unicentric Model of the Observable UNiverse (UNIMOUN). The model relies on employing a new time-dependent $\mathcal{H}$-metric for the GR field equations, which enables reversible phase transitions between normal compressible fluids and incompressible quantum superfluids, necessary for studying the cosmic evolution of the observable universe. The main properties of UNIMOUN read: 1) The observable universe was born in a flat spacetime environment, which is a tiny fraction of our infinitely large and flat parent universe, 2) Our big bang (BB) happened to occur in our neighbourhood, thereby endowing the universe the observed homogeneity and isotropy, 3) The energy density in the universe is upper-bounded by the universal critical density ρ_{cr}^{uni}, beyond which matter becomes purely incompressible, rendering formation of physical singulareties, and in particular black holes, impossible, 4) Big bangs are neither singular events nor invoked by external forces, but rather, they are common self-sustaining events in our parent universe, 5) The progenitors of BBs are created through the merger of cosmically dead and inactive neutron stars and/or through "supermassive black holes" that are currently observed at the centres of most massive galaxies, 6) The progenitors are made up of purely incompressible entropy-free superconducting gluon-quark superfluids with $\rho = \rho_{cr}^{uni}$ (SuSu-matter), which endows these giant objects measurable sizes, 7) Spacetimes embedding SuSu-matter are conformally flat. It is shown that UNIMOUN is capable of dealing with or providing answers to several fundamental open questions in astrophysics and cosmology without invoking inflation, dark matter or dark energy.

Keywords

General Relativity: Big Bang, Black Holes, QSOs, Neutron Stars, QCD, Condensed Matter, Incompressibility, Superfluidity, Super-Conductivity

1. Introduction

For thousands of years, the geocentric model was accepted as the unrivalled model which visibly describes the cosmos: celestial bodies and objects, including the moon, planets, the Sun, stars and etc., move across the sky, whereas the Earth residing in the centre of the cosmos. Theoretically, the model was first discussed by the famous Greek philosophers Plato and Aristotle and completed about 450 years later by the Greek astronomer Ptolemy [1] [2]. Accordingly, the Earth is a perfect sphere, stationary and located at the centre of the cosmos, whilst all other celestial objects orbit it. The first orbit was devoted to the moon and followed respectively by Mercury, Venus, the Sun, Mars, Jupiter and Saturn.

The model continued to be valid until Nicolaus Copernicus in 1543 published his new radical heliocentric model of the universe. Here the Sun, rather than the Earth, lies in the centre of the universe, whilst all other celestial objects, including the Earth, moon and planets, are orbiting the Sun. Moreover, together with Galileo Galilei, it was argued that the Earth even rotates around its axis once a day. Hence the centuries-long divine role of the Earth in the cosmos was suddenly cancelled and doomed the Earth to a normal celestial object [3] [4].

Several years later, Thomas Digges proposed replacing the heliocentric model with an alternative one, in which the universe is completely flat, static and infinite in space and time. The model was ignored due to missing support from astronomers.

Despite the modification of Johannes Kepler and Isaac Newton, the heliocentric model did not survive the early years of the nineteenth century, when observations revealed that the solar system, together with the embedding milky way galaxy, are just tiny fractions of a much larger universe. Based thereon, an alternative model was suggested by Einstein in 1917, in which the universe is spatially finite but temporally infinite [5]. Here Einstein included the cosmological constant in his field equations to relax the expansion of the spacetime at the background. However, several years later, Edwin Hubble discovered that the universe is expanding rather than static. When combining this finding with the observed homogeneity and isotropy of the universe, it was concluded that the milky way, as well as other galaxies, are uniformly distributed on the surface of an inflating ballon-like structure that lacks a central symmetric point, hence why the FLRW-metric was considered to be the correct metric for describing the expanding universe (see [6] [7] and the references therein). The current ΛCDM-cosmologies use this metric to study the universe's accelerating expansion. However, this simple model was found to still be inconsistent with various observed properties of the universe, and therefore new exotic components were invoked to solely match observations, though their physical origins continued to be a mystery [8] [9].

ΛCDM-cosmology is currently widely accepted as the standard model of cosmology, in which inflation, dark matter (DM) and dark energy are its main building blocks. DM was invoked to enable the formation of galaxies, large-scale

structures and reasonable distributions of galaxies in the observable universe, whereas dark energy, generally identified as the cosmological constant Λ in the field equations, is the driver for accelerating the expansion of the universe [10] [11]. The role of inflation is to enable an abrupt expansion of the universe, through which observations of the early universe, the absence of magnetic monopoles, homogeneity and geometrical flatness of our observable universe may nicely be explained [12] [13] [14].

On the other hand, despite advanced BH theoretical research and the recent tremendous efforts by the EHT observations, which placed the existence of BHs beyond doubt, it is, however still unclear why the universe chose to adopt exponential inflation in the early universe rather than collapsing into a supermassive black hole [15] [16] [17] which is the preferable evolutionary track, when taking into account the short length and time-scales characterizing the system. Moreover, the ΛDCM-cosmologies failed to resolve other fundamental problems in astrophysics and cosmology, e.g. the coincidence and fine-tuning problems, the voids crisis, the nature of dark matter and dark energy and how to resolve the current persistent Hubble tension [8] [18].

The related fundamental question to be answered is: Do the laws of nature permit the existence of a maximum energy density in the universe? If they do, BHs become superfluous and their existence should be ruled out.

Worth noting here is that the BH-paradigm was rejected at least two times by Einstein: in 1915 and 1939 when he mentioned that "Schwarzschild singularities do not exist in physical reality."

Indeed, UNIMOUN is a self-consistent model of the universe and a promising alternative to ΛDCM-cosmologies; no exotic components are needed, and in most cases, it complies nicely with observations whilst suggesting simple and reasonable answers to still open questions is astrophysics and cosmology.

In the present paper, we present an alternative model to the evolution of the observable universe, abbreviated UNIMOUN. In the following sections, we discuss the physical basis of the model and its mathematical foundation and briefly propose answers to selected open questions in astrophysics and cosmology. Finally, I end up with Section 5, where I summarise the model's main aspects and highlight the relevant consequences.

2. Pulsars: The Fabric of Incompressible Gluon-Quark Superfluids

The state of matter inside massive neutron stars (NSs) cannot be probed under terrestrial conditions, though multi-messenger observations may be used to limit the range of possibilities. In particular, the observed glitch phenomena in pulsars, together with the recently discovered under and over-shootings found to associate the glitch events in the Vela pulsar, confirm the predicated exchange of mass and angular momentum in the geometrically thin boundary layer between the rigid-body rotating quantum core and the differentially rotating dissipative matter in the overlying shells [19] [20] [21] [22]. Recalling that the density of

degenerate matter inside the cores of massive pulsars is larger than the nuclear density ρ_0, then the cooling down of pulsars on cosmic times should transfer their contents into entropy-free superfluids. Further confirmation comes from the recently detected merger of the NS-binary in GW170817, in which the remnant is apparently not a BH but rather a NS with a hypermassive superfluid core [23]. Similar to massive stars, the luminous lifetimes of NSs correlate inversely with their masses, which, among others, may explain the missing first generation of NSs formed from the collapse of population III stars (see [24], and the references therein).

In the following, I address additional properties of NSs that are relevant to UNIMOUN:

• Had NSs radiated away their entire secondary energies[1], then their contents would settle down to the truly lowest possible quantum energy state. It is hypothesized here that this supranuclear dense matter with zero-entropy would consist of paired gluon-quarks that collectively behave as a single quantum entity. In the absence of secondary energies, internal communications between the constituents are mediated with the speed of light, which make the matter well-equipped to resist all types of external perturbations, including self-collapse.

• The glitches of the well-observed Crab and Vela pulsars are abrupt events through which considerable amounts of rotational anergies are ejected from their cores into the ambient media, where they viscously diffuse through the whole shell, thereby triggering their observed spin-up (**Figure 1**). Indeed, it was shown that pulsar cores evolve in accord with the Onsager-Feynman equation [19]:

$$\frac{\mathrm{d}(S\Omega)}{\mathrm{d}t} = \frac{h}{2m}\frac{\mathrm{d}N}{\mathrm{d}t}, \tag{1}$$

where S, Ω, N are the cross-section, angular frequency, and the number of vortices inside the core, respectively.

During the glitch event, the cross-section of the core, S, must increase, and due to incompressibility, its mass and dimension increase linearly as well. Consequently, in the limit of $t \to \infty$, the angular frequency $\Omega \to 0$, and therefore $S \to S_\infty$, which is equal to the total cross-section of the object. This implies that the dead NS is effectively metamorphosed into an invisible object that consists solely of its rest mass, as shown in **Figure 1**. These objects are termed dark energy objects (DEO).

• Observations indicate that newly born pulsars undergo glitching more frequently than older ones [25] [26]. The Crab and Vela follow these tendencies. This indicates that pulsars are born with embryonic SuSu-cores, but their effects become measurable once their relative inertias became dynamically significant (see Figure 4 in [22]).

• The spacetime embedding incompressible entropy-free SuSu-matter should be flat.

[1]e.g. $E_{thermal} = E_{kinetic} = E_{magnetic} = \cdots = 0$.

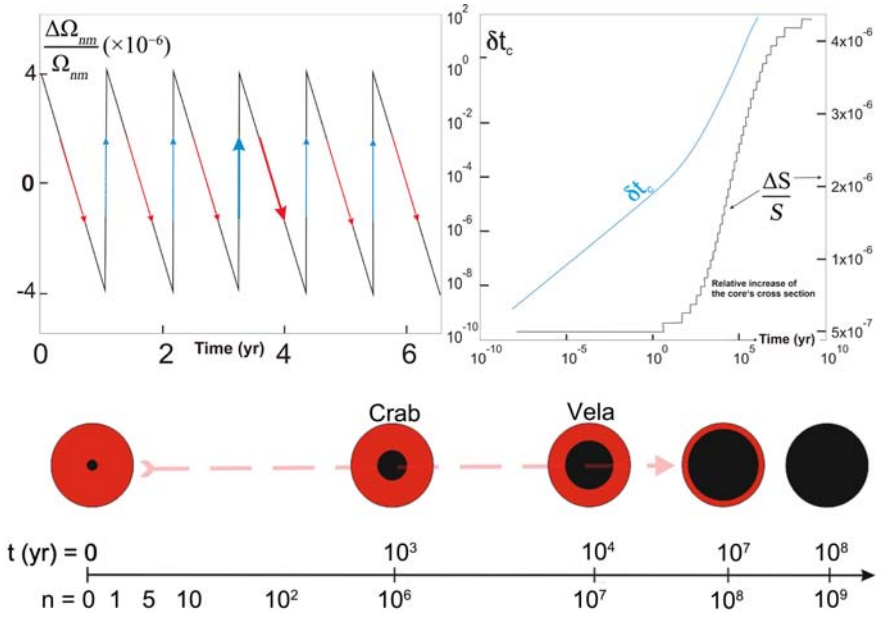

Figure 1. The time-evolution of the relative change of the angular frequency, $\Delta\Omega_{nm}/\Omega_{nm}$ of normal matter inside the boundary layer between the rigid-body rotating SuSu-core and the normal matter in the ambient shell is shown during two successive glitch events (top-left). In the top-right panel the duration between two successive glitch events, δt_c, and the corresponding increase of the relative cross-section of the DEO-core, $\Delta S/S$, versus cosmic time are shown. In the lower panel, the cosmic evolution (yr) of the size of a SuSu-core (black circle) of an arbitrary pulsar relative to the surrounding shell of normal matter and the corresponding total number of glitch-events are shown. Here, the Crab and Vela pulsars are predicated to have undergone million and ten million glitching events during their lives, respectively. They are expected to fully metamorphose into DEOs after having undergone several billion glitching events, which correspond to roughly one hundred million years.

In a previous study, it was argued that the amount of enclosed total mass of normal matter in a system should be readable from the curvature of the embedding spacetime, in accord with ADM-mass calculated from the positive energy theorem [17].

Assume we are given a cosmically dead NS, and the enclosed matter is on the verge of making a phase transition from maximally compressible into an incompressible state. In this case, there is no volume change as the separation between three quark flavours inside a baryon at ρ_{max}^{uni} and $T=0$ is 0.85 fm (see Figure 4 in [17]) is identical to the average separation between any pair of quarks. Here it was conjectured that the energy stored in the curvature of the embedding spacetime during the phase transition goes into a macroscopic confining of the ocean of the incompressible SuSu-matter. The process here is reversible: once the SuSu-core undergoes hadronization, the macroscopic confining energy goes back into curving the embedding spacetime.

• Purely incompressible SuSu-matter is insensitive to further compression by external forces, and therefore all types of gradients of physical quantities vanish. Hence the regularity condition usually imposed at the centre of astrophysical

objects is met everywhere inside SuSu-cores, therefore rendering the geometrical centre physically unimportant and endowing the constituents with the same physical conditions irrespective of their locations.

For an observer inside the sphere (save the boundary), the matter distribution is perfectly homogenous and isotropic. This implies that the probability for the hadronization front to start its runaway precisely at the centre would be inversely proportional to the number of particles inside the sphere, which is vanishingly small.

On the other hand, a runaway front that starts off-centre would be amplified during the cosmic expansion and therefore would violate the homogeneity and isotropy of the observable universe.

Moreover, a runaway front that starts inside the core would lead to local energy enhancement and therefore to over-dense sectors relative to the background energy density ρ_{max}^{uni}, which would violate the incompressibility condition, and therefore is forbidden by construction. The property of homogeneity and isotropy holds if hadronization is triggered by surface effects on a perfectly spherical symmetric object, which, under the here-discussed conditions, should be connected to an abrupt decay of the macroscopic force confining the ocean of SuSu-superfluid.

• A $10^{24} M_{\odot}$ progenitor with $\rho > \rho_0$ would not survive the collapse into a BH if the embedding spacetime were not flat.

3. UNIMOUN: Mathematical Foundation

The basic argument of UNIMOUN is that the observable universe is a perturbed local sub-domain of the infinitely large and flat parent universe, which is populated by all types of astrophysical objects, including stellar-mass DEOs and supermassive DEOs (SMDEOs). The giant perturbation was derived the hadronization of a $10^{24} M_{\odot}$ progenitor, which is deemed big bang. However, apart from mass and dimension, the structure of the progenitor is physically identical to DEOs. These are assumed to have conglomerated into clusters that subsequently merged to form SMDEOs. Due to their universal low energy states, their mergers should proceed smoothly. Alternatively, the massive black objects that are observed to reside at the centre of most massive galaxies, usually called supermassive BBs, may also function as powerful machines for converting normal matter into incompressible SuSu-matter. Accreting of matter, formation of powerful jets and merger with other objects are possible mechanisms for enhancing the mass and dimensions of SMDEOs.

Based thereon, the field equations to be solved read:

$$R_{\mu\nu} - \frac{1}{2} g_{\mu\nu} = -\kappa T_{\mu\nu}, \tag{2}$$

where R is the Ricci tensor, $g_{\mu\nu}$ is the metric coefficients and $\kappa = 8\pi G/c^4$ [27]. $\{\mu,\nu\}$ run from 0 to 3. Following [28], the following new time-dependent $\mathcal{H}$-metric was introduced:

$$\mathrm{d}s_{\mathcal{H}}^2 = g_{\mu\nu}\mathrm{d}x^{\mu}\mathrm{d}x^{\nu} = g_{00}\,\mathrm{d}t^2 + g_{11}\,\mathrm{d}\bar{r}^2 + g_{22}\,\mathrm{d}\theta^2 + g_{33}\,\mathrm{d}\varphi^2 \tag{3}$$

where

$$g_{00} = c^2\mathrm{e}^{2\mathcal{V}(r,t)}, g_{11} = -\mathrm{e}^{2\lambda(r,t)} g_{22} = -\mathrm{e}^{2\mathcal{C}(t)}r^2, g_{33} = -\mathrm{e}^{2\mathcal{C}(t)}r^2\sin^2\theta. \tag{4}$$

Here $\mathcal{V}$ and λ are functions of the comoving radius $\bar{r}(r,t) = r\mathrm{e}^{\mathcal{C}}$, and $\mathcal{C}(t)$ is a function of time only. All physical and geometrical events are measured with respect to the preferred observer $\mathcal{H}_0$ located at $r = 0$.

Depending on the underlying physical problem, the $\mathcal{H}$-metric may reduce to the classical metrics of Minkowski, Schwarzschild and Friedmann [28].

Using the Christoffel symbol:

$$\Gamma^{\lambda}_{\mu\nu} = \frac{1}{2}g^{\lambda\kappa}\left\{g_{\kappa\nu,\mu} + g_{\kappa\mu,\nu} - g_{\mu\nu,\kappa}\right\}, \tag{5}$$

to calculate the Ricci tensor, see [28] [29]:

$$R_{\mu\nu} = \Gamma^{\alpha}_{\mu\alpha,\nu} - \Gamma^{\alpha}_{\mu\nu,\alpha} + \Gamma^{\alpha}_{\mu\beta}\Gamma^{\beta}_{\alpha\nu} - \Gamma^{\alpha}_{\mu\nu}\Gamma^{\beta}_{\alpha\beta}, \tag{6}$$

we then obtain the following Ricci components:

$$\begin{aligned}
R_{00} &= \ddot{\lambda} + \dot{\lambda}^2 - \dot{\mathcal{V}}\dot{\lambda} + 2\ddot{\mathcal{C}} + 2\dot{\mathcal{C}}^2 - 2\dot{\mathcal{V}}/r + \left(-\mathcal{V}'' + \mathcal{V}'\lambda' - (\mathcal{V}')^2 - 2\mathcal{V}'/r\right)\mathrm{e}^{2(\mathcal{V}-\lambda)}\\
R_{11} &= \left(-\ddot{\lambda} - \dot{\lambda}^2 + \dot{\mathcal{V}}\dot{\lambda} - 2\dot{\lambda}\dot{\mathcal{C}}\right)\mathrm{e}^{2(\lambda-\mathcal{V})} + \mathcal{V}'' + (\mathcal{V}')^2 - \mathcal{V}'\lambda' - 2\lambda'/r\\
R_{22} &= -\left\{\ddot{\mathcal{C}} + \dot{\mathcal{C}}\dot{\lambda} + 2\dot{\mathcal{C}}^2 - \dot{\mathcal{V}}\dot{\mathcal{C}}\right\}r^2\mathrm{e}^{2(\mathcal{C}-\mathcal{V})} + \left(1 + r\mathcal{V}' - r\lambda'\right)\mathrm{e}^{2(\mathcal{C}-\lambda)} - 1\\
R_{33} &= -r^2\sin^2\theta\left[\ddot{\mathcal{C}} + 2\dot{\mathcal{C}}^2 - \dot{\mathcal{V}}\dot{\mathcal{C}} + \dot{\mathcal{C}}\dot{\lambda}\right]\mathrm{e}^{2(\mathcal{C}-\mathcal{V})} + \sin^2\theta\left[\left(1 + r' - r\lambda'\right)\mathrm{e}^{2(\mathcal{C}-\lambda)} - 1\right]
\end{aligned} \tag{7}$$

where $\dot{\square}, \square'$ denote the time and spatial derivatives of the variables, respectively.

Performing detailed algebraic manipulations, re-arrangements and carrying partial integration of certain terms, we end up with the following two equations [28]:

$$\begin{aligned}
&\left[\frac{\ddot{R}}{R} - (1+\mathcal{Z}_b)\left(\frac{\dot{R}}{R}\right)^2 - \dot{F}\left(\frac{\dot{R}}{R}\right)\right]\mathrm{e}^{-2\mathcal{V}} + \frac{1}{2r}\left[\frac{\partial}{\partial t}\left(\mathrm{e}^{-2\mathcal{V}}\right) + \frac{\mathrm{e}^{-2\lambda}}{\mathrm{e}^{-2\mathcal{V}}}\frac{\partial}{\partial r}\left(\mathrm{e}^{-2\mathcal{V}}\right) + \frac{\partial}{\partial r}\mathrm{e}^{-2\lambda}\right]\\
&= -\frac{1}{2}\kappa(\mathcal{E}+p)\left[\Gamma^2\left(g_{00} - g_{11}V^2\right)\right]
\end{aligned} \tag{8}$$

$$\begin{aligned}
&\frac{1}{2}\left(\frac{1}{r} - Y\right)\frac{\partial}{\partial t}\left(\mathrm{e}^{-2\mathcal{V}}\right) - \left[(3+2\mathcal{Z}_b)\left(\frac{\dot{R}}{R}\right)^2 + 2\dot{F}\left(\frac{\dot{R}}{R}\right)\right]\mathrm{e}^{-2\mathcal{V}}\\
&= -\kappa(\mathcal{E}+p)V^2\mathrm{e}^{-2(\mathcal{V}-\lambda)} + \frac{1}{r^2R^2}\frac{\mathrm{d}}{\mathrm{d}r}\left(r\mathcal{X}_b\right) - \kappa\mathcal{E},
\end{aligned} \tag{9}$$

where $\mathcal{E}, p, V, \Gamma = 1/\sqrt{g_{00} + g_{11}V^2}, R$ are the energy density, pressure, transport velocity, Lorentz factor and scaling factor, respectively. The subscript b denotes the comoving values, and $\dot{F}$ is the flux of normal matter injected into the system through hadronization. Here $Y = \dot{R}/R$, $\mathcal{Z}_b = \mathcal{X}_b/(1-\mathcal{X}_b)$, and $\mathcal{X}(r,t) = \alpha_{bb}\left(\frac{m_n(r,t)}{r}\right)$, where $m_n(r,t)$ is the enclosed mass of normal matter and α_{bb} is the so-called compactness parameter.

In addition, the conservation of energy and momentum of matter is taken into account by requiring that the stress-energy tensor must be divergence-free, *i.e.* $\nabla_\mu T^{\mu\nu}=0$. This yields the following set of GR hydrodynamical equations:

$$\frac{1}{\sqrt{-g}}\frac{\partial}{\partial t}\left(\sqrt{-g}\mathcal{D}\right)+\frac{1}{R}\frac{1}{\sqrt{-g}}\frac{\partial}{\partial r}\sqrt{-g}\left(\mathcal{D}V\right)=0 \tag{10}$$

$$\begin{aligned}&\frac{1}{\sqrt{-g}}\frac{\partial}{\partial t}\left(\sqrt{-g}\mathcal{M}^r\right)+\frac{1}{R}\frac{1}{\sqrt{-g}}\frac{\partial}{\partial r}\left(\sqrt{-g}\mathcal{M}^rV\right)\\&=-\frac{1}{R}\frac{\partial P}{\partial r}+\frac{\mathcal{M}^t}{2R}\left(g_{tt,r}+V^2g_{rr,r}\right),\end{aligned} \tag{11}$$

where $\sqrt{-g}=r^2R^3\sin(\theta)\mathrm{e}^{\nu+\lambda}$, $\mathcal{D}$, and V are the determinant of the metric, the relativistic energy-density, and the transport velocity, respectively. The four-momenta is defined as $\mathcal{M}^\sigma=\mathcal{D}hu^\sigma$, where h stands for enthalpy and u^σ for the four-velocity; $\sigma=\{t,r,\theta,\varphi\}$. Here, the Lorentz factor reads:

$$u^t=\frac{1}{g_{tt}+V^2g_{rr}}. \tag{12}$$

The continuity equation may be re-written in the following compact form:

$$\frac{\partial}{\partial t}\left(\bar{\mathcal{D}}_b\right)+\frac{1}{R}\frac{1}{r^2}\frac{\partial}{\partial r}\left(r^2\bar{\mathcal{D}}_bV\right)=0, \tag{13}$$

where $\bar{\mathcal{D}}_b=\mathcal{D}_b\mathrm{e}^{\nu+\lambda}$ and $\mathcal{D}_b=\mathcal{D}R^3$.

To close the system, an equation of state (EOS) should be included, e.g. $P=P(\mathcal{E})=P\left(\mathcal{D}/u^t\right)$.

In the present model, the evolutions of matter and spacetime's topology are followed with respect to a fixed observer at the centre. In this case $R=const.$ and therefore $\dot{R}=Y=0$.

Equations (8) and (9) are then integrated with time to follow the time-evolution of the topology of spacetime, which is in turn dictated by the spatial distribution of mass-energy obtained by time-integrating the hydrodynamical Equations (10) and (11).

The initial configuration is a progenitor of $10^{24}M_\odot$, which set to levitate at the background of the infinitely large and flat spacetime of the parent universe. The progenitor is made of purely incompressible SuSu-matter, whose matter-density is set to be equal to universal critical density $\rho=\rho_{cr}=3\times\rho_0$. At $t=0$, the membrane confining SuSu-matter is removed and a hadronization front starts propagating from the surface inward, converting thereby SuSu-matter into normal compressible and dissipative matter. The created pressure of normal matter generates extraordinary strong pressure-gradients that jettisons the newly created normal matter into the ambient space with ultra-relativistic speeds, as shown in **Figure 2**. Here the gradual increase of both the modified Lorentz factor $\bar{u}^t$ and the kinetic energy E_{kin} with radius is due to the inward-increasing gravitational redshift of the fireball. The shock front follows the traces of the expansion front separating the enclosed curved spacetime from the unperturbed ambient flat one.

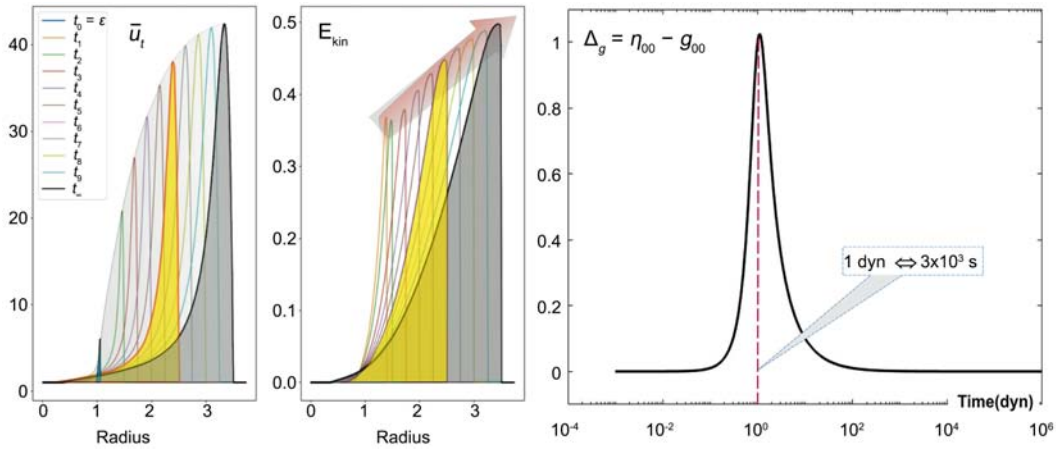

Figure 2. Different snapshots of the radial distributions of the modified Lorentz factor $\bar{\mathbf{u}}_t$ and the kinetic energy E_{kin} during hardonization and thereafter are displayed. The radii and time here are in r_p and dynamical time scale units. The time-sequence of the snapshots is marked with different colours, starting with blue and ending with black. In the right panel the deviation of the topology of the dynamical spacetime from the flat spacetime, Δ_g, during hadronization and at much later times is shown.

4. Viability of UNIMOUN as a Cosmological Model

In this section, we intend to discuss selected problems in observational astronomy and the possible answers that can be provided by the current models.

- **The SMBH in M87: Is the existence of BHs a proven hypothesis?**

Distant BHs still may not exist, even if currently, both theory and resolution-limited observations allude to their existence. Directly observing event horizons of BH is forbidden by construction, and their vicinities are far beyond the resolution sensitivities of today's telescopes, including the event horizon telescopes (EHT). The object residing inside the central dark region of the famous figures published by the EHT must not be a BH, but a highly compact supermassive dark object that is hiding an entropy-free incompressible SuSu-matter at its centre with a radius r_{core}, and surrounded by a shell of weakly compressible and dissipative normal matter. As the spacetime inside the SuSu-core is flat, but curved in the surrounding space, the configuration is immune to collapse into a true BH. To clarify the idea: consider the supergiant galaxy M87. The mass of the supermassive black hole (SMBH) is predicated to be $M_{BH}^{obs} = [6.0 \pm 0.4] \times 10^9 M_\odot$, yielding $r_{\mathcal{H}}^{obs} \approx 1.92 \times 10^{15}$ cm for the event horizon. On the other hand, UNIMOUN suggests that these values correspond solely to the content of normal matter. Hence the true radius of the black object in M87 and the corresponding compactness parameter α_{M87}, read:

$$r_{true} = r_{\mathcal{H}}^{obs} + r_{core} \Rightarrow \alpha_{M87} = \frac{1}{1 + \frac{r_{core}}{r_{\mathcal{H}}^{obs}}}, \tag{14}$$

which is upper-bounded by unity for any non-vanishing SuSu-core.

This implies that measuring the trajectories of orbiting stars around the central object does not necessarily infer the true radius of the event horizon $r_{\mathcal{H}}^{true}$.

Here multi-messenger observations may be used to detect the behaviour of M87 during mergers with other astrophysical objects, carrying precise measurements of the dynamics of the proton-dominated jet in the vicinity of the predicted event horizon [30], as well as the dynamics of the plasma in the boundary layer between the optically this accretion disk, and the central object may enable observers to infer the difference $\Delta_H = r_{\mathcal{H}}^{obs} - r_{\mathcal{H}}^{true}$.

Currently, the observational data of M87 are unable to accurately determine the dynamics of plasmas inside [$r_{\mathcal{H}} < r \le 4r_{\mathcal{H}}$].

This leave us with a gross uncertainty, as setting a SMDEO with a mass $6.5\times10^9 M_\odot$ and constant density $\rho = 3\times\rho_0 = const.$ at the centre of the dark region in M87 would merely increase $r_{\mathcal{H}}^{obs}$ by a factor of 10^{-6}, which far below the measurement sensitivities of today's telescopes, including the VLBI and EHT.

- **The life cycle of BBs in the parent universe**

The progenitors of BBs are reproducible giant objects in the parent universe. There are several clues that indirectly support this conjecture:

1) Almost all massive NSs that should have formed from the collapse of the first generation of stars are observationally missing. According to standard cosmologies, the first generation of stars should have formed within the first several hundred million years after the BB. These stars must have been relatively very massive and metal-free and therefore their lifetimes must have been significantly shorter than those in the local universe. If Pop III stars did really form, then a significant number should have collapsed to form massive pulsars and NSs, that by now, should be metamorphosed into invisible DEOs. These in turn, may conglomerate into tight clusters and/or merge with other objects from the observable universe or from the parent universe to form the progenitors for the next generations of BBs.

2) The multi-messenger observations of the merger event in GW170817 didn't exclude the possibility that the remnant may be a massive NS [31] [32]. Here, due to the low energy states of both incompressible SuSu-cores, the merger of these cores is expected to proceed smoothly toward forming a massive incompressible SuSu-core. For a sufficiently long cosmic time, the remnant would undergo repeated mergers to end up as a SMDEO which and serve as a progenitor for the next BB.

3) The supermassive black objects observed to reside the centres of most massive galaxies are ultracompact and massive objects that harbour SMDEOs that evolving toward forming the progenitors of the next generation of BBs.

- **What is the origin of the SMBHs in high redshift galaxies?**

Irrespective of the counter arguments against BHs, observations indicate that most high redshift galaxies host supermassive BHs at their cenres with masses beyond $10^8 M_\odot$. The currently suggested growth mechanisms, such as merger and accretion, are not sufficiently effective to enable their formation and rapid growth during the first 400 Myr after the big bang.

According to UNIMOUN, these host galaxies are relics of old and inactive

ones that were levitating in the infinitely large and flat parent universe that happened to be surrounding the progenitor prior big bang. Matter and the associated enormous momentum from the fireball tuned these galaxies into active modes and set them into outward-oriented accelerating motions.

- **What is the origin of the dark matter and dark energy in our cosmos?**

Supermassive BHs in UNIMOUN correspond to evolving supermassive DEOs. Similar to massive pulsars and NSs, whose cores are set to grow in mass and size as they evolve on cosmic times, the central regions of SMBHs should be occupied by cores that are made incompressible SuSu-matter surrounded by compressible and dissipative matter. As the latter cools down on cosmic times, then the matter in the geometrically thin boundary layer between these two fluids is set to convert into SuSu-matter and to subsequently integrate into the core, thereby increasing its mass and size in a discrete quantum manner. Consequently, the spacetime embedding the matter in the boundary layer (BL) is ought to change topology from a curved into a flat one, thereby weakening the central gravitational attraction of the orbiting objects. In UNIMOUN, the changes of spacetime's topologies resulting from the discrete growth of SMDEOs should be observed through the radial motion of the objects orbiting the central supermassive object. Here the prompt reduction of the gravitational mass of the central object should lead to an excess of kinetic energy that would force these orbiting objects to migrate outwardly, thereby giving rise to a total velocity that grows with distance from the central object, *i.e.* $V \sim r^{\alpha}$, where $\alpha \geq 1/2$.

Moreover, as UNIMOUN predicts the infinitely large and flat parent universe to be populated by all type of astrophysical objects, the possibility that invisible old, cold, inactive matter and/or objects maybe involved or effecting the formation of galaxies should not be excluded.

UNIMOUN doesn't require dark energy to accelerate the universe. Recalling that the observable universe is a perturbed sub-domain of our infinitely large and flat parent universe, which would diffuse out and return to the initial state, then invoking dark energy is neither a conformal process with the parent universe nor needed. According to UNIMOUN, the mechanisms underlying the acceleration of high redshift galaxies are a consequence of matter and momentum transfer from the powerfully expanding fireball into the old and inactive galaxies that surrounded the progenitor prior to its explosion. The bombardment of these galaxies with matter associated with tremendous momentum from the fireball may easily set quiet galaxies into outward accelerating motions (see **Figure 3** as well as [33] [34] for further details).

- **Why is the observable universe incredibly flat?**

During the hadronization phase of the progenitor, incompressible SuSu-matter was converted into normal compressible and dissipative matter, which in turn dictated how the embedding spacetime should curve. At the end of this epoch, which lasted for roughly 46 minutes, the created total mass of normal matter attained its maximum value, at which the embedding spacetime was maximally curved (see Δ_g/**Figure 2**).

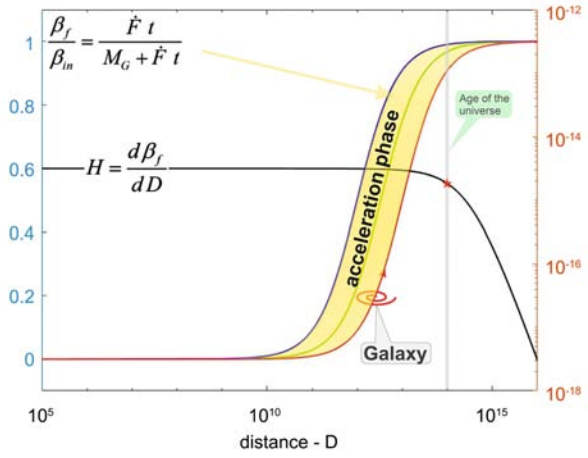

Figure 3. The time development of the receding velocity, β_f of galaxies for different incident fluxes $\dot{F}_{in} = 10^{-11}, 5\times10^{-12}, 10^{-12}$ denoted respectively by blue, green and red lines. The depicted yellow region denotes the domain of galaxy accelerations, where the galaxies are assumed to have a fixed mass of $M_G = 10$. Also, the cosmic evolution of the Hubble parameter, $H = \mathrm{d}V/\mathrm{d}D$ is displayed in black-colored line. Here H decreases slowly with the cosmic time from relatively high values in the early universe to low ones on later times.

As predicted by the minimum energy theorem, the equivalence of energy and curvature implies that the amount of energy stored in the spacetime should be readable from the curvature of the embedding spacetime. However, when the fireball expands, the embedding spacetime should flatten, and therefore the corresponding compactness parameter must decrease with cosmic time. In this case, the evolution of the deviation of the spacetime's topology from the flat spacetime may be measured as follows:

$$\Delta_g = \eta_{00} - g_{00} = \mathcal{X}(r,t) = \alpha_{bb}\left(\frac{m_n(r,t)}{r}\right) = \begin{cases} 0 & t \le 0 \\ \alpha_{bb}/2 & t = \tau_{dyn} \\ \alpha_{bb}/t & t > \tau_{dyn} \\ \mathcal{O}\left(10^{-17}\right) & t = \tau_{age}^{uni} \approx \text{universe's age,} \end{cases} \tag{15}$$

where $m_n(r,t)$ is the enclosed total mass of normal matter and α_{bb} is the compactness parameter, which, under normal astrophysical conditions, must be smaller than or equal to unity.

Hence, as the progenitor is made up of incompressible SuSu-matter, then the spacetime at the background was flat. During the hadronization of the progenitor, the spacetime was continuously enhancing its curvature. Once the hadronization process is completed, the fireball starts expanding and the embedding spacetime should flatten to become today almost indistinguishable from flat spacetime (Figure 4).

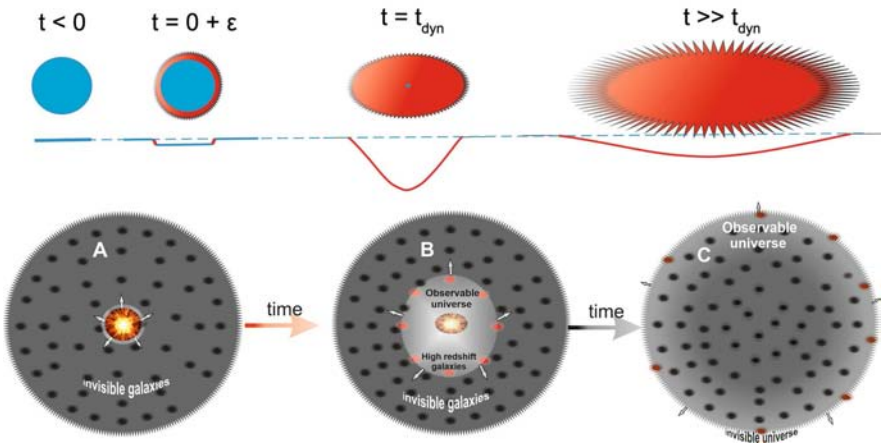

Figure 4. A schematic description of the progenitor's spacetime (upper panel): prior to hadronization $t<0$, the progenitor is made up of incompressible SuSu-matter embedded in flat spacetime. During the hadronization phase: *i.e.* $0 \le t \le \tau_{dyn}$, the creation of normal matter enhances the curvature of the embedding spacetime and reaches its maximum possible value at $t=\tau_{dyn}$, at which the progenitor is entirely hadronized, and the total mass of normal matter has attained its maximum value. At later times, $t>\tau_{dyn}$, the total mass of normal matter remains constant, whereas the expanding spacetime becomes increasingly flatter. In the lower panel, the spacetime embedding the fireball continues to expand and diffuse into the flat parent universe, whose innermost shells are populated with quiet and inactive galaxies, though they may turn active once the expansion front marches through them.

- **Hubble parameter and the local universe**

The motions of galaxies in the local universe display relatively low redshift compared to their remote counterparts. This behaviour is a logical consequence of the measurable duration of the progenitor's hadronization process, which may be explained as follows: During the hadronization phase, which lasted for roughly 46 minutes, the embedding spacetime, which was initially flat, started to enhance its curvature almost in a continuous manner and to finally become maximally curved when the hadronization phase was completed. This implies that the early and lately created normal normal matter fluids evolve under different gravitational redshift conditions. The created normal matter near the geometrical centre is relatively deeply trapped in the potential-well and therefore, a significant kinetic energy is lost while climbing up the well, which slows its motion and delays its escape into the ambient space. This enables the normal matter in the central region to cool down and possibly to form the observed galaxies of our local universe (see Figure 3 in [34]).

- **Entropy of DEOs versus black holes**

According to BH-thermodynamics, the entropy of a star collapsing into a BH should increase roughly by a factor of 10^{19} [35]. To avoid loss of quantum information that may result from the collapse of massive stars into BHs, the event horizon my serve as a 2D complex construct, where the information are stored in accordance with the holographic principle [36]. In our scenario, however, BHs are replaced by DEOs that are made up of incompressible SuSu-superfluid

occupying just one single quantum state, and therefore they have zero entropy. These cores are surrounded by normal compressible and dissipative matter, whose compactness parameter is close to but still smaller than unity. Similar to glitching pulsars, when the normal matter liberates its secondary energies entirely and cools down on cosmic time, the mass and dimensions of the cores should grow discretely in accord with Onsager-Feynman's analysis of superfluidity. In this respect, the jet in M87 serves as a mechanism, not only to transfer angular momentum out of the system but also to expel the other types of energy as well as entropy from the central SMDEO into the intergalactic medium (see [30], and the references therein).

Both the glitch phenomena of pulsars and their metamorphosis into entropy-free objects suggest that there might be a hidden connection between entropy and gravity: isolated entropy-free DEOs appear to be incapable of communicating with the outside world and therefore cease to affect the topology of the embedding spacetimes. While the present approach differs from the emerging gravity scenario [37], investigating the gravity-entropy connection might turn out to be a rewarding effort.

Assuming these communications to be mediated by a certain elementary particle, say via entropytons, then these particles appear to be trapped inside the object once the state of matter making up the object undergoes a phase transition into incompressible entropy-free SuSu-superfluid.

5. Summary

UNIMOUN is a mathematically founded and physically viable model for the observable universe: it has the capability of competing with modern astronomical observations as well as with experimental data. It is based on thorough theoretical and numerical calculations for modeling glitching pulsars, namely of the Crab and Vela, as well as on the merger of the binary NSs in GW170817, but also on the recently observed perfect fluidity of gluon-quark plasma at the LHC and RHIC (see [38], and the references therein). The main outcome of these investigations is that massive pulsars and NSs are capable of creating the exotic and extraordinarily stable state of matter inside their cores: incompressible gluon-quark superfluid. This, however, suggests the following two possibilities:

• The laws of nature may have placed an upper limit on the maximum energy density in the universe, which, among others, forbid the formation of physical singularities, and in particular black holes.

• The cosmic time required for pulsars to evolve, starting from their births, then going through NS and DEO-phases to finally conglomerate into tight clusters, that subsequently merge to form hypermassive progenitors, is predicated to be much longer than the current age of the universe. This open the possibility that objects originating from the parent universe could, in principle, be involved in the merger process. In this case the ultimate deaths of massive neutron stars and the formation of big bang's progenitors may be strongly interconnected more than current research could suggest.

When these theoretical possibilities are put together, it becomes inevitable to conclude that our observable universe must be a tiny fraction of an infinitely large, homogeneous and isotropic flat parent universe. And as the parent universe is populated by all types of astrophysical objects, e.g. planets, stars, galaxies and galaxy clusters, etc. then the origin of the SMBH-candidates hosted by high redshift galaxies become straightforward: The black objects so far classified as SMBH should have been there already before the big bang, but they started growing, once the hosting galaxies have been hit by the fireball-matter and the expansion front of the spacetime.

Based thereon, our big bang is just one of countless big bangs that occur in a sequence or in parallel manner at the same time or in different locations of the parent universe. These BBs may be classified as local and power-limited perturbations that are doomed to decay and diffuse out in the ambient parent universe (Figure 5).

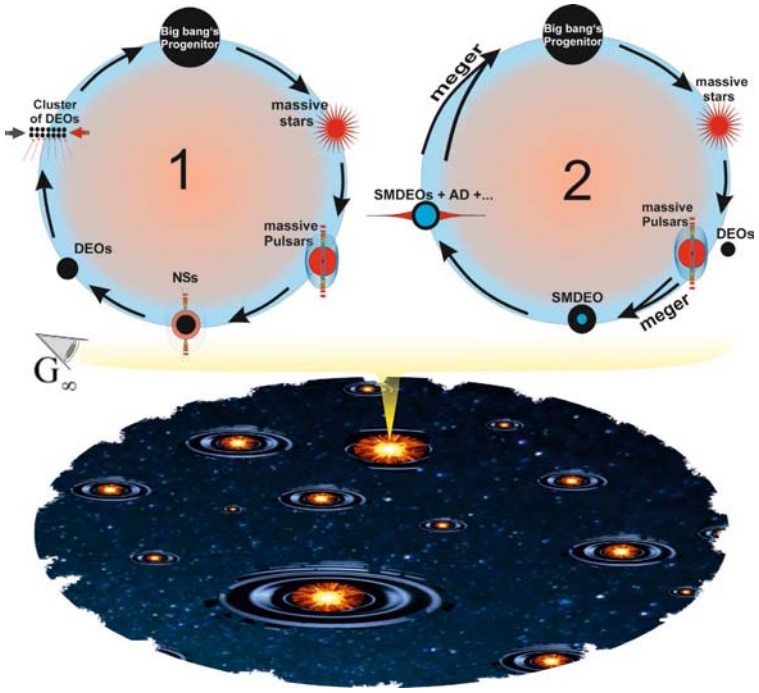

Figure 5. A schematic description of two possible life cycles of BBs in the parent universe, as seen by the supra-observer $\mathbf{G}_{\infty}$. Cycle "1": The trapped cold matter from the BB collapse to form massive stars, which subsequently collapse to form pulsars. These pulsars are born with embryonic incompressible SuSu-cores, whose masses grow with cosmic time to finally turn into DEOs. These objects may conglomerate into tight clusters to subsequently merge and BB-progenitors. In cycle "2": during mergers of NSs-NSs, BHs-BHs and NSs-BHs the SuSu-cores merge smoothly to form SMDEOs surrounded by shells of normal matter that is sufficiently compact to enable conversion of the normal matter in the BL into incompressible SuSu-matter. This, in turn, adopts the same quantum numbers of the core's matter and subsequently joins the core, thereby increasing its mass and size. This is currently the operating process in the supermassive BH-candidates that are observed to reside in the centres of massive galaxies. In our infinitely large and flat parent universe, BBs may occur sequentially and/or in parallel at the same or different locations.

The evolution of these perturbations is similar to water droplets falling into large water containers: the strongest spatial and temporal variations occur immediately after the droplet splash but start decaying once the generated waves set in their expansion, they diffuse out and disappear finally.

Finally, there is an additional fundamental outcome of UNIMOUN:

As the parent universe is populated with all types of astrophysical objects, then the possibility that part of these objects may have been involved in the formation of the progenitor of our big bang should not be excluded. On the other hand, this raises the possibility that the governing laws of nature and the underlying physical constants and therefore the type of matter are unalterable throughout the infinite parent universe. In this case, the probability of finding habitable planets in the parent universe is certain.

Acknowledgements

The author acknowledges the financial support from the IWR and KAUST. Max Camenzind, Mario Livio and Adi Nasser are deeply acknowledged for their valuable comments and suggestions.

Conflicts of Interest

The author declares no conflicts of interest regarding the publication of this paper.

References

[1] Murschel, A. (1995) *Journal for the History of Astronomy*, **26**, 33-61. https://doi.org/10.1177/002182869502600102

[2] John, A. (2017) *Journal for the History of Astronomy*, **48**, 238-241. https://doi.org/10.1177/0021828617706254

[3] Swerdlow, N.M. (1973) *Proceedings of the American Philosophical Society*, **117**, 424-434.

[4] Kuhn, T.S. (1985) The Copernican Revolution-Planetary Astronomy in the Development of Western Thought. Harvard University Press, Cambridge.

[5] Einstein, A. (1917) Kosmologische Betrachtungen zur allgemeinen Relativitätstheorie. Sitzungsb. Sitzungsberichte der Königlich Preußischen Akademie der Wissenschaften, Berlin, 142-152.

[6] Ellis, G.R. and van Elst, H. (1998) *NATO Advanced Study Institute Ser. C. Mathematical and Physical Sciences*, **541**, 1-116.

[7] Caroll, S.M. (2001) *LRR*, **4**, 1.

[8] Di Valentino, E., Mena, O., *et al.* (2021) *Classical and Quantum Gravity*, **38**, Article ID: 153001.

[9] Efstathiou, G. (2023) *Astronomy & Geophysics*, **64**, 1.21-1.24. https://doi.org/10.1093/astrogeo/atac093

[10] Trimble, V. (1987) *Annual Review of Astronomy and Astrophysics*, **25**, 425-472. https://doi.org/10.1146/annurev.aa.25.090187.002233

[11] Perlmutter, S., *et al.* (1999) *ApJ*, **517**, 565.

[12] Sato, K. (1981) *MNRAS*, **195**, 467-479. https://doi.org/10.1093/mnras/195.3.467

[13] Steinhardt, P.J. (2011) *Scientific American*, **304**, 18. https://doi.org/10.1038/scientificamerican0311-18b

[14] Ade, P.A.R., *et al.* (2014) *Astronomy & Astrophysics*.

[15] The Event Horizon Telescope Collaboration, *et al.* (2021) *ApJL*, **910**, L13.

[16] Hujeirat, A.A. (2018) *Journal of Modern Physics*, **9**, 70-83.

[17] Hujeirat, A.A. (2021) *Journal of Modern Physics*, **12**, 937-958.

[18] Aghanim, N., *et al.* (2020) *A&A*, **641**, A5-A6.

[19] Hujeirat, A.A. (2018) *Journal of Modern Physics*, **9**, 532-553.

[20] Hujeirat, A.A. and Samtaney, R. (2019) *Journal of Modern Physics*, **10**, 1696-1712. https://doi.org/10.4236/jmp.2019.1014111

[21] Ashton, G., Lasky, P.D., *et al.* (2019) *Nature Astronomy*, **3**, 1143-1148. https://doi.org/10.1038/s41550-019-0844-6

[22] Hujeirat, A.A. and Samtaney, R. (2020) *Journal of Modern Physics*, **11**, 395-406. https://doi.org/10.4236/jmp.2020.113025

[23] Hujeirat, A. and Samtaney, R. (2020) *Journal of Modern Physics*, **11**, 1779-1784. https://doi.org/10.4236/jmp.2020.1111110

[24] Haemmerl, L., Mayer, L., *et al.* (2020) *Space Science Reviews*, **216**, Article No. 48. https://doi.org/10.1007/s11214-020-00673-y

[25] Espinoza, C.M., Lyne, A.G., Stappers, B.W. and Kramer, C. (2011) *Monthly Notices of the Royal Astronomical Society*, **414**, 1679-1704. https://doi.org/10.1111/j.1365-2966.2011.18503.x

[26] Roy, J., Gupta, Y. and Lewandowski, W. (2012) *Monthly Notices of the Royal Astronomical Society*, **424**, 2213-2221. https://doi.org/10.1111/j.1365-2966.2012.21380.x

[27] Glendenning, N.K. (2007) Special and General Relativity. Springer, Berlin. https://doi.org/10.1007/978-0-387-47109-9

[28] Hujeirat, A.A. (2022) *Journal of Modern Physics*, **13**, 1474-1498. https://doi.org/10.4236/jmp.2022.1311091

[29] Hobson, M.P., Efstathiou, G. and Lasenby, A.N. (2015) CUP.

[30] Hujeirat, A.A., Livio, M., *et al.* (2003) *A&A*, **408**, 415-430. https://doi.org/10.1051/0004-6361:20031040

[31] Abbott, *et al.* (2017) *ApJL*, **848**, L12.

[32] Piro, L., Troja, E. and Zhang, B. (2019) *Monthly Notices of the Royal Astronomical Society*, **483**, 1912-1921. https://doi.org/10.1093/MNRAS/sty3047

[33] Hujeirat, A.A. (2022) *Journal of Modern Physics*, **13**, 1581-1597. https://doi.org/10.4236/jmp.2022.1312096

[34] Hujeirat, A.A. (2023) *Journal of Modern Physics*.

[35] Brousso, R. (2002) *Reviews of Modern Physics*, **74**, 825. https://doi.org/10.1103/RevModPhys.74.825

[36] 't Hooft, G. (2001) Basics and Highlights in Fundamental Physics. *Proceedings of the International School of Subnuclear Physics*, Erice, August-September 2000, 72-100.

[37] Verlinde, E.P. (2010) *JHEP*, **1104**, 29.

[38] Eskola, K.J. (2019) *Nature Physics*, **15**, 1111-1112. https://doi.org/10.1038/s41567-019-0643-0

Journal of Modern Physics, 2023, 14, 432-444
https://www.scirp.org/journal/jmp
ISSN Online: 2153-120X
ISSN Print: 2153-1196

Explanation of the Necessity of the Empirical Equations That Relate the Gravitational Constant and the Temperature of the CMB

Tomofumi Miyashita

Miyashita Clinic, Osaka, Japan
Email: tom_miya@plala.or.jp

How to cite this paper: Miyashita, T. (2023) Explanation of the Necessity of the Empirical Equations That Relate the Gravitational Constant and the Temperature of the CMB. *Journal of Modern Physics*, **14**, 432-444.
https://doi.org/10.4236/jmp.2023.144024

Received: February 6, 2023
Accepted: March 13, 2023
Published: March 16, 2023

Abstract

In previous papers, we proposed an empirical equation for the fine-structure constant. Using this equation, we proposed a refined version of our own former empirical equations about the electromagnetic force and gravity in terms of the temperature of the cosmic microwave background. The calculated values of the temperature of the cosmic microwave background (T_c) and the gravitational constant (G) were 2.726312 K and 6.673778 × 10^{-11} $m^3 \cdot kg^{-1} \cdot s^{-2}$, respectively. Then, for the values of the factors 9/2 and π in our equations, we used 4.488519503 and 3.132011447, respectively. However, we could not provide a theoretical explanation for the necessity of these empirical equations. In this paper, using the redefinition method for the UNIT, we show the necessity for our empirical equations.

Keywords

Gravitational Constant, Temperature of the Cosmic Microwave Background

1. Introduction

The symbol list is shown in Section 2. Previously, we discovered Equations (1)-(3) [1] [2] [3] in terms of the temperature of the cosmic microwave background (CMB), which are mathematically connected [3].

$$\frac{Gm_p^2}{hc} = \frac{4.5}{2} \times \frac{kT_c}{1\,\mathrm{kg} \times c^2} \tag{1}$$

$$\frac{Gm_p^2}{\left(\frac{e^2}{4\pi\varepsilon_0}\right)} = \frac{4.5}{2\pi} \times \frac{m_e}{e} \times hc \times \left(\frac{\mathrm{C}}{\mathrm{J \cdot m}} \times \frac{1}{\mathrm{kg}} = \frac{1}{\mathrm{V \cdot m}} \times \frac{1}{\mathrm{kg}}\right) \tag{2}$$

$$\frac{m_e c^2}{e} \times \left(\frac{e^2}{4\pi\varepsilon_0} \right) = \pi \times kT_c \times \left(\frac{\mathrm{J \cdot m}}{\mathrm{C}} = \mathrm{V \cdot m} \right) \tag{3}$$

We attempted to reduce the errors in the previous papers by changing the values of 4.5, π and the temperature of the cosmic microwave background (T_c) [4] [5]. Next, we discovered an empirical equation for the fine-structure constant [6].

$$137.0359991 = 136.0113077 + \frac{1}{3 \times 13.5} + 1 \tag{4}$$

$$13.5 \times 136.0113077 = 1836.152654 = \frac{m_p}{m_e} \tag{5}$$

We thought that Equations (4) and (5) should be related to the transference number [7] [8]. Then, we proposed an equivalent circuit and the following values as the deviation for the values of 9/2 and π [8].

$$3.13201\,\Omega = \frac{\left(\frac{m_p}{m_e} + \frac{4}{3} \right) m_e c^2}{ec} \tag{6}$$

$$4.48852 = \frac{q_m c}{\left(\frac{m_p}{m_e} + \frac{4}{3} \right) m_p c^2} \tag{7}$$

Then, $\left(\frac{m_p}{m_e} + \frac{4}{3} \right)$ have the unit of $\left(\frac{\mathrm{m}}{\mathrm{C}} \right)$. We can freely define the UNITs for 1 C, 1 Wb and 1 kg. Therefore, we must show the necessity for Equations (6) and (7) that these values are related to 4.5 and π. Using the redefinition method for the UNIT, we can show the necessity for our empirical equations in this report.

The remainder of the paper is organized as follows. In Section 2, we show the symbol list. In Section 3, we discuss the purpose of this report. In Section 4, we explain the redefinition method for the UNIT. In Section 5, using the redefinition method, we can refine Equations (1)-(3). Furthermore, we propose a fourth empirical equation that relates the gravitational constant and the temperature of the cosmic microwave background. In Section 6, our conclusions are described.

2. Symbol List (These Values Were Obtained from Wikipedia)

G: gravitational constant: 6.6743×10^{-11} ($m^3 \cdot kg^{-1} \cdot s^{-2}$)
(we used the compensated value 6.673778×10^{-11} in this report).

T_c: temperature of the cosmic microwave background: 2.72548 (K)
(we used the compensated value 2.726312 K in this report).

k: Boltzmann constant: 1.380649×10^{-23} ($J \cdot K^{-1}$).

c: speed of light: 299792458 (m/s).

h: Planck constant: $6.62607015 \times 10^{-34}$ ($J \cdot s$).

ε_0: electric constant: $8.8541878128 \times 10^{-12}$ ($N \cdot m^2 \cdot C^{-2}$).

μ_0: magnetic constant: $1.25663706212 \times 10^{-6}$ ($\mathrm{N \cdot A^{-2}}$).

e: electric charge of one electron: $-1.602176634 \times 10^{-19}$ (C).

q_m: magnetic charge of one magnetic monopole: $4.13566770 \times 10^{-15}$ (Wb)
(this value is only a theoretical value, $q_m = h/e$).

m_p: rest mass of a proton: $1.6726219059 \times 10^{-27}$ (kg)
(we used the compensated value $1.672621923 \times 10^{-27}$ kg in this report).

m_e: rest mass of an electron: $9.1093837 \times 10^{-31}$ (kg).

Rk: von Klitzing constant: 25812.80745 (Ω).

Z_0: wave impedance in free space: 376.730313668 (Ω).

α: fine-structure constant: 1/137.035999081.

3. Purpose

In this section, we show the purpose of this report. For convenience, Equations (5) and (6) are rewritten as follows. The units have been corrected.

$$3.132011447\left(\mathrm{V \cdot m}\right) = \frac{\left(\frac{m_p}{m_e} + \frac{4}{3}\right) m_e c^2}{ec} \left(\frac{\mathrm{m^2}}{\mathrm{s}} \times \frac{\mathrm{J}}{\mathrm{A \cdot m}} = \frac{\mathrm{J \cdot m}}{\mathrm{C}} = \mathrm{V \cdot m}\right) \tag{8}$$

$$4.488519503\left(\frac{1}{\mathrm{A \cdot m}}\right) = \frac{q_m c}{\left(\frac{m_p}{m_e} + \frac{4}{3}\right) m_p c^2} \left(\frac{\mathrm{s}}{\mathrm{m^2}} \times \frac{\mathrm{V \cdot m}}{\mathrm{J}} = \frac{\mathrm{V}}{\mathrm{J}} \times \frac{\mathrm{s}}{\mathrm{m}} = \frac{\mathrm{s}}{\mathrm{C \cdot m}} = \frac{1}{\mathrm{A \cdot m}}\right) \tag{9}$$

Then, $\left(\frac{m_p}{m_e} + \frac{4}{3}\right)$ have the unit of $\left(\frac{\mathrm{m^2}}{\mathrm{s}}\right)$. Next, the deviation from 4.5 and π can be explained as follows.

$$\frac{4.5}{\pi} \times \frac{3.132011447}{4.488519503} = 0.999500154 \doteq 1 \tag{10}$$

Then, we can freely define the UNITs for 1 C, 1 Wb and 1 kg. It does not seem necessary that these values are related to 4.5 and π. Unfortunately, we could not establish the background theory. Using the redefinition method for the UNIT, we can show the necessity why these values should be related to 4.5 and π.

4. Methods

4.1. Redefinitions for the Electric Charge of One Electron and the Magnetic Charge of One Magnetic Monopole

We redefine the electric charge of one electron as follows.

$$e_{\mathrm{new}} = e \times \frac{4.48852}{4.5} = 1.59809E-19\left(\mathrm{C}\right) \tag{11}$$

We redefine the magnetic charge of one magnetic monopole as follows.

$$q_{m\_\mathrm{new}} = q_m \times \frac{\pi}{3.13201} = 4.14832E-15\left(\mathrm{Wb}\right) \tag{12}$$

Then, we can redefine the Planck constant and von Klitzing constant as follows.

$$h_{\text{new}} = e_{\text{new}} \times q_{m\_\text{new}} = h \times \frac{4.48852}{4.5} \times \frac{\pi}{3.13201} = 6.62938E-34 \tag{13}$$

$$Rk_{\_\text{new}} = \frac{q_{m\_\text{new}}}{e_{\_\text{new}}} = Rk \times \frac{4.5}{4.48852} \times \frac{\pi}{3.13201} = 25958.0(\Omega) \tag{14}$$

Then, we can redefine the wave impedance in free space, electric constant and magnetic constant.

$$Z_{0\_\text{new}} = \alpha \times \frac{2h_{\text{new}}}{e_{\text{new}}^2} = 2\alpha \times Rk_{\text{new}} = Z_0 \times \frac{4.5}{4.48852} \times \frac{\pi}{3.13201} = 378.849(\Omega) \tag{15}$$

$$\mu_{0\_\text{new}} = \frac{Z_{0\_\text{new}}}{c} = \mu_0 \times \frac{4.5}{4.48852} \times \frac{\pi}{3.13201} = 1.26371E-06\left(\text{N}\cdot\text{A}^{-2}\right) \tag{16}$$

$$\varepsilon_{0\_\text{new}} = \frac{1}{Z_{0\_\text{new}} \times c} = \varepsilon_0 \times \frac{4.48852}{4.5} \times \frac{3.13201}{\pi} = 8.80466E-12\left(\text{F}\cdot\text{m}^{-1}\right) \tag{17}$$

Next, we must ensure that there are no contradictions.

$$c_{\_\text{new}} = \frac{1}{\sqrt{\varepsilon_{0\_\text{new}}\mu_{0\_\text{new}}}} = \frac{1}{\sqrt{\varepsilon_0\mu_0}} = c = 299792458\left(\text{m}\cdot\text{s}^{-1}\right) \tag{18}$$

$$\begin{aligned} Z_{0\_\text{new}} &= \sqrt{\frac{\mu_{0\_\text{new}}}{\varepsilon_{0\_\text{new}}}} = \sqrt{\frac{\mu_0}{\varepsilon_0}} \times \frac{4.5}{4.48852} \times \frac{\pi}{3.13201} \\ &= Z_0 \times \frac{4.5}{4.48852} \times \frac{\pi}{3.13201} = 378.849(\Omega) \end{aligned} \tag{19}$$

The value in the speed of light should not be changed because the UNITs for 1 m and 1 s are unchanged. In Equation (19), the value of the impedance in free space is the same as the value in Equation (15).

4.2. The Macroscopic Explanation of Our Redefinition Method

By our redefinition method for the units of the particles, 1 C and 1 Wb as MKSA units are not fixed. We redefine the electric charge of one electron. Then, the number of electrons in 1 C is changed.

$$N_1 = \frac{1\,\text{C}}{e} = \frac{1}{1.60218E-19} = 6.24151E+18 \tag{20}$$

$$N_2 = \frac{1\,\text{C}}{e_{\text{new}}} = \frac{1\,\text{C}}{\frac{4.48852}{4.5} \times e} = \frac{4.5}{4.48852} \times 6.24151E+18 \tag{21}$$

Then, the number of magnetic monopoles in 1 Wb is changed.

$$N_3 = \frac{1\,\text{Wb}}{q_m} = \frac{1}{4.13567E-15} = 2.41799E+14 \tag{22}$$

$$N_4 = \frac{1\,\text{Wb}}{q_{m\_\text{new}}} = \frac{1\,\text{Wb}}{\frac{\pi}{3.13201} \times 1q_m} = \frac{3.13201}{\pi} \times 2.41799E+14 \tag{23}$$

The number of electrons in 1 C is related to the Faraday constant and the Avogadro's number. Therefore, we redefined the Faraday constant and the Avo-

gadro's number, which will be explained in the later section.

$$\frac{1\,\mathrm{C}_{\mathrm{new}}}{1\,\mathrm{C}}=\frac{4.5}{4.48852} \tag{24}$$

$$\frac{1\,\mathrm{Wb}_{\mathrm{new}}}{1\,\mathrm{Wb}}=\frac{3.13201}{\pi} \tag{25}$$

However, the relationship between Equations (26) and (27) should hold.

$$1\,\mathrm{J}\cdot\mathrm{s}_{\mathrm{new}}=1\,\mathrm{C}_{\mathrm{new}}\times 1\,\mathrm{Wb}_{\mathrm{new}} \tag{26}$$

$$1\,\Omega_{\mathrm{new}}=\frac{1\,\mathrm{Wb}_{\mathrm{new}}}{1\,\mathrm{C}_{\mathrm{new}}} \tag{27}$$

We used $\mathrm{A}\cdot\mathrm{m}_{\_\mathrm{new}}$ and $\mathrm{C}_{\mathrm{new}}$ in the later sections. Then, these units are from the microscopic redefinition. From the macroscopic redefinition, $\mathrm{A}\cdot\mathrm{m}_{\_\mathrm{new}}$ and $\mathrm{C}_{\mathrm{new}}$ should be different values.

4.3. Redefinitions of the Mass of One Electron and One Proton

The Compton wavelength (λ) is as follows.

$$\lambda=\frac{h}{mc} \tag{28}$$

This value should (λ) be unchanged since the UNIT for 1 m is unchanged. However, in Equation (13), the Planck constant is changed. Therefore, the UNIT for the mass of one electron and one proton should be redefined.

$$m_{e\_\mathrm{new}}=\frac{4.48852}{4.5}\times\frac{\pi}{3.13201}\times m_e=9.11394E-31(\mathrm{kg}) \tag{29}$$

$$m_{p\_\mathrm{new}}=\frac{4.48852}{4.5}\times\frac{\pi}{3.13201}\times m_p=1.67346E-27(\mathrm{kg}) \tag{30}$$

Next, we must ensure that the following equation is satisfied.

$$\frac{m_{p\_\mathrm{new}}}{m_{e\_\mathrm{new}}}=\frac{1.67346E-27}{9.11394E-31}=1836.152654=\frac{m_p}{m_e} \tag{31}$$

4.4. Redefinitions of Equations (8) and (9)

Equations (8) and (9) can be redefined as follows.

$$\begin{aligned}\frac{\left(\frac{m_p}{m_e}+\frac{4}{3}\right)\times m_{e\_\mathrm{new}}c^2}{e_{\mathrm{new}}c}&=3.13201(\mathrm{V}\cdot\mathrm{m})\times\frac{4.5}{4.48852}\times\frac{4.48852}{4.5}\times\frac{\pi}{3.13201}\\&=\pi(\mathrm{V}\cdot\mathrm{m})\end{aligned} \tag{32}$$

$$\begin{aligned}\frac{q_{m\_\mathrm{new}}c}{\left(\frac{m_p}{m_e}+\frac{4}{3}\right)m_{p\_\mathrm{new}}c^2}&=4.48852\left(\frac{1}{\mathrm{A}\cdot\mathrm{m}}\right)\times\frac{\pi}{3.13201}\times\frac{4.5}{4.48852}\times\frac{3.13201}{\pi}\\&=4.5\left(\frac{1}{\mathrm{A}\cdot\mathrm{m}}\right)\end{aligned} \tag{33}$$

Using Equations (32) and (33), Equations (34) and (35) can be obtained.

$$\frac{\left(\frac{m_p}{m_e}+\frac{4}{3}\right)\times m_{e\_\mathrm{new}}c^2}{e_{\mathrm{new}}c}\times\frac{q_{m\_\mathrm{new}}c}{\left(\frac{m_p}{m_e}+\frac{4}{3}\right)m_{p\_\mathrm{new}}c^2} = \frac{m_{e\_\mathrm{new}}}{e_{\mathrm{new}}}\times\frac{q_{m\_\mathrm{new}}}{m_{p\_\mathrm{new}}} = 4.5\times\pi\left(\frac{\mathrm{V\cdot m}}{\mathrm{A\cdot m}}=\Omega\right) \tag{34}$$

$$\frac{\frac{q_{m\_\mathrm{new}}c}{\left(\frac{m_p}{m_e}+\frac{4}{3}\right)m_{p\_\mathrm{new}}c^2}}{\frac{\left(\frac{m_p}{m_e}+\frac{4}{3}\right)\times m_{e\_\mathrm{new}}c^2}{e_{\mathrm{new}}c}} = \frac{h_{\mathrm{new}}c^2}{\left(\frac{m_p}{m_e}+\frac{4}{3}\right)^2\times m_{e\_\mathrm{new}}c^2\times m_{p\_\mathrm{new}}c^2} = \frac{4.5}{\pi}\left(\frac{1}{\mathrm{A\cdot m}\times\mathrm{V\cdot m}}=\frac{\mathrm{s}}{\mathrm{J}\times\mathrm{m}^2}\right) \tag{35}$$

5. Results

5.1. Explanation for the Necessity of Using the Values of 4.5 and π

When we define the Avogadro's number (N_A) and the Faraday constant (F) as follows,

$$N_A = \frac{1\,\mathrm{g}}{m_p} = 5.97565E+23 \approx 6.02214076E+23 \tag{A}$$

$$F = e\times N_A = 9.57405E+04 \approx 9.6485E+04 \tag{B}$$

The redefined Avogadro's number(N_A) and the refined Faraday constant (F) are as follows,

$$N_{A\_\mathrm{new}} = \frac{1\,\mathrm{g}}{m_{p\_\mathrm{new}}} = \frac{1\,\mathrm{g}}{m_p}\times\frac{4.5}{4.48852}\times\frac{3.13201}{\pi} \tag{C}$$

$$F_{\mathrm{new}} = e_{\mathrm{new}}\times N_{A\_\mathrm{new}} = \frac{1\,\mathrm{g}}{m_p}\times\frac{3.13201}{\pi} \tag{D}$$

Next, we can define 1 J freely. Using arbitrary number (a), N_5 and N_6 can be calculated as follows.

$$N_5 = \frac{a\times 1\,\mathrm{J}}{\left(\frac{m_p}{m_e}+\frac{4}{3}\right)m_{e\_\mathrm{new}}c^2}\left(\frac{\mathrm{s}}{\mathrm{m}^2}\right) = a\times 6.64398E+09\left(\frac{\mathrm{s}}{\mathrm{m}^2}\right) \tag{36}$$

$$N_6 = \frac{a\times 1\,\mathrm{J}}{e_{\_\mathrm{new}}c}\left(\frac{\mathrm{J}}{\mathrm{A\cdot m}}\right) = a\times 2.08726E+10\left(\frac{\mathrm{J}}{\mathrm{A\cdot m}}\right) \tag{37}$$

$$\frac{N_6}{N_5} = \frac{2.08726E+10}{6.64398E+09}\left(\frac{\mathrm{J}}{\mathrm{A\cdot m}}\times\frac{\mathrm{m}^2}{\mathrm{s}}=\frac{\mathrm{J\cdot m}}{\mathrm{C}}=\mathrm{V\cdot m}\right) = \pi\left(\mathrm{V\cdot m}\right) \tag{38}$$

The ratio should be π V·m and constant. Next,

$$N_7 = \frac{a \times 1\,\mathrm{J}}{\left(\frac{m_p}{m_e} + \frac{4}{3}\right) m_{p\_\mathrm{new}} c^2} \left(\frac{\mathrm{s}}{\mathrm{m}^2}\right) = a \times 3.61843E+06 \left(\frac{\mathrm{s}}{\mathrm{m}^2}\right) \tag{39}$$

$$N_8 = \frac{a \times 1\,\mathrm{J}}{q_{m\_\mathrm{new}} c} \left(\frac{\mathrm{J}}{\mathrm{Wb} \cdot \mathrm{m/s}} = \frac{\mathrm{J} \cdot \mathrm{s}}{\mathrm{Wb} \cdot \mathrm{m}} = \frac{\mathrm{C}}{\mathrm{m}}\right) = a \times 8.04095E+05 \left(\frac{\mathrm{C}}{\mathrm{m}}\right) \tag{40}$$

$$\frac{N_7}{N_8} = \frac{3.61843E+06}{8.04095E+05} = 4.5 \left(\frac{\mathrm{s}}{\mathrm{m}^2} \times \frac{\mathrm{m}}{\mathrm{C}} = \frac{1}{\mathrm{A} \cdot \mathrm{m}}\right) \tag{41}$$

The ratio should be 4.5 and π are constant. Consequently, we can explain the necessity for the values of 4.5 and π in Equations (8) and (9).

5.2. Explanation for the Necessity of Using the Values of 4.5 and π in Equations (1)-(3)

5.2.1. Our Main Three Equations

Equations (1)-(3) are our main three equations. Then, the unit (V·m and 1/A·m) should be replaced. Alternatively, the redefinition of V·m and 1/A·m is needed in the equations.

$$\frac{G m_p^2}{hc} = \frac{4.48852}{2} \frac{kT_c}{1\,\mathrm{kg} \times c^2} \times (\mathrm{A} \cdot \mathrm{m}) \tag{42}$$

$$\frac{G m_p^2}{\left(\frac{e^2}{4\pi\varepsilon_0}\right)} = \frac{4.48852}{2 \times 3.13201} \times \frac{m_e}{e} \times hc \times \left(\mathrm{A} \cdot \mathrm{m} \times \mathrm{V} \cdot \mathrm{m} \times \frac{1}{\mathrm{V} \cdot \mathrm{m}} \times \frac{1}{\mathrm{kg}} = \mathrm{A} \cdot \mathrm{m} \times \frac{1}{\mathrm{kg}}\right) \tag{43}$$

$$\frac{m_e c^2}{e} \times \left(\frac{e^2}{4\pi\varepsilon_0}\right) = 3.13201 \times kT_c \times \left(\frac{1}{\mathrm{V} \cdot \mathrm{m}} \times \mathrm{V} \cdot \mathrm{m} = 1\right) \tag{44}$$

5.2.2. Our Fourth Equation

Our fourth equation can be derived as follows. From Equation (43),

$$\frac{G m_p^2}{\left(\frac{e^2}{4\pi\varepsilon_0}\right)^2} = \frac{4.48852}{2 \times 3.13201} \times \frac{m_e}{e} \times \frac{2\pi}{\alpha} \times \left(\mathrm{A} \cdot \mathrm{m} \times \frac{1}{\mathrm{kg}}\right) \tag{45}$$

From Equation (44),

$$\frac{e^2}{4\pi\varepsilon_0} = 3.13201 \times kT_c \times \frac{e}{m_e c^2} \tag{46}$$

From Equations (45) and (46),

$$\frac{G m_p^2}{\left(3.13201 \times kT_c \times \frac{e}{m_e c^2}\right)^2} = \frac{4.48852}{2 \times 3.13201} \times \frac{m_e}{e} \times \frac{2\pi}{\alpha} \times \left(\mathrm{A} \cdot \mathrm{m} \times \frac{1}{\mathrm{kg}}\right) \tag{47}$$

Therefore,

$$\frac{G m_p^2}{(kT_c)^2} = 4.48852 \times 3.13201 \times \frac{e}{m_e c^4} \times \frac{\pi}{\alpha} \times \left(\mathrm{A} \cdot \mathrm{m} \times \frac{1}{\mathrm{kg}}\right) \tag{48}$$

Here,

$$4.48852\times 3.13201(\Omega)=\frac{q_m}{e}\times\frac{m_e}{m_p}(\Omega) \tag{49}$$

In Equation (48), the unit of Ω is already considered. Therefore,

$$Gm_p^2=\frac{q_m}{m_p c^4}\times\frac{\pi}{\alpha}\times(kT_c)^2\times\left(\mathrm{A\cdot m}\times\frac{1}{\mathrm{kg}}\right) \tag{50}$$

Equation (50) is our fourth equation.

5.2.3. Redefinition for Equation (42)

We define G free from 1 kg (G_N) as follows.

$$G_N=G\times 1\,\mathrm{kg} \tag{51}$$

The UNIT for G_N is $\mathrm{m^3\cdot s^{-2}}$. By our redefinition method, the UNITs for 1 m and 1 s are unchanged. However, when G_N is a function of C or Wb, G_N should be changed.

$$G_{N\_new}\neq G_N \tag{52}$$

From Equations (42) and (51),

$$\frac{G_N m_p^2}{hc}=\frac{4.4885}{2}\frac{kT_c}{c^2}\times(\mathrm{A\cdot m}) \tag{53}$$

Therefore,

$$\frac{G_N m_{p\_\mathrm{new}}^2\times\left(\frac{4.5}{4.48852}\times\frac{3.13201}{\pi}\right)^2}{h_{\mathrm{new}}\times\frac{4.5}{4.48852}\times\frac{3.13201}{\pi}c}=\frac{4.48852}{2}\frac{kT_c}{c^2}\times\mathrm{A\cdot m} \tag{54}$$

Therefore,

$$\frac{G_N m_{p\_\mathrm{new}}^2}{h_{\mathrm{new}}c}=\frac{4.5}{2}\times\left(\frac{4.48852}{4.5}\right)^2\times\frac{\pi}{3.13201}\times\frac{kT_c}{c^2}\times(\mathrm{A\cdot m}) \tag{55}$$

Next, using G_{N_new} and kT_{c_new}, we proposed the following equation, which is the same formula as Equation (1). Then, the unit of 4.5 is 1/A·m in Equation (9).

$$\frac{G_{N\_\mathrm{new}}m_{p\_\mathrm{new}}^2}{h_{\mathrm{new}}c}=\frac{4.5}{2}\times\frac{kT_{c\_\mathrm{new}}}{c^2}\times(\mathrm{A\cdot m})_{\mathrm{new}} \tag{56}$$

Therefore,

$$\frac{G_{N\_\mathrm{new}}}{G_N}=\left(\frac{4.5}{4.48852}\right)^2\times\frac{3.13201}{\pi}\times\frac{kT_{c\_\mathrm{new}}}{kT}\times\frac{(\mathrm{A\cdot m})_{\mathrm{new}}}{\mathrm{A\cdot m}} \tag{57}$$

5.2.4. Redefinition of Equation (43)

Using G_N, Equation (43) is rewritten as follows.

$$\frac{G_N m_p^2}{\left(\frac{e^2}{4\pi\varepsilon_0}\right)}=\frac{4.48852}{2\times 3.13201}\times\frac{m_e}{e}\times hc\times(\mathrm{A\cdot m}) \tag{58}$$

Therefore,

$$G_N m_{p\_\text{new}}^2 = \frac{m_{e\_\text{new}} e_{\text{new}} h_{\text{new}} c}{4\pi\varepsilon_{0\_\text{new}}} \times \frac{4.48852}{2\times 3.13201} \times \frac{4.5}{4.48852} \times \frac{4.48852}{4.5} \times \frac{3.13201}{\pi} \times (\text{A}\cdot\text{m}) \tag{59}$$

Using G_{N_new} and $\text{A}\cdot\text{m}_{\text{new}}$, we propose the following equation, which is the same formula as Equation (2).

$$\frac{G_{N\_\text{new}} m_{p\_\text{new}}^2}{\left(\frac{e^2}{4\pi\varepsilon_0}\right)_{\text{new}}} = \frac{4.5}{2\times\pi} \times \frac{m_{e\_\text{new}}}{e_{\_\text{new}}} \times h_{\_\text{new}} c \times (\text{A}\cdot\text{m})_{\text{new}} \tag{60}$$

Therefore,

$$\frac{G_{N\_\text{new}}}{G_N} = \frac{4.5}{4.48852} \times \frac{(\text{A}\cdot\text{m})_{\text{new}}}{\text{A}\cdot\text{m}} \tag{61}$$

5.2.5. Redefinition of Equation (44)

Equation (44) is rewritten as follows.

$$\frac{m_e c^2}{e} \times \left(\frac{e^2}{4\pi\varepsilon_0}\right) = 3.13201 \times kT_c \tag{62}$$

Therefore,

$$\frac{m_{e\_\text{new}} c^2}{e_{\text{new}}} \times \frac{e_{\text{new}}^2}{4\pi\varepsilon_{0\_\text{new}}} \times \frac{4.5}{4.48852} \times \frac{3.13201}{\pi} = \pi \times kT_c \tag{63}$$

Next, using kT_{c_new}, we propose the following Equation, which is the same formula as Equation (3).

$$\frac{m_{e\_\text{new}} c^2}{e_{\text{new}}} \times \frac{e_{\text{new}}^2}{4\pi\varepsilon_{0\_\text{new}}} = \pi \times kT_{c\_\text{new}} \tag{64}$$

Therefore,

$$\frac{kT_{c\_\text{new}}}{kT_c} = \frac{4.48852}{4.5} \times \frac{\pi}{3.13201} \tag{65}$$

5.2.6. Redefinition of Equation (50)

Using G_N, Equation (50) is rewritten as follows.

$$G_N m_p^2 = \frac{q_m}{m_p c^4} \times \frac{\pi}{\alpha} \times (kT_c)^2 \times (\text{A}\cdot\text{m}) \tag{66}$$

Therefore,

$$G_N = \frac{q_{m\_\text{new}}}{m_{p\_\text{new}}^3} \times \frac{\pi}{\alpha} \times \frac{(kT_c)^2}{c^4} \times \left(\frac{4.48852}{4.5}\right)^3 \times \left(\frac{\pi}{3.13201}\right)^2 \times (\text{A}\cdot\text{m}) \tag{67}$$

Next, using G_{N_new}, kT_{c_new} and $\text{A}\cdot\text{m}_{\text{new}}$, we propose the following equation.

$$G_{N\_\text{new}} = \frac{q_{m\_\text{new}}}{m_{p\_\text{new}}^3} \times \frac{\pi}{\alpha} \times \frac{(kT_{c\_\text{new}})^2}{c^4} \times (\text{A}\cdot\text{m})_{\text{new}} \tag{68}$$

Therefore,

$$\frac{G_{N\_new}}{G_N}=\left(\frac{4.5}{4.48852}\right)^3\times\left(\frac{3.13201}{\pi}\right)\times\left(\frac{kT_{c\_new}}{kT_c}\right)^2\times\frac{(\mathrm{A\cdot m})_{new}}{\mathrm{A\cdot m}} \tag{69}$$

5.2.7. Redefinition of kT_c and Vm

Equations (57), (61), (65) and (69) are rewritten as follows.

$$\frac{G_{N\_new}}{G_N}=\left(\frac{4.5}{4.48852}\right)^2\times\frac{3.13201}{\pi}\times\frac{kT_{c\_new}}{kT}\times\frac{(\mathrm{A\cdot m})_{new}}{\mathrm{A\cdot m}} \tag{70}$$

$$\frac{G_{N\_new}}{G_N}=\frac{4.5}{4.48852}\times\frac{(\mathrm{A\cdot m})_{new}}{\mathrm{A\cdot m}} \tag{71}$$

$$\frac{kT_{c\_new}}{kT_c}=\frac{4.48852}{4.5}\times\frac{\pi}{3.13201} \tag{72}$$

$$\frac{G_{N\_new}}{G_N}=\left(\frac{4.5}{4.48852}\right)^3\times\left(\frac{3.13201}{\pi}\right)\times\left(\frac{kT_{c\_new}}{kT_c}\right)^2\times\frac{(\mathrm{A\cdot m})_{new}}{\mathrm{A\cdot m}} \tag{73}$$

In Equation (72), kT_c is redefined and determined. Next,

$$\frac{(\mathrm{A\cdot m})_{new}}{\mathrm{A\cdot m}}=\frac{(\mathrm{C\times m/s})_{new}}{\mathrm{C\times m/s}}=\frac{\mathrm{C}_{new}}{\mathrm{C}}=\frac{4.48852}{4.5} \tag{74}$$

From Equations (71) and (74),

$$\frac{G_{N\_new}}{G_N}=1 \tag{75}$$

Then, Equations (70) and (73) can be explained. In Equation (72), redefinition of $kT_c$is from redefinition of the mass of the particle as follows:

$$\frac{kT_{c\_new}}{kT}=\frac{4.48852}{4.5}\times\frac{\pi}{3.13201}=\frac{m_{e\_new}}{m_e} \tag{76}$$

However, the unit Am remains in the three equations. We proposed the following unit. We will explain the unit ($G_{N/Am}$) in a future report, which maybe different from the standard approach for G and thermodynamics [9].

$$\frac{G_{N/Am\_new}}{G_{N/Am}}=\frac{\left(G\times\frac{1\,\mathrm{kg}}{\mathrm{A\cdot m}}\right)_{new}}{G\times\frac{1\,\mathrm{kg}}{\mathrm{A\cdot m}}}=\frac{\left(\frac{G_N}{\mathrm{A\cdot m}}\right)_{new}}{\frac{G_N}{\mathrm{A\cdot m}}}=\frac{4.5}{4.48852} \tag{77}$$

5.2.8. Making Sure for the Calculation

Equation (56) is rewritten as follows:

$$\frac{G_{N/Am\_new}m_{p\_new}^2}{h_{new}c}=\frac{4.5}{2}\times\frac{kT_{c\_new}}{c^2}=9.4279464618E-40 \tag{78}$$

Equation (60) is rewritten as follows:

$$\frac{G_{N/Am\_new}m_{p\_new}^2}{\left(\frac{e^2}{4\pi\varepsilon_0}\right)_{new}}=\frac{4.5}{2\times\pi}\times\frac{m_{e\_new}}{e_{\_new}}\times h_{\_new}c=8.1176747490E-37 \tag{79}$$

Equation (64) is rewritten as follows:

$$\frac{m_{e\_\mathrm{new}}c^2}{e_{\mathrm{new}}}\times\frac{e_{\mathrm{new}}^2}{4\pi\varepsilon_{0\_\mathrm{new}}}=\pi\times kT_{c\_\mathrm{new}}=1.18311202E-22 \tag{80}$$

Equation (68) is rewritten as follows:

$$G_{N/Am\_\mathrm{new}}=\frac{q_{m\_\mathrm{new}}}{m_{p\_\mathrm{new}}^3}\times\frac{\pi}{\alpha}\times\frac{\left(kT_{c\_\mathrm{new}}\right)^2}{c^4}=6.6908477020E-11 \tag{81}$$

Consequently, our four equations can be redefined successfully.

5.2.9. The Other Equations

From Equation (8),

$$3.132011447\left(\mathrm{V}\cdot\mathrm{m}\right)=\frac{\left(\frac{m_p}{m_e}+\frac{4}{3}\right)m_ec^2}{ec}\left(\frac{\mathrm{m}^2}{\mathrm{s}}\times\frac{\mathrm{J}}{\mathrm{A}\cdot\mathrm{m}}=\frac{\mathrm{J}\cdot\mathrm{m}}{\mathrm{C}}=\mathrm{V}\cdot\mathrm{m}\right) \tag{82}$$

From Equation (44),

$$\frac{m_ec^2\times ec}{4\pi\varepsilon_0c}=3.132011447\left(\mathrm{V}\cdot\mathrm{m}\right)\times kT_c \tag{83}$$

In Equation (83), there are no dimension mismatch problems. From Equations (81) and (82),

$$\frac{m_ec^2\times ec}{4\pi\varepsilon_0c}=\frac{\left(\frac{m_p}{m_e}+\frac{4}{3}\right)m_ec^2}{ec}\times kT_c \tag{84}$$

Therefore,

$$\frac{kT_c}{\frac{e^2c}{4\pi\varepsilon_0}}=\frac{1}{\left(\frac{m_p}{m_e}+\frac{4}{3}\right)}\left(\frac{\mathrm{s}}{\mathrm{m}^2}\right)=\frac{1}{1837.485988}\left(\frac{\mathrm{s}}{\mathrm{m}^2}\right) \tag{85}$$

Therefore,

$$\left(\frac{kT_c}{\frac{e^2c}{4\pi\varepsilon_0}}\right)_{\mathrm{new}}\frac{1}{1837.485988}\left(\frac{\mathrm{s}}{\mathrm{m}^2}\right)=\frac{1}{\left(\frac{m_p}{m_e}+\frac{4}{3}\right)}\left(\frac{\mathrm{s}}{\mathrm{m}^2}\right) \tag{86}$$

Consequently, Equation (85) can be successfully redefined. Therefore,

$$\left(\frac{kT_c}{hc^2}\right)_{\mathrm{new}}=\frac{1}{6.3206454E-07}=\frac{1}{\left(\frac{m_p}{m_e}+\frac{4}{3}\right)}\times\frac{\alpha}{2\pi} \tag{87}$$

Furthermore, Equation (87) can also be redefined.

6. Conclusions

In this report, using the redefinition method for the UNIT, we showed the necessity for our empirical equations. The redefinition method was explained in

detail. Then, we proposed four empirical equations.

$$\frac{G_{N/Am\_new}m_{p\_new}^2}{h_{new}c}=\frac{4.5}{2}\left(\frac{1}{\mathrm{A\cdot m}}\right)\times\frac{kT_{c\_new}}{c^2}=9.4279464618E-40 \tag{88}$$

where $G_{N/Am}=G\times 1\ \mathrm{kg/A\cdot m}$

$$\frac{G_{N/Am\_new}m_{p\_new}^2}{\left(\frac{e^2}{4\pi\varepsilon_0}\right)_{new}}=\frac{4.5}{2\times\pi}\left(\frac{1}{\mathrm{A\cdot m\times V\cdot m}}\right)\times\frac{m_{e\_new}}{e_{\_new}}\times h_{\_new}c=8.1176747490E-37 \tag{89}$$

$$\frac{m_{e\_new}c^2}{e_{new}}\times\frac{e_{new}^2}{4\pi\varepsilon_{0\_new}}=\pi\left(\mathrm{V\cdot m}\right)\times kT_{c\_new}=1.18311202E-22 \tag{90}$$

$$G_{N/Am\_new}=\frac{q_{m\_new}}{m_{p\_new}^3}\times\frac{\pi\left(\mathrm{V\cdot m}\right)}{\alpha}\times\frac{\left(kT_{c\_new}\right)^2}{c^4}=6.6908477020E-11 \tag{91}$$

Furthermore, we derived four important equations.

$$\frac{m_{e\_new}}{e_{new}}\times\frac{q_{m\_new}}{m_{p\_new}}=4.5\times\pi\left(\frac{\mathrm{V\cdot m}}{\mathrm{A\cdot m}}=\Omega\right) \tag{92}$$

$$\frac{h_{new}c^2}{\left(\frac{m_p}{m_e}+\frac{4}{3}\right)^2\times m_{e\_new}c^2\times m_{p\_new}c^2}=\frac{4.5}{\pi}\left(\frac{1}{\mathrm{A\cdot m\times V\cdot m}}=\frac{\mathrm{s}}{\mathrm{J\times m^2}}\right) \tag{93}$$

$$\frac{kT_c}{\frac{e^2c}{4\pi\varepsilon_0}}=\frac{1}{1837.485988}\left(\frac{\mathrm{s}^2}{\mathrm{m}}\right)=\frac{1}{\left(\frac{m_p}{m_e}+\frac{4}{3}\right)}\left(\frac{\mathrm{s}^2}{\mathrm{m}}\right) \tag{94}$$

$$\left(\frac{kT_c}{hc^2}\right)_{new}=\frac{1}{6.3206454E-07}=\frac{1}{\left(\frac{m_p}{m_e}+\frac{4}{3}\right)}\times\frac{\alpha}{2\pi}\left(\frac{\mathrm{s}^2}{\mathrm{m}}\right) \tag{95}$$

About numerical connections considering the units, our redefinition is perfect, in which there are not any dimension mismatch problems. About the unit ($G_{N/Am}$), we will explain in the future report.

Conflicts of Interest

The author declares no conflicts of interest regarding the publication of this paper.

References

[1] Miyashita, T. (2020) *Journal of Modern Physics*, **11**, 1180-1192. https://doi.org/10.4236/jmp.2020.118074

[2] Miyashita, T. (2021) *Journal of Modern Physics*, **12**, 623-634. https://doi.org/10.4236/jmp.2021.125040

[3] Miyashita, T. (2021) *Journal of Modern Physics*, **12**, 859-869. https://doi.org/10.4236/jmp.2021.127054

[4] Miyashita, T. (2020) *Journal of Modern Physics*, **11**, 1159. https://doi.org/10.4236/jmp.2020.118074

[5] Miyashita, T. (2021) *Journal of Modern Physics*, **12**, 1160-1161. https://doi.org/10.4236/jmp.2021.128069

[6] Miyashita, T. (2022) *Journal of Modern Physics*, **13**, 336-346. https://doi.org/10.4236/jmp.2022.134024

[7] Miyashita, T. (2018) *Journal of Modern Physics*, **9**, 2346-2353. https://doi.org/10.4236/jmp.2018.913149

[8] Miyashita, T. (2023) *Journal of Modern Physics*, **14**, 160-170. https://doi.org/10.4236/jmp.2023.142011

[9] Jacobson, T. (1995) *Physical Review Letters*, **75**, 1260-1263. https://doi.org/10.1103/PhysRevLett.75.1260

Scientific Research Publishing

Journal of Modern Physics, 2023, 14, 445-449
https://www.scirp.org/journal/jmp
ISSN Online: 2153-120X
ISSN Print: 2153-1196

On the Superconductivity in High-Entropy Alloy $(NbTa)_{1-x}(HfZrTi)_x$

Snehadri B. Ota

Government of India, New Delhi, India
Email: snehadri@hotmail.com

How to cite this paper: Ota, S.B. (2023) On the Superconductivity in High-Entropy Alloy $(NbTa)_{1-x}(HfZrTi)_x$. *Journal of Modern Physics*, **14**, 445-449.
https://doi.org/10.4236/jmp.2023.144025

Received: December 24, 2022
Accepted: March 18, 2023
Published: March 21, 2023

Abstract

The superconductivity in $(NbTa)_{1-x}(HfZrTi)_x$ high-entropy alloy is analyzed using the theory of strong-coupled superconductor. It is concluded that $(NbTa)_{1-x}(HfZrTi)_x$ is a strong coupled superconductor. The variation in the superconducting transition temperature from 7.9 K to 4.6 K as x increases from 0.2 to 0.84 arises because of the decrease in electronic band width due to localization and broadening of the band. It is suggested that the decrease in electronic band width is due to crystalline randomness which gives rise to the mobility edge.

Keywords

High-Entropy Alloys, Disordered Metals, Strong-Coupled Superconductivity, Localization, Cocktail Effect

1. Introduction

The high-entropy alloys (HEA) have attracted considerable attention in recent years [1] [2]. These alloys consist of several principal elements that are stabilized due to high configurational entropy. The atoms in HEA are randomly distributed on ordered lattice as has been inferred from the sharp X-ray diffraction peaks. Distortion of the lattice of the order of 1 percent has also been concluded from theoretical calculations [3]. These alloys show better mechanical properties and superparamagnetism. Recently, superconductivity has been observed in transition metal based HEA $(Nb_{0.33}Ta_{0.34})_{1-x}(Hf_{0.08}Zr_{0.14}Ti_{0.11})_x$, which has bcc lattice structure [4] [5] [6] [7]. (Hereafter, we replace $(Nb_{0.33}Ta_{0.34})_{1-x}(Hf_{0.08}Zr_{0.14}Ti_{0.11})_x$ by $(NbTa)_{1-x}(HfZrTi)_x$, for simplicity.) The superconducting transition temperature (T_C) has been found to vary from 7.9 K to 4.6 K as the atomic fraction x increases from 0.2 to 0.84. The elements Nb, Ta, Hf, Zr and Ti have T_C s; 9.5 K, 4.5 K, 0.1 K, 0.5 K and 0.4 K, respectively, which ranges from 0.1 K to 9.5 K [8]. One

important observation is the "cocktail-effect" which refers to the enhancement of T_C beyond the simple mixture of those of constituent elements [7]. The occurrence of superconductivity is often considered empirically using the variation of T_C as a function of number of outer electrons/atom (e/a) [5] (aka Matthias rule). The variation of T_C with e/a in this HEA falls between that of crystalline and amorphous transition metals and alloys. A maximum of T_C occurs for e/a = 4.7 which is within the range of values of e/a (4.3 to 5.0) for the crystalline system. In this paper, the superconductivity in $(NbTa)_{1-X}(HfZrTi)_X$ HEA is explained using the theory of strong-coupled superconductors [9].

2. Superconductivity in $(NbTa)_{1-X}(HfZrTi)_X$ HEA

The effect of disorder on superconductivity has been studied before, for example, the universal degradation of T_C in A15 compounds ([10] and the references in [10]). Here, the effect of disorder in $(NbTa)_{1-X}(HfZrTi)_X$ HEA is explained in terms of localization of electronic states [11]. The randomness of transition metal atoms in the lattice positions of $(NbTa)_{1-X}(HfZrTi)_X$ is expected to affect the electronic band structure. In this regard, localization of electronic states can occur when the electronic band width (U) is comparable to the distribution width (W) of the site energy. The site energy can be taken to be the first ionization energy of the constituent atoms. The first ionization energies of Nb, Ta, Hf, Zr and Ti are 6.77 eV, 7.88 eV, 7 eV, 6.95 eV and 6.83 eV, respectively, which ranges from 6.77 eV to 7.88 eV [8] and therefore, W in this alloy is of the order of eV. Since the typical width of d-band is of the order of eV [12], one expects localization of electronic states, as U~W. Next, one can examine what can be concluded from the Ioffe-Regel criterion, which states that electronic states can be localized for $kl < 1$ and are extended, otherwise [13]. Here, k and l are wave vector and mean-free path, respectively, of the electron in the solid. The mean-free path in this HEA is of the order of 10^{-7} cm [6] and from the Ioffe-Regel criterion one obtains $k < 10^7$ cm^{-1}, which is fairly low compared to the typical value of k_F in metals (~10^8 cm^{-1}) [8]. Localization can give rise to mobility edges of electronic band. In addition, disorder can also broaden the width of the d-band density of states.

Approximate solutions of the Gor'kov-Eliashberg form of the theory of strong-coupled superconductors has been of interest for a long time [9]. First, the T_C of $(NbTa)_{1-X}(HfZrTi)_X$ HEA, is examined with some redundancy in the weak coupling limit [14]. **Table 1** gives various parameters relevant for the superconductivity in this HEA. The Debye temperature (Θ_D) in **Table 1** for x = 0.3 is from [5]. For other compositions of this HEA in **Table 1**, Θ_D is calculated from the well known proportionality: $\Theta_D \propto 1/\sqrt{M}$, where M is the molecular weight. T_C s of the HEA in **Table 1** are obtained from Figure 3 of [5]. In the weak-coupling limit T_C is given as follows [14]:

$$T_C = 1.14 \cdot \Theta_D \cdot \exp\left(\frac{-1}{N(0)V}\right) \tag{1}$$

Table 1. Measured and calculated values of T_C, M, Θ_D and N(0)V for $(Nb_{0.33}Ta_{0.34})_{1-X}(Hf_{0.08}Zr_{0.14}Ti_{0.11})_X$ HEA.

HEA alloy	x	T_C (K)	M	Θ_D (K)	N(0)V
$(TaNb)_{0.80}(ZrHfTi)_{0.20}$	0.20	7.6	129.7	220.5	0.286
$(TaNb)_{0.75}(ZrHfTi)_{0.25}$	0.25	7.9	127.7	222.2	0.288
$(TaNb)_{0.70}(ZrHfTi)_{0.30}$	0.30	7.9	125.7	223.9	0.288
$(TaNb)_{0.67}(ZrHfTi)_{0.33}$	0.33	7.8	124.5	225.0	0.286
$(TaNb)_{0.65}(ZrHfTi)_{0.35}$	0.35	7.5	123.7	225.7	0.283
$(TaNb)_{0.60}(ZrHfTi)_{0.40}$	0.40	7.2	121.7	227.6	0.279
$(TaNb)_{0.55}(ZrHfTi)_{0.45}$	0.45	6.7	119.7	229.4	0.273
$(TaNb)_{0.50}(ZrHfTi)_{0.50}$	0.50	6.4	117.8	231.3	0.269
$(TaNb)_{0.40}(ZrHfTi)_{0.60}$	0.60	6.2	113.8	235.3	0.265
$(TaNb)_{0.30}(ZrHfTi)_{0.70}$	0.70	5.3	109.8	239.6	0.254
$(TaNb)_{0.20}(ZrHfTi)_{0.80}$	0.80	4.6	105.9	244.0	0.244
$(TaNb)_{0.16}(ZrHfTi)_{0.84}$	0.84	4.6	104.3	245.8	0.243

where, N(0)V is a dimensionless electron-phonon coupling constant. It is noted that in the weak-coupling limit the frequency dependence of the interaction is ignored. The calculated values of N(0)V using Equation (1) are given in Table 1, which are nearly 0.3. N(0)V is found to increase with x until x = 0.3 and then decreases with further increase in x. The decrease of N(0)V with increase of x can be attributed primarily due to the reduction of N(0).

The theory of strong-coupled superconductors includes frequency dependences of phonon-induced interaction and instantaneous Coulomb repulsion. In order to understand the influence of Coulomb interaction on the phonon induced interaction, the strong-coupling case is considered. In the strong-coupling case, T_C is obtained as a function of electron-phonon and electron-electron coupling constants, which is given by (aka McMillan equation) [15]:

$$T_C = \frac{\Theta_D}{1.45} \cdot \exp\left(\frac{-1.04(1+\lambda)}{\lambda - \mu^*(1+0.62\lambda)}\right) \tag{2}$$

where λ is the electron-phonon coupling constant and μ^* is the Coulomb pseudopotential. The Coulomb pseudopotential is given by [14]:

$$\mu^* = \frac{\mu}{1+\mu\ln\frac{E_B}{\omega_0}} \tag{3}$$

where E_B and ω_0 are cutoffs of instantaneous Coulomb repulsion and phonon induced interactions, respectively. Since Θ_D is known (Table 1) and there are two unknown parameters in the exponential of Equation (2), λ is taken from the weak-coupling limit. Using Equation (2) and Equation (3) and taking ω_0 as that corresponding to the Debye temperature, the e/a dependence of E_B is obtained, which is shown in Figure 1.

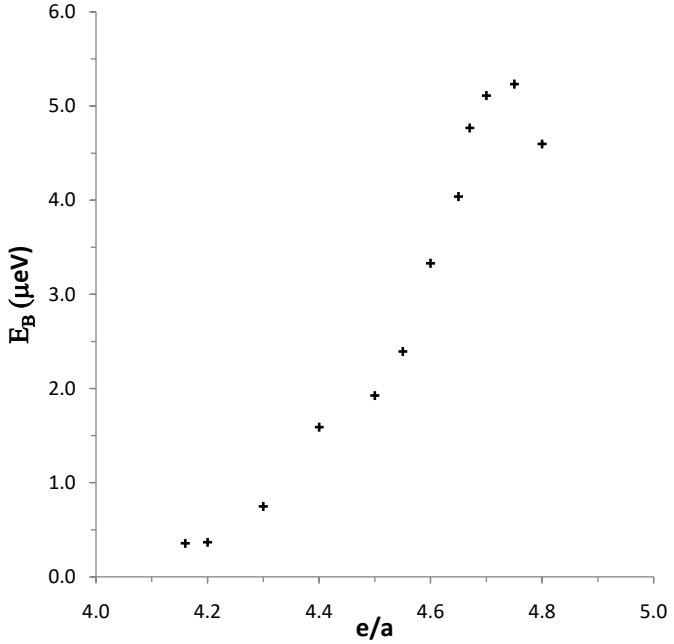

Figure-1. E_B as a function of (e/a) in superconducting $(Nb_{0.33}Ta_{0.34})_{1-X}(Hf_{0.08}Zr_{0.14}Ti_{0.11})_X$ HEA. e/a decreases from 4.8 to 4.16 as x increases from 0.2 to 0.84.

3. Discussion and Conclusions

It is seen that E_B is of the order of μeV, which is considerably smaller than ω_0. The small value of E_B can be attributed to the formation of mobility edge. The peak in **Figure 1** can be due to initial broadening of the electronic band and with the increase of x beyond 0.3, E_B reduces due to localization of electronic states. The nearly temperature independent high resistivity (~50 μΩ·cm) which is nearly 0.2 times the resistivity saturation value (~ 250 μΩ·cm) [16] also supports this conclusion. This occurs since the energy range for scattering is limited by E_B rather than kT. Enhancement of T_C is also expected in the approximate solution to the theory when $E_B \ll \omega_0$, which accounts for the cocktail effect in this HEA [7]. Superconductivity has been studied in (NbTaTiZr)-based HEA with the addition of Hf, Fe, Ge, Si and V [6]. The ionization energies of Hf, Fe, Ge, Si and V are comparable to that of Nb, Ta, Ti and Zr. The ionization energy of La is 5.61 eV, which is considerably smaller than Nb (6.77 eV). It is therefore, suggested that metal to insulator transition can occur in $(NbTa)_{1-X}(HfZrTi)_X$ HEA by the replacement of Hf with La, which increases the distribution width W.

In conclusion, the experimental results on superconductivity in $(NbTa)_{1-X}(HfZrTi)_X$ have been analyzed using the Gor'kov-Eliashberg form of the theory for strong-coupled superconductors. The variation in the superconducting transition temperature from 7.9 K to 4.6 K as x increases from 0.2 to 0.84 is explained in terms of decrease in electronic band width due to localization and broadening of the band. The formation of the mobility edge is found to reduce the effective band width in these alloys. The cocktail effect in this HEA is

explained in terms of the enhancement of T_C, when $E_B \ll \omega_0$.

Acknowledgements

The author is benefited from his visit to Europe in 1988-92 for HTSC research; Xiamen, China, during 1995 for STATPHYS19 conference and New Orleans and Dallas, USA during 2008 and 2011, respectively, for APS March meeting. The author thanks the referee for several helpful suggestions. The author thanks Joseph for constant encouragement.

Conflicts of Interest

The author declares no conflicts of interest regarding the publication of this paper.

References

[1] Ye, Y.F., *et al.* (2016) *Materials Today*, **19**, 349. https://doi.org/10.1016/j.mattod.2015.11.026

[2] Chen, S., Tong, Y. and Liaw, P.K. (2018) *Entropy*, **20**, 937. https://doi.org/10.3390/e20120937

[3] Song, H., *et al.* (2017) *Physical Review Materials*, **1**, 23404.

[4] Koželj, P., *et al.* (2014) *Physical Review Letters*, **113**, Article ID: 107001. https://doi.org/10.1103/PhysRevLett.113.107001

[5] von Rohr, F., *et al.* (2016) *Proceedings of the National Academy of Sciences of the United States of America*, **113**, E7144-E7150.

[6] Wu, K.Y., Chen, S.K. and Wu, J.M. (2018) *Natural Science*, **10**, 110-124. https://doi.org/10.4236/ns.2018.103012

[7] Ishizu, N. and Kitagawa, J. (2019) *Results in Physics*, **13**, Article ID: 102275. https://doi.org/10.1016/j.rinp.2019.102275

[8] Kittel, C. (1976) Introduction to Solid State Physics. 5th Edition, Wiley Eastern Limited, New Delhi.

[9] Lynn, J.W. (1991) High Temperature Superconductivity. World Publishing Corporation, Beijing, Ch. 9, 303.

[10] Ota, S.B. (1987) *Physical Review B*, **35**, 8730. https://doi.org/10.1103/PhysRevB.35.8730

[11] Thouless, D.J. (1974) *Physics Reports*, **13**, 93-142. https://doi.org/10.1016/0370-1573(74)90029-5

[12] Liu, Z.H. and Shang, J.X. (2011) *Rare Metals*, **30**, 354-358. https://doi.org/10.1007/s12598-011-0302-9

[13] Skipetrov, S.E. and Sokolov, I.M. (2018) *Physical Review B*, **98**, 64207. https://doi.org/10.1103/PhysRevB.98.064207

[14] Morel, P. and Anderson, P.W. (1962) *Physical Review*, **125**, 1263. https://doi.org/10.1103/PhysRev.125.1263

[15] McMillan, W.L. (1968) *Physical Review*, **167**, 331. https://doi.org/10.1103/PhysRev.167.331

[16] Sundqvist, B. (2022) *Journal of Physics and Chemistry of Solids*, **165**, Article ID: 110686. https://doi.org/10.1016/j.jpcs.2022.110686

Scientific Research Publishing

Journal of Modern Physics, 2023, 14, 450-460
https://www.scirp.org/journal/jmp
ISSN Online: 2153-120X
ISSN Print: 2153-1196

Could Long-Term Stability Last Forever?

Maria K. Koleva

Institute of Catalysis, Bulgarian Academy of Sciences, Sofia, Bulgaria
Email: mkoleva_1113@yahoo.com

How to cite this paper: Koleva, M.K. (2023) Could Long-Term Stability Last Forever? *Journal of Modern Physics*, **14**, 450-460.
https://doi.org/10.4236/jmp.2023.144026

Received: February 23, 2023
Accepted: March 19, 2023
Published: March 22, 2023

Abstract

The subject of the present paper is to prove that the recently introduced conjecture of boundedness puts a ban over the view of stability as asymptotic property. This result comes in sharp contrast with the prescription of the traditional thermodynamics and statistical physics which consider the existence of equilibrium as asymptotic property of all systems. The difference commences from the use of infinitesimal calculus as the basic implement for modelling by the latter while the primary premise of the conjecture of boundedness is sustaining the energy/matter/information permanently bounded and finite. The latter property overrules the infinitesimal calculus as the major implement of modelling because, among all, it is proven that the traditional one suffers unsoluble difficulties.

Keywords

Long-Term Stability, Equilibrium, Infinitesimal Calculus, Boundedness, Decomposition Theorem, Certain Information, Universal Mechanism for Collapse

1. Introduction

The major goal of the present paper is to prove that long term stability of any complex system never is their asymptotic property: that is, it cannot last forever. This assertion is in fundamental contradiction with the central conjecture of the traditional thermodynamics and statistical physics, namely the conjecture that stable equilibrium has it's asymptote so that the corresponding system arrives at it in finite time interval and stays there forever regardless to the initial conditions and irrespectively to the boundary ones, and regardless to the structure, functional properties and environment where the system is put in. However, an unforeseen so far flaw of the traditional conjecture is that, if so, the total amount of energy and matter involved in maintaining the stable asymptote gradually and permanently increases in the course of evolution eventually and inevitably reach-

ing infinite values. The latter consideration holds for any asymptote since the cumulative effect of its maintaining always reaches infinite and ever-increasing values in the time course, despite the fact that it could involve only finite amount of energy/matter/information at each and every step of evolution. A few paragraphs below it are demonstrated that the convergence of corresponding indefinite integrals does not help solving that problem.

Consequently, the above considerations immediately imply that, if it would be possible to maintain each and every system in stable state arbitrary long time, the Nature would turn to be a giant perpetuum mobile such that each and every its constituent also would be a perpetuum mobile.

It is worth noting that the above conundrum provokes a cascade of questions some of which are: if all systems, both natural and tailor-made inevitably turn unstable in due time, are there any early warning signs for their collapse and if so, for which systems are they available? Does a universal mechanism for "dying out" of any system, even the best organized and the most stable one, exist? Is it possible to define the "life-time" of each and every system? Further, is there universally available operational protocol such that to provide answers to the above mentioned questions?

Let us start with the obvious fact that infinite systems are excluded from the present consideration because, being infinite either in size, and/or in energy/matter necessary for functioning as such, it takes infinite amount of energy/matter to sustain a system not only asymptotically but at each and every instant. Thus, the obvious consequence is that only systems of finite size and such that their construction and functioning involve and exchange only bounded amount of energy/matter at each and every step of their evolution are the appropriate candidates for being subject of present consideration. This premise renders the primary importance of taking into account explicitly the size of each and every constituent viewed as boundary conditions, and its permanent interaction with the environment viewed as highly non-trivial interplay with the corresponding initial conditions. It is worth noting that this highly non-trivial interplay suggests that there exists a specific spatio-temporal domain where the corresponding unit evolves in a stable way. The intuitive clue hints that whenever the size of any spatio-temporal domain is bounded, it takes bounded time of a system to cross the boundaries of that domain regardless to the direction and nature of its motion (ballistic or diffusive).

In more familiar terms, the role of boundary is that, though restraining the motion to stay within a domain by means of reflection back from it, the reflected flow of matter/energy interacts with the bulk and thus eventually the boundary turns overcome and certain amount of matter/energy "leaks" beyond. In turn, the latter changes the functional properties of the system within the domain which in turn provokes another "break" in the boundary restraint. Thus, eventually a system approaches moment of functional instability and eventually collapses.

The tacitly presupposed assumption in the above consideration is that the

boundaries are supposed not absolutely rigid and forever intact. The crucially important consequence of the withdrawal from intactness of the boundary in the above example is that stability turns out not to be asymptotic property. To prove the latter is the subject of the present paper.

In a nutshell, it will be proven that stability holds only until a system evolves so that to stay within specific margins, called by the author thresholds of stability and never reaches either of them. Indeed, in order to sustain its stability intact, a system should make a smooth "U-turn" back on reaching either threshold. At this point, however, the traditional modelling of the evolution needs major revision because, as proven next, it suffers an up to now unforeseen inherent contradiction. Indeed, the traditional science asserts that the notion of smoothness is adequately modelled by means of infinitesimal calculus. Consequently, the latter defines the notion of smoothness as a lack of restraint over the number of significant digits necessary for characterization of an information unit and/or the distance between nearest points. Yet, the price of that conjecture comes as follows: each smooth exertion of a "U-turn" takes infinite number of steps, accordingly infinite energy/matter and time for its substantiation. The unforeseen so far point is that convergence of the corresponding integral(s) suffer(s) inherent contradiction, namely: the lack of restraint over the number of significant digits means that the smaller the infinitesimal number is the more energy/matter is involved/exchange for its substantiation regardless to whether it is a point and/or distance. Thus, though the integral over the information units converges, at the same time, the integral over the energy/matter involved in providing that convergence diverges. Thus, convergence is mathematical property which, however, is inappropriate for modelling real processes.

In order to overcome the problem, the author has put forward a new approach grounded on the conjecture [1] that the evolution of stable systems involve/exchange only finite and bounded amount of energy/matter at each and every state/step at its execution. In turn, this brings about a restraint over the values of each information unit characterizing a point and/or step; that is, their values are bounded and finite, e.g. number of significant digits is always finite and bounded both from below and from above. It is worth noting that that restraint is a fundamental property which must not be associated with imperfections of resolution and/or insufficiency of our current knowledge about a given process.

It is worth noting that, to the author's knowledge, neither of the traditional or latest approaches put restraints over the values of information means. Thus, all sorts of modeling share the same property of the infinitesimal calculus, that is, the lack of restraint over the information means. In turn, the lack of restraint makes possible the execution of a smooth "U-turn", even though a model is described by, for example, a discrete mapping. To compare, both infinitesimal calculus and all current approaches render execution of a smooth "U-turn" available but optional (*i.e.* it depends on the concrete modelling) while the conjecture of boundedness puts a ban over execution of each and every smooth "U-turn"

for a fundamental physical reason.

Now the major difference with the traditional approaches becomes apparent. To compare, the latter prescribes existence of stable equilibrium as asymptotic property because a system is open to make a smooth "U-turn" on reaching either threshold (to remind: a smooth "U-turn" implies tangential approach to a threshold). On the contrary, the conjecture of boundedness [1] renders the approach to any threshold to be always non-tangential and thus the execution of a "U-turn" inevitably to go some beyond either threshold. However, going beyond either threshold, inevitably makes the corresponding system to experience certain damages, either in its structure and/or its functioning. This opens the door to further malfunctioning and on exerting other "U-turn(s)" eventually to collapse.

In a nutshell, the exertion of a "U-turn" turns out to be the demarcation line for our understanding of the future evolution of any system. To remind, the smoothness of a "U-turn" sets the generic property of stability to be its holding forever. On the contrary, the setting of boundedness renders the generic property of the execution of each and every "U-turn" to be always non-tangential which in turn makes stability rather transient property, that is, it lasts only until the first "U-turn" is completed.

It is worth noting on the analogy between the above consideration and the mentioned in the beginning example about the role of boundary conditions viewed as either absolutely intact (traditional approach) or viewed as having specific margins (thresholds of stability) such that their overcoming is available.

Outlining, the major suggestion of the approach put forward by the author and called by her boundedness [1], is that the long-term stability holds intact only until reaching either of its thresholds for the first time. Now the following questions stand: are "U-turn(s)" inevitable and are there early warning signs for their execution? The corresponding considerations and the answers to these questions are presented in the next section.

Then, in Section 3, the consideration about how the functional organization of a complex system should be organized so that to "prolong" its "life-time".

A very important and, to certain extent unexpected, outcome is the opportunity to extract confident information even about the evolution of systems, the information about whose behavior is uncertain and/or incomplete. The corresponding considerations are presented in Section 4.

2. Boundedness Conjecture and Universal Protocol for Collapse

The major conjecture of the present paper is that the evolution could develop in a stable way only when a system evolves so that to stay within specific thresholds of stability never reaching either of them. Next the elucidation why the author's approach sets the role of reaching either threshold so crucial for the collapse of any system, even the best ones in construction and functioning, comes. The core of that approach turns out to be the following conjecture: it asserts that all natural phenomena involve/exchange only bounded and finite amount of energy/

matter in each state and/or step. The major consequence is that this assertion puts a general restraint over the values of the information units used for modelling the corresponding phenomena. Put in other words the major conjecture reads: the phenomena subject to the conjecture of boundedness evolve so that the corresponding rates and amplitudes are constrained within specific for each and every process, system and environment margins, called by the author thresholds of stability. At this point the major novelty comes: due to that restraint, on reaching either threshold, neither system can make a smooth "U-turn" because it approaches the corresponding threshold always in non-tangential way. Thus, the execution of any "U-turn" always goes some beyond either threshold. However, doing that, the corresponding system certainly experiences specific damages either in its structure and/or its functioning. This opens the door to further malfunctioning which on exerting other "U-turn(s)" eventually brings collapse.

Let us now consider how to confirm mathematically the above described setting.

The major breakthrough of the author's idea is to consider the above mentioned setting as general operational protocol not as law. To elucidate the latter difference, let us remind that the notion of a law implies establishing of a stable relation among specific variables characterizing a given process which re-occur the same on repetition. On the contrary, the notion of operational protocol implies existence of a stable pattern which stays intact in an ever-changing environment. Yet, the ever-changing environment is where all natural systems "live" and interact. To compare, controlled environment is available for only few model systems such as ideal gases and/or other tailor-made systems such as computers and other electronic devices whose energetic needs are supplied artificially. Yet, systems like Internet, power and water grids etc. are put in semi-autonomously changing environment just because different users plug to them semi-randomly. That is why the matter about stability of the behavior of a system in an ever-changing environment is of primary importance.

Next it is demonstrated that the successful modelling is rigorously derived from the proved by the author and called by her the decomposition theorem. The latter proves that each system, put in an ever-changing environment and subject to boundedness of rates and amplitudes, exhibits the same type decomposition of the power spectrum of each time series characterizing its behavior. More precisely, it is proven that the power spectrum of each and every time series comprises 3 parts, namely: a specific to a system discrete pattern, universal continuous band of shape $1/f^{\alpha(f)}$ and components which commence from the thresholds. Since the derivation of that decomposition is grounded on the boundedness of rates and amplitudes alone and does not require any knowledge about the nature and origin of a system, neither about its dimension, size and or other specifications, it can serve as the major implement of a universal operational protocol for modelling the behavior of such systems.

Crucial for our considerations is the major outcome of the decomposition

theorem which proves that stable and predictable behavior is available only when the specific discrete band and the universal continuous band of shape $1/f^{\alpha(f)}$ are additively superimposed. That additivity ensures that the specific for the system information encapsulated in the discrete band stays intact and thus could serve as the major specific characteristic of the corresponding system which does not change in an ever-changing environment. This happens because the additivity of those bands prevents development of emergent phenomena and thus sustains robustness and stability of the discrete pattern.

However, the things become different with regard to the components in a power spectrum which come from thresholds: emergence of new phenomena is unavoidable and started going on at the execution of the first "U-turn". The inevitability of those phenomena is grounded on the facts that: 1) simultaneous additivity of all three bands is impossible since, if otherwise, the components which come from thresholds would belong either to the discrete or to the continuous band. To elucidate this consideration better let us remind that the lines in a power spectrum are permutation sensitive: any permutation yields a new pattern. 2) the ubiquity of the non-tangential approach to a threshold, (a "U-turn" in the setting of boundedness) is the one which launches the emergence and development of new phenomena, each of which is associated with specific "leak" beyond the corresponding threshold. Remember the "leaking" beyond the physical boundaries at the example given in the Introduction; 3) each line in a power spectrum is characterized by bounded means of information and thus each new phenomenon emerges in a specific bounded time interval set by the concrete path to approach the threshold.

Outlining, the break in additivity commences from the emergence of any new phenomenon and is characterized by the emergence of a new line(s) in the corresponding power spectrum. The importance of the latter emergence is that it turns out impossible to maintain any longer the discrete pattern stable and intact because the new phenomenon starts its development immediately after it's commence due to the interaction with the entire system. The emergence and development of a new phenomenon could be traced by monitoring the development of the new line(s) and the changes it makes to the power spectrum. Since the exclusive property of the execution of a "U-turn" is the persistent non-tangential approach to either threshold, it is certain that it produces specific damages either to the structure and/or functioning. So, the execution of "U-turns" serves as a general protocol for launching destructive phenomena which eventually yields collapse. Further, the collapse is inevitable and happens in a finite time interval since any "U-turn" inevitably happens in a specific, yet finite and bounded spatio-temporal time interval.

Summarizing, each and every system, whose behavior is subject to the boundedness of rates and amplitudes, is subject to unavoidable collapse which occurs even for best organized and functioning ones. However, establishing of the "lifetime" of each system is mathematically decidable with certainty only for the time periods before the first new line emerges. This is so because the break in additiv-

ity between a discrete pattern and a continuous band renders the individual properties extremely sensitive to the specific and highly non-trivial interplay between already developed and newly emergent phenomena for each item, system, individual etc., the. The high sensitivity makes the evolution after the first "U-turn" subject to individual circumstances which, to a much extent, appear as unique ones.

Now, a question comes: whether it is ever possible to "prolong" stability by other means? This question is suggested by our daily experience about the role of medicine: for example, most of people take dietary supplements in order to keep their health in a good shape as long as possible. But, the author's interest is focused on the following subject: does a universal protocol governing the interaction of different units, systems etc. exist and could it help to "extend" stability? That issue is the subject of the next section.

3. Protocol of Compatibility and Early Warning Signs for a Change

Let us start with establishing how to model interactions in the setting of boundedness. Up to now, the traditional modelling is grounded on the idea about linear superposition among interactions. It conjectures that the total interaction consists of linearly superposed interactions among clusters of two, three, etc. numbers of units. However, the corresponding approach suffers of so far unavoidable infrared and/or ultraviolet catastrophes, a fact which is in conflict with the energy saving law.

Further, the idea about linear superposition is also in conflict with the idea of boundedness since linear superposition does not put bounds on the partial and/or total energy/matter involved and/or exchanged in any point.

In order to resolve the above conflict, the author has conjectured withdrawal from the principle of linear superposition and instead she replaces it with the primary role of saving boundedness of the involved and/or exchanged matter/energy. The later implies that the interactions are non-linear and non-homogeneous throughout a system and both in space and in time. Since different functional units, modules etc. in a complex system have different thresholds of stability, the interplay between the corresponding units makes some new phenomena emerging from a local "U-turn" to affect other unit(s) without the latter to reach their own thresholds. Thus, an alternative to inevitability of destructivity of a "U-turn" arises and this is adaptation. A few paragraphs below it is consider whether an emergent line implies adaptation or destruction.

At this point the question stands: how different units should be organized so that to provide stability of the discrete pattern as long as possible? The answer is given by the put forward by the author conjecture about a bi-directional hierarchy of interactions [1]. Its major idea asserts that the response of a system could be strengthened and its "life-time" prolonged when the response is diversified so that its functioning to be a subject to the called by the author protocol of compatibility [2]. Diversification is substantiated by means of letting only

specific units to response to a given stimuli; for example, our vision responses to visible light, but not to temperature etc. The exclusive property of the bi-directional hierarchy is that the diversification of the response goes via the organization of the functional units in functional hierarchical layers so that the boundedness is self-maintained on each and every level. The latter is substantiated by means of the following: the outcome of each level serves as environment for the others. The bi-directionality comes from the fact that the "environment" for each given level comes both from lower and from the higher levels and thus generally it goes simultaneously both bottom up and top down.

Now the general operational protocol, called by the author "protocol of compatibility", comes into consideration. Its major value is that it provides general rules for establishing bi-directional hierarchy.

The general protocol of compatibility comprises two interconnected rules which come as follows: the first one asserts that in order to postpone emergence of a new phenomenon as long as possible, the lower and higher level discrete patterns must appear as closer as possible to be in overtone positions to a given discrete pattern.

An obvious consequence of that rule is that, because the functioning of all units is interconnected, the emergence of a new phenomenon of any single unit affects all others. This is characterized by emergence of specific new lines in the power spectra of each unit. Yet, now different functional units and hierarchical levels are subject to highly a non-trivial interplay among mutual interactions, remember the major conjecture about non-linearity and non-homogeneity of interactions so that to save energy/matter bounded, which makes some of those interactions to turn from originally destructive to adaptive ones.

However, as proven in [3], it is mathematically undecidable whether the newly emergent line(s) means adaptation and thus eventually prolonging stabilization, or it triggers malfunctioning of the entire system which eventually brings almost immediate collapse. At this point, the role of other knowledge comes of decisive importance: Thus, with the primary knowledge that the collapse of a system and/or unit is generally unavoidable, could and when other appropriate knowledge helps the stabilization of the entire system and in this way to "prolong" its "life-time"? Obviously, the answer to this question is subject to each concrete case. For example, the EEG and EKG time series of an ill person exhibit specific deviations from an established standard but it is the medical knowledge which prescribes the appropriate for a given case medicines.

The second part of the protocol of compatibility is provided by the following rule: the processes at each hierarchical level should be organized so that all of them to share the same "strip" of energy/matter involved/exchanged. Thus the functioning of specific units (self)-organizes in a stable system (hierarchical level). The major value of the second part of the protocol of compatibility is that it puts under control any increase of a quantal error regardless to its origin and location by means of not allowing it's growth over the thresholds as long as possible. Consequently, the "interactions" among hierarchical levels stay under

control as long as possible.

Put in a nutshell, along with the straightening of the response by means of its diversification, the two rules of the protocol of compatibility provide that other levels emergent phenomena appear as small disturbances to a given level ones for a longer time. However, it is crucially important to stress that, though being prolonged and the response strengthened, the total life-time of a system turns again to be finite and bounded.

An exclusive property of the protocol of compatibility, viewed as a protocol of stable (self)-organization, and the boundedness, viewed as universal protocol for stable functioning, is their self-consistency. It is worth noting the major exclusive property of that self-consistency: that is the property that the decomposition theorem holds for each and every so organized system and /or hierarchical level. The major consequence of that holding comes as follows: since the author considers only systems of bounded finite size, the hierarchy of functional levels has its lowest and its highest one, a fact which makes the collapse unavoidable.

Further, the emergence of a new line(s) in a power spectrum appears as a generic type of early warning sign(s) for a change. However, it is mathematically undecidable whether the emergence of a new line in any power spectrum is an early warning sign for adaptation or for fast collapse even for systems subject to the protocol of compatibility.

The "life-time" of any system could be prolonged and the response enhanced by means of highly specific for each system and environment interplay between the general means of "the protocol of compatibility" and other appropriate for each and every given system knowledge.

And last but not least, the "protocol of compatibility" serves as a criterion for demarcation between stable systems and "bunches" of units. Indeed, only systems subject to that protocol stay stable and predictable in a definite period of time that is, until reaching a threshold for the first time. On the contrary, for a "bunch of units", that is systems which are not subject to that protocol, it does not exists a definite period of time when any of them evolves in a stable and predictable way.

4. How to Get Certain Information from Uncertain Data

Let us start with establishing what certain information is.

The novelty of the author's approach lies in the suggestion that stable functioning of a system is modelled by means of "locking" the values for matter/energy/information involved and/or exchanged in every instant and throughout the system within specific margins called by the author thresholds of stability. This restraint commences from the basic assumption of the theory of boundedness, that is: the hypothesis about primary role of keeping boundedness of energy/matter involved/exchanged in each step. As it is demonstrated in the previous sections one of the far going consequences is the one which asserts that stability is rather transient phenomenon than asymptotic one.

An immediate consequence of that reminding is that the evolution of each

process and each system put in an ever-changing environment is modelled by means of monitoring its behavior for a given period of time. The exclusive property of the boundedness conjecture is that the values of the members of the corresponding time series belong to the same specific bounded both from above and from below "strip" of discrete values. Thus, when a system is put in an ever-changing environment, the time series in study comprises some, probably most of all available values from the corresponding "strip". It is important to stress that the obtained sequence is not random because each its member is defined by the current environment and the previous member(s). Yet, an exclusive property of those sequences is that all members in each one appear of equal significance in their contribution. So, a question comes: which member is the true and the certain one? An intuitive answer is that this could be only that information, which stays intact in an ever-changing environment.

An immediate interpretation of the above consideration comes as follows: Does the decomposition theorem holds for the case when factors such poor resolution, human reluctance to say true to some questionnaires etc. persists? The answer is positive and comes as follows: the proof of the decomposition theorem does not involve any knowledge about the nature and the concrete values of the members in the time series under study. The only necessary knowledge is that about their permanent boundedness. Thus, it holds also for time series whose members comprise uncertain/incomplete and even false information let alone they stay bounded within the original thresholds.

Thus, as long as the decomposition theorem holds, there is knowledge obtainable with certainty and that is the information encapsulated in the corresponding discrete pattern. More precisely, each discrete pattern carries the information about stable spatio-temporal landscape of causal relations [3] which characterize a given system.

It is worth noting once again that the information encapsulated in a discrete pattern is certain, although the members of the corresponding time series could comprise uncertain/incomplete (even false) information. The only necessary condition for obtaining certain information is that the uncertainty of information in each and every member of a time series not to exceed the original thresholds.

Thus, an immediate consequence of the above generalization of the decomposition theorem is: again the appearance of a new line in the power spectra suggests that some threshold is reached. And again it is mathematically undecidable whether the new line(s) is early warning sign for adaptation or for collapse. And again, the role of other knowledge turns out to be of primary importance.

5. Conclusions

The major outcome of the considerations presented in the present paper commences from the withdrawal from the infinitesimal calculus as the basic implement for modelling the dynamics and the evolution of complex systems. The infinitesimal calculus suffers inherent contradiction which comes as follows: the

smaller the infinitesimally numbers are, the larger the amount of energy/matter involved in their substantiation is. On the contrary, the conjecture of boundedness puts specific restraint over the amount of energy/matter involved in substantiation of any state and/or step in evolution of each and every system. Hence, the information characterizing the functioning of a stable system turns out to be restrained into a specific "strip" of values.

The new conjecture comes at price: it is that stability turns rather transient phenomenon since the stability is well-defined only until the first "U-turn" is executed. The decisive role of reaching thresholds is that the withdrawal of infinitesimal calculus renders any approach to either of the thresholds non-tangential; hence, the exertion of a "U-turn" goes some beyond the corresponding threshold thus causing specific damages to a system. Then, the stability of a system has a well-defined life-time which is the time before the first "U-turn" happens. To compare, the infinitesimal calculus makes "U-turns" smooth which in turn provides the stability to last arbitrary long time.

Yet, it is worth noting on an exclusive advantage of the conjecture of boundedness which comes as follows: a design which puts under restraint the available values characterizing the corresponding processes into operational "strips" each of which stands for a given hierarchical level, renders the maximum possible stability towards any accidental growth of any quantal error wherever and whenever it occurs. To compare, any lack of restraint over the current values makes the corresponding "software" vulnerable to accidental growth of a quantal error which inevitably is accompanied with the corresponding "hardware" malfunctioning such as overheating, sintering etc.

Summarizing, the major conclusion drawn from the present paper is that the stability never could be asymptotic property that is, it cannot last forever. Yet, with the primary knowledge about the inevitability of collapse in mind, along with other knowledge specific to a given system, the lifetime of a system could be prolonged and/or strengthened. Further, the knowledge about the principle of compatibility and the mathematically non-decidability of early warning signs viewed as parts of a universal protocol for functional organization, along with appropriate specific knowledge, could serve as guiding lines for our understanding of natural systems and for a successful tailoring of artificial ones.

Conflicts of Interest

The author declares no conflicts of interest regarding the publication of this paper.

References

[1] Koleva, M.K. (2012) Boundedeness and Self-Organized Semantics: Theory and Applications. IGI-Global, Hershey. https://doi.org/10.4018/978-1-4666-2202-9

[2] Koleva, M.K. (2018) *Journal of Modern Physics*, **9**, 335-348. https://doi.org/10.4236/jmp.2018.93024

[3] Koleva, M.K. (2020) *Journal of Modern Physics*, **11**, 767-778. https://doi.org/10.4236/jmp.2020.116049

Journal of Modern Physics, 2023, 14, 461-500
https://www.scirp.org/journal/jmp
ISSN Online: 2153-120X
ISSN Print: 2153-1196

Imagine the World, New Insight into Creation, Gravity and Evolution*

Jarl-Thure Eriksson

Åbo Akademi University, Åbo, Finland
Email: jarl.thure.eriksson@gmail.com

How to cite this paper: Eriksson, J.-T. (2023) Imagine the World, New Insight into Creation, Gravity and Evolution. *Journal of Modern Physics*, **14**, 461-500.
https://doi.org/10.4236/jmp.2023.144027

Received: February 6, 2023
Accepted: March 20, 2023
Published: March 23, 2023

Abstract

Since the publication of Einstein's theory of general relativity, a variety of interpretations have been suggested. In 1937, Paul Dirac presented his Large Number Hypothesis (LNH) based on the large difference between gravitational and electromagnetic forces. As a consequence, the energy is proportional to the radius squared and the gravitational constant is inversely proportional to the radius of the universe. The energy increases during expansion, Dirac used the term "additive creation". The objective is to prove the validity of Dirac's claims. A new theory, CBU (Continuously Breeding Universe), has been developed. The universe is considered a black hole originating from the single fluctuation of a positron-electron pair. The expansion is driven by the formation of new pairs. The negative gravitational potential energy balances the increase in matter energy. Due to G ~ 1/r, the Planck length ℓ_p and Planck time t_P depend on the curvature of space. The Schrödinger solution of an initial positron-electron fluctuation contains a parameter equal to the Planck length. The CBU theory postulates that the primordial universe undergoes a transition from a black hole to a photon-filled universe. After the transition, one half of the energy is bound to numerous "small" black holes, the seeds for galaxies, while the other half propagates as CMB (Cosmic Microwave Background) radiation. The CMB photons are due to e^+ - e^- annihilations. Characteristically, the CMB photons are pairwise entangled, the radiation loses wave energy but compensates by increasing the photon numbers. According to a new model for black holes, a continuous inflow of matter prevents the black holes from becoming singularities. An energy gap between the event horizon and the inner photon sphere is the source of real matter from a QED vacuum foam. There is evidence that all stellar matter originates from a proton-antiproton outflow from the galaxy central black hole.

*Die Welt ist alles, was der Fall ist-Ludwig Wittgenstein, Tractatus, 1921. (The World is all that is the case).

Keywords

General Relativity, Gravitation, Black Holes, Singularity, CMB

1. Introduction

Astronomy opens windows to the universe. To understand the physics behind the clockwork of the world, we must use our imagination (Einstein's Gedanken experiment). Step by step, the theory emerges from observations and scientific methodology.

Astronomy has deep roots in history, early observations have been important for the timing of historical events and for the understanding of astrophysical phenomena. However, astronomy as a scientific discipline started with Galileo Galilei at the beginning of the 17th century. The invention of the telescope made it possible to observe the motions of the planets and their moons, giving support to the Copernican heliocentric model.

The accumulation of observational data and the development of tools of increasing sophistication, most recently the Hubble Telescope and the James Webb Space Telescope, have greatly improved our view of the cosmos and its past.

The Big Bang theory, the basis of the present standard model (ΛCDM), was first proposed by the Belgian priest Georges Lemaitre, who used the term "the Primeval Atom" for the Big Bang event [1]. As a religious person, Lemaitre interpreted this as an act of creation, a view that has been accepted by the Vatican and the Catholic Church. Lemaitre also described the expansion of the universe.

The discovery of the cosmic microwave background radiation (CMB) in 1964 has been a key piece of evidence for the Big Bang. Photons following a black body intensity distribution come from all directions of the universe. The spatially even distribution at a time very close to the initial event has been interpreted as very strong argument.

There are several problems related to the standard theory, however. It is assumed that all the energy was packed into the singularity from which the bang started. What was the origin of this energy? To get on track for the coming expansion, the universe had to make a rapid transition from the singularity scale to a scale leading to the current size. One had to introduce inflation, ingeniously developed by Alan Guth [2].

The introduction of dark energy and dark matter, concepts required to explain the expansion and the motions of the celestial bodies, is an extraordinary intervention in science, especially in physics. These concepts are invented just to defend a specific theory, the roots of which are blurred. So far all attempts to find a candidate for dark matter have failed. Dark energy is a trickier question, in this study we will present a solution based on quantum mechanics, which will give a plausible explanation to the dark energy concept.

In the standard model, there is no theoretical derivation or equation for the Hubble constant de facto a time dependent parameter (Edwin Hubble made his observations of the expanding universe in 1923, but only published in 1929 [3]). For practical reasons astronomers use a statistical formula, where the components of matter (dark matter included), dark energy and radiation are fitted in. Here we derive an equation that yields a result 0.5% from observations.

In 1916, Albert Einstein published the Theory of General Relativity (GR) [4]. The theory has formed the backbone of our understanding of gravity. Time and time again, the theory has been proven correct. Einstein's field equation combines the geometry of the universe with energy and momentum. Gravity is explained as a result of the curvature of space. Energy bound to matter or electromagnetic radiation follows a geodesic line as it travels through space. In the empty space around a point-like mass, the ultimate geodesic line coincides with the arc of the radius of curvature. In reality, near celestial bodies, the curvature is distorted.

There were many things that Einstein did not know when he formulated his equations. For instance, the expansion of the universe was still hidden in the veil of the unknown. Not to mention an accelerated expansion. The theory at the time was an unchanging steady state universe. To Einstein Newton's gravitational constant G was a physical fact needed to describe the special case of Newtonian gravitation.

But there was a problem that bothered him, the field equation was unstable, it required an extra term to fulfill the steady state condition. Less than a year after the publication of the GR theory Einstein introduced the idea of a cosmological constant, [5]. Later he would call this as his biggest blunder. This remark received great publicity; it was hard to believe that a genius should admit a mistake. However, the article was not that bad. Much later the cosmological constant was reintroduced to explain the expansion. In the cosmological constant article Einstein defines the curvature radius R_E, also called the Einstein radius, which appears to be close to the present estimate of the radius of the observable universe. The radius is $R_E = c/\sqrt{4\pi G\rho} = 4.6\times10^{26}$ m, which should be compared to $R_\Lambda = 4.4 \times 10^{26}$ m (the standard model). Here, the density of real matter was taken to 5×10^{-28} kg/m^3, a representative value.

Einstein also estimated the total mass by multiplying the density by the volume $V = 2\pi^2 R_E^3$, which is a 4d surface projected into 3d. It is also the volume of a horn torus, **Figure 1(a)**. By using this choice, Einstein sought a 3d shape that would illustrate how light circulates throughout the universe and returns to the point of origin.

In this study, we will stick to Einstein's field equation and interpret the geometry as the interior of a 4d black hole (*BH*). It is impossible to imagine a 4d configuration without an outer surface and without a centre. Instead, we use a 3d projection as shown in **Figure 1(b)**. This assumption leads to solutions that eliminate some problems with the standard model. The *universe BH* has a very

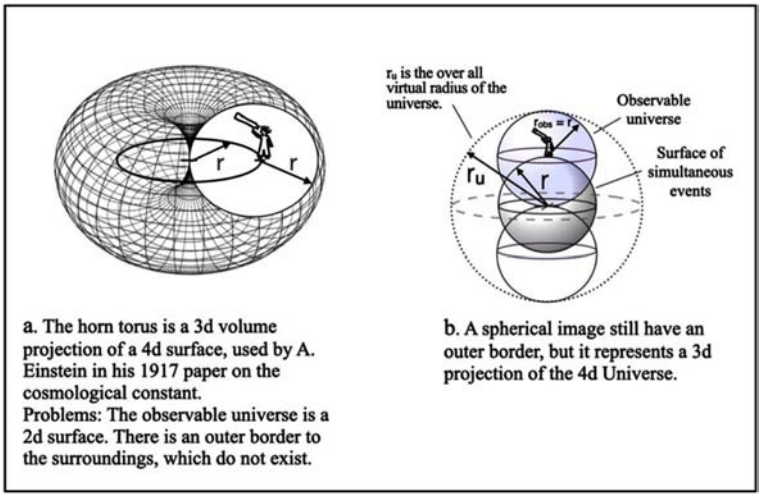

Figure 1. Geometric 3d interpretations of a 4d black hole universe.

low energy density. A steady addition of matter, electrons and positrons, say, prevents a contraction and the formation of a singularity. The influx is a quantum mechanical process made possible by a "momentum-space window" in accordance with the Heisenberg uncertainty principle. The energy of the new matter is balanced by the growth of space and an increase in the gravitational negative potential energy. This important principle was proposed by Alan Guth in an Appendix to [2].

By introducing an acceleration parameter B, we can define the pressures responsible for the expansion, all of which can be formulated as functions of B: Eulerian pressure (introduced by Einstein), a momentum change pressure caused by the influx of new matter, and the pressure responsible for the acceleration. The last-mentioned component is linked to an intrinsic acceleration of space expansion giving rise to a Coriolis effect, which in turn eliminates the need for dark matter.

The most speculative suggestions are omitted. These are inflation, dark matter, singularities, wormholes and the multiverse. We do not deny their existence but do not find them necessary for this study. Though, the theory requires two bold postulates:

1) The CMB radiation is the result of a transition, where the primordial black hole universe releases 50% of its energy as photons from electron-positron annihilations and agglomerates the rest of the energy as matter into a vast array of black holes, the seeds for future galaxies.

2) All stellar matter is the product of proton and antiproton excitations from the event horizon of the galaxy's central black hole.

The study is based on a theory developed by the author in a series of publications during 2018-2022, [6]-[11]. The theory is called CBU, which stands for the Continuously Breeding Universe. The goal is to prove that the CBU theory obeys known laws of physics, the predictions agree with observations and the applied physics proves that the postulates are credible and not coincidences.

2. The Black Hole Universe

The principle that a celestial body possesses such gravity that even light cannot escape was first proposed by the French mathematician Pierre-Simon Laplace and the English physicist John Michell in the late 18th century. A modern approach was implemented by the German mathematician Karl Schwarzschild in 1916, right after the publication of the GR theory. He was the first person to present a solution to the Einstein Field Equation by creating his own metric and deriving the Schwarzschild radius, *i.e.* the radius of the event horizon of a black hole.

Major theoretical work has been going on since the 60s. Stephen Hawking and Roger Penrose became well known for their work on black hole entropy, Hawking radiation and the singularity problem. Some attempts to describe the universe as a black hole have been made, most on purely theoretical grounds, without being able to produce testable predictions. The first serious suggestion to a black hole universe was published by R. K. Pathria in 1972, [12]. The question then—as well as today—was "is the universe closed or open?" By postulating a closed universe Pathria saw a possibility to find explanations to observations of distant phenomena. He proclaims: "Here I demonstrate that the universe may not only be a closed structure but may also be a black hole, confined to a localized region of space which cannot expand without limit."

In 2013, Bernard McBryan published a comprehensive analysis of alternative geometrical solutions for black holes, [13]. He used various metrics as proposed by theorists in previous years. In conclusion he states that one could live in a low-density black hole without really knowing it. But in his study the gravitational parameter G is kept constant. We are going to show that this is not consistent with a black hole universe.

The current study differs from previous attempts in a radical way, the black hole is a main actor in the celestial interplay between time, space and energy. The quantum mechanical activity across the characteristic boundaries, the event horizon, $r_s = 2GM/c^2$ (Schwarzschild radius), and the real black hole radius (the inner photon radius) $r_B = GM/c^2$, makes the black hole's vicinity a cauldron of tumultuous creation. M is the total internal energy in mass units.

The Heisenberg uncertainty principle allows virtual particles from a vacuum ground state to become real not by creating new energy but by balancing the addition of matter with an increasing portion of negative potential energy due to gravitation.

This is the explanation for gravity. The growth of matter requires an expansion of space to increase the negative energy. Thus, the radius of curvature r becomes a measure of gravity. A parameter G, inversely proportional to r, is a convenient way to estimate the gravitational force at a specific time and for a specific size of the universe.

We must make a distinction between the universe black hole and the black holes in the centres of the galaxies. Often the former is described as a cocoon,

the surface of a sphere expanding like the universe, without a centre, however, we are on the inside. The universe includes everything: space, time, matter and radiation. Einstein's theory of General Relativity is about the 4d geometry of a black hole and the interpretation that the curved space is an indication of the gravitational effect. The Einstein Field Equation joins geometry with the content of energy and momentum.

The black holes in the centres of galaxies should be treated as spherical cosmological objects, the properties of which have so far remained mysterious. By interpreting the observations made and accepting the postulate of matter influx, we can create a more accurate picture of the black holes and their physical behaviour. A common characteristic of both the *universe* BH and the *galaxy* BH is that they are not singularities. They are dynamic objects that grow by letting streams of elementary particles enter the interior space. The *universe BH* expands, while the *galaxy BH* increases its density.

3. Basic Equations and Geometry

The official view of a black hole is incomplete. On the one hand, it has a mass, a temperature and an entropy, on the other hand, it is just a dive of the fabric of space into an infinitely deep well, the singularity. We claim that this description is inconsistent and incorrect. The black hole contains energy in the form of matter and radiation. The outer surface of the black hole has a distinct radius, half the Schwarzschild radius. We have called this limit the inner photon sphere, it is motivated by the fact that the ultimate photon energy required to escape the BH is $hf = GMhf/(r_B c^2)$, h is the Planck constant and f is the radiation frequency, from which we have the BH radius

$$r_B = \frac{GM}{c^2}. \tag{1}$$

Here G is the gravitational parameter and M the mass of the black hole. Instead of hf we could put any mass energy mc^2 and obtain the same radius. We can also interpret r_B as the distance from a mass centre M required to create a particle m.

Postulating that the universe is a black hole means that Equation (1) also is valid for the universe. The limit for our range is also the radius of the universe:

$$r_u = \frac{r_s}{2} = \frac{GM_u}{c^2}. \tag{2}$$

Here M_u is the total energy of the universe in mass units. Equation (2) is familiar from several significant proposals, most important those by Brans and Dicke [14] and Dirac [15]. For practical reasons we introduce

$$r = \frac{r_u}{2} = \frac{GM_u}{2c^2}. \tag{3}$$

Later we will show that r equals the radius of the observable universe and the Einsteinian curvature radius.

Figure 1(b) visualizes the 3d projection of the 4d universe black hole. The interpretation is relevant as we will see throughout this analysis. The volume and surface of the 3d projection are

$$V_u = \frac{32\pi r^3}{3}, \tag{4}$$

$$A_u = 16\pi r^2. \tag{5}$$

From Equation (3) we have

$$\frac{G}{r} = \frac{2c^4}{W_u}, \tag{6}$$

where $W_u = M_u c^2$ is the total energy, matter and radiation, of the universe.

The first electron-positron pair appears at the initial event, at which point the following condition is satisfied

$$\frac{G_i}{r_i} = \frac{2c^2}{2m_e} = \frac{c^2}{m_e}, \tag{7}$$

Here G_i is the initial gravitational parameter, r_i is the radius and m_e the electron rest mass. The radius is calculated by forming the energy balance equation, Figure 2. The distance between the particles is obtained by multiplying with π: πr_i.

The energy equation is

$$2m_e c^2 = G_i \frac{m_e^2}{\pi r_i} + \frac{e^2}{4\pi\varepsilon_0 (\pi r_i)}, \tag{8}$$

where e is the electron charge and ε_0 is the vacuum permittivity. From Equation (8) we obtain the initial radius

$$r_i = \frac{e^2}{4\pi\varepsilon_0 m_e c^2 (2\pi - 1)}. \tag{9}$$

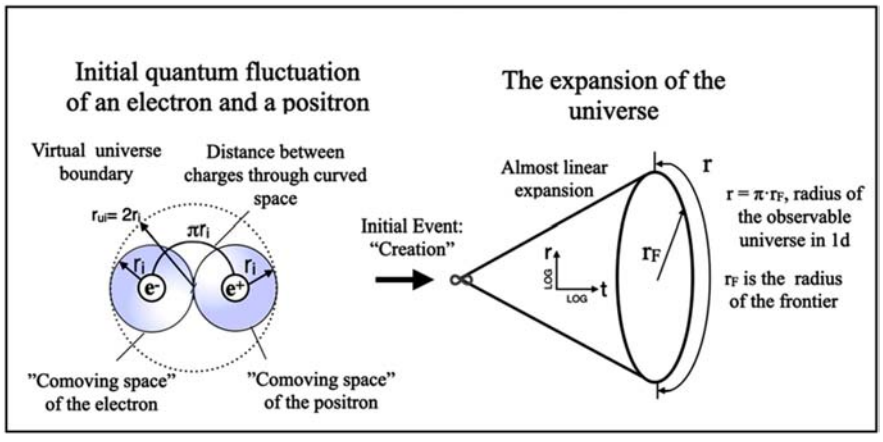

Figure 2. A description of the Genesis event and schematically the expanding universe as the 2d surface of the cone figure. The radius of the observable universe equals πr_F, where r_F is the radius of the frontier circumference (the same presentation as used by NASA, cf. Figure 6).

The value is $r_i = 0.53337905 \times 10^{-15}$ m. It will be shown later that the radius r_i is a fundamental cosmological quantity.

In [9] it was demonstrated that the following relation is valid

$$G_i r_i = Gr = \frac{r_i^2 c^4}{W_e} = constant. \tag{10}$$

As the present value of the Newton gravitational parameter is known, $G_0 = 6.6743015 \times 10^{-11}$ N·m^2/kg^2, we obtain the radius of the observable universe

$$r_0 = \frac{1}{G_0} \cdot \frac{r_i^2 c^4}{W_e} = 4.20550 \times 10^{26} \text{ m}. \tag{11}$$

The value differs from the official figure of 4.4×10^{26} m by −4.6%, a small discrepancy considering the uncertainties in the estimation chain. When G_0 from Equation (11) is substituted into Equation (6), we have

$$W_{u0} = 2W_e \left(\frac{r_0}{r_i} \right)^2 = 1.018 \times 10^{71} \text{ J} \sim 1.133 \times 10^{54} \text{ kg}. \tag{12}$$

The value in kg divided by 8 (the observable universe), $M_{uobs} = 1.42 \times 10^{53}$ kg, matches almost exactly the estimate given by Wikipedia/Observable Universe: $M_{uobs} = 1.46 \times 10^{53}$ kg.

Equation (12) proves that the real energy content is proportional to r^2. The author has defined the following definition

$$W_u = 4\pi b r^2. \tag{13}$$

Here b is a universal energy "pressure" constant, J/m^2, which is obtained from the initial event conditions

$$b = \frac{2W_e}{4\pi r_i^2} = 0.458017 \times 10^{17} \text{ J/m}^2. \tag{14}$$

There are some equations that are of vital importance for the study. The gravitational parameter is

$$G(r) = \frac{c^4}{2\pi b r}. \tag{15}$$

The density of matter (m) and radiation (x) is obtained from

$$\rho_{mx} = \frac{W_u}{V_u c^2} = \frac{3b}{8rc^2}. \tag{16}$$

In his original text on GR Albert Einstein introduces the Eulerian hydrodynamic pressure P_E, capital P is used for pressure to distinguish it from momentum p. From basic thermodynamical principles we have $\mathrm{d}W_u = -P_E \mathrm{d}V_u$. We differentiate the energy relation of Equation (13) and obtain $\mathrm{d}W_u = 8\pi b r \cdot \mathrm{d}r = -P_E \mathrm{d}V_u$, then by substituting $dV_u/\mathrm{d}r = 32\pi r^2$ we have

$$P_E = -\frac{b}{4r}. \tag{17}$$

The ingredients needed for a deeper exploration of the dynamic behaviour of

the universe are now at hand.

4. The Expanding Universe

4.1. Acceleration

The first observations of an accelerated expansion of the universe were made in the late 1990ies by two independent groups, cf. [16]. The result is significant, because it implies that either there is an unknown form of energy (dark energy) involved or the influx of new matter causes the rate change. Actually, both approaches may be compatible, a virtual quantum ground state energy provides the source of a particle influx. The theoretical dark energy is an integrated rating of the instantaneous ground state values. It is important to determine an approximation of the acceleration, even if there does not exist a purely mathematical solution.

The Einstein Field Equation in its original form is

$$G_{\mu\nu} = 8\pi G T_{\mu\nu}, \tag{18}$$

where $G_{\mu\nu}$ is the Einstein tensor and $T_{\mu\nu}$ is the energy-momentum tensor. The Friedmann solution in Robertson-Walker metrics is, cf. [17],

$$\left(\frac{\dot{a}}{a}\right)^2 = \frac{8\pi G\rho}{3} - \frac{kc^2}{\left(ar_{cur0}\right)^2}. \tag{19}$$

Here a is the scale factor, such that $r = ar_0$, and r_{cur} is the curvature radius. The curvature factor k is −1, 0, +1 for negative, zero and positive curvature respectively.

We derivate Equation (19) with respect to time

$$2\dot{a}\ddot{a} = \frac{8\pi}{3}\left(Ga^2\dot{\rho} + 2G\rho a\dot{a} + \dot{G}\rho a^2\right). \tag{20}$$

We have

$$\frac{\ddot{a}}{a} = \frac{4\pi G}{3}\left(\frac{a}{\dot{a}}\dot{\rho} + 2\rho + \frac{\dot{G}}{G}\rho\frac{a}{\dot{a}}\right). \tag{21}$$

Equation (21) differs from the accustomed equation by accounting for the time derivative of G.

The time derivative of the density $\dot{\rho}$ contains the pressure P responsible for the expansion. The 1. Law of Thermodynamics states that $\mathrm{d}W + P\mathrm{d}V = 0$. We have

$$\frac{\mathrm{d}W}{\mathrm{d}t} + P\frac{\mathrm{d}V}{\mathrm{d}t} = 0. \tag{22}$$

The rate of volume change is

$$\frac{\mathrm{d}V}{\mathrm{d}t} = \frac{32\pi}{3}\frac{\mathrm{d}}{\mathrm{d}t}\left(r^3\right) = 3V\frac{\dot{a}}{a}. \tag{23}$$

On the other hand the change of work is

$$\frac{\mathrm{d}W}{\mathrm{d}t} = V\dot{\rho}c^2 + \rho c^2 \frac{\mathrm{d}V}{\mathrm{d}t} = Vc^2\left(\dot{\rho} + 3\rho\frac{\dot{a}}{a}\right). \tag{24}$$

Now, by combining Equations (23) and (24) with Equation (22) we have

$$\dot{\rho}\frac{a}{\dot{a}} = -3\left(\rho + \frac{P}{c^2}\right). \tag{25}$$

We may now write the complete equation of acceleration

$$\frac{\ddot{a}}{a} = -\frac{4\pi G}{3}\left[\rho\left(1 - \frac{\dot{G}}{G}\frac{a}{\dot{a}}\right) + 3\frac{P}{c^2}\right]. \tag{26}$$

It is easy to show that $\frac{\dot{G}}{G}\frac{a}{\dot{a}} = -1$. When G, ρ_{mx} and P_E from Equations (15), (16) and (17) are substituted into Equation (26), the result is 0. This can be interpreted as the equation being correct, as well as the variable definitions, and that the need for the cosmological constant is necessary. However, we have solved the problem in a more plausible way, the difference between the density and the pressure (divided by c^2) terms must be diminutive. Therefore we introduce a factor $B + 1$ before the pressure term. B is small, roughly $1/\pi^2$, a more precise definition will be presented in Section 4.4. The new acceleration equation is

$$\frac{\ddot{a}}{a} = \frac{c^2}{2r^2}B. \tag{27}$$

We use the following relation as an Ansatz:

$$g = r_0\ddot{a} = \frac{Bc^2}{2r_0 a} = \frac{Bc^2}{2r}. \tag{28}$$

Here g has been used as the symbol for acceleration because a is reserved for the scale factor.

We conclude that r^2 in the denominator of Equation (27) should be multiplied with π^2 (cf. **Figure 2**) to indicate that $\ddot{a}$ is an intrinsic 3d acceleration acting at each point of the space and giving rise to a Coriolis effect.

4.2. The Hubble Parameter

By integrating Equation (27) we obtain the rate of the universe expansion, *i.e.* the Hubble parameter. First

$$\dot{a}\mathrm{d}\dot{a} = \frac{c^2}{r_0^2}B\frac{\mathrm{d}a}{a}, \tag{29}$$

and further

$$\dot{a} = \frac{c}{r_0}\sqrt{B\ln\frac{a}{a_i}} = \frac{c}{r_0}\sqrt{B\ln\frac{r}{r_i}}. \tag{30}$$

This is the Hubble parameter, $a_i = r_i/r_0$. As a first approximation we use $B = 1/\pi^2$ and obtain

$$h_0 = \frac{c}{\pi r_0}\sqrt{\ln\frac{r_0}{r_i}} = 2.229\times10^{-18}\,\mathrm{s}^{-1} \sim H_0 = 68.8\frac{\mathrm{km}}{\mathrm{s}\cdot\mathrm{Mpc}}. \tag{31}$$

H_0 is close to the present best value of 67.7 km/sMpc.

4.3. The Age of the Universe

The passage of time since the initial event is thought to be anchored to the curvature radius due to the relation $\ell_p/t_p = c$, where ℓ_p and t_P are the Planck length and the Planck time respectively, that is, length and time are synchronized even if the pull of gravity changes. Accordingly, we can treat universe size and time as synchronized variables, without considering the decreasing G.

The propagation of time is obtained by integration. We substitute $u = \ln(a/a_i)$ into Equation (30)

$$\int a_i \frac{e^u du}{\sqrt{u}} = \int \frac{c}{r_0}\sqrt{B}dt. \tag{32}$$

The integral on the left-hand side has an error function solution

$$\int a_i \frac{e^u du}{\sqrt{u}} = -a_i i\sqrt{\pi}\cdot erfi\left(\sqrt{u}\right). \tag{33}$$

The real part solution of the right-hand side is obtained by using the Dawson integral function $D_+\left(\sqrt{\ln(a/a_i)}\right)$, to be found in Wolfram-Alpha.

The time as a function of the radius is obtained from

$$t(r) = D_+ \frac{2r}{c\sqrt{B}}. \tag{34}$$

In our first approximation $D_+\left(\sqrt{\ln(r_0/r_i)}\right) = 0.05111$, $B = 1/\pi^2$ we get the age of the universe: $t_0 = 4.51 \times 10^{17}$ s ~ 14.3 Gyr, a slightly higher value than the official 13.8 Gyr.

4.4. A Specified Estimate of the Hubble Parameter and Universe Age

Our attempt is to determine B as a function of time. It can be proved that $\lim\left(\sqrt{L}D_+\left(\sqrt{L}\right)\right) = 1/2$ for $\sqrt{L} \to \infty$. We define a parameter

$$\nu_B = \frac{1}{4LD_+^2}, \tag{35}$$

where $L = \ln(r/r_i) + 1/4$. The addition of 1/4 stems from the need of considering the momentum change caused by the continuous influx of new matter. The momentum force is

$$\begin{aligned} F_M &= \frac{dp}{dt} = M_u\frac{\partial V_u}{\partial t} + V_u\frac{\partial M_u}{\partial t} = M_u\frac{\partial V_u}{\partial r}\frac{dr}{dt} + V_u\frac{\partial M_u}{\partial r}\frac{dr}{dt} \\ &= 8\pi brB\left(\ln\frac{r}{r_i} + \frac{1}{4}\right) = 8\pi brBL, \end{aligned} \tag{36}$$

where $p = M_u V_u$ is the momentum and V_u the velocity of expansion.

It can be shown that

$$B = \left(\frac{\nu_B}{\pi}\right)^2. \tag{37}$$

As r goes towards ∞, ν_B approaches 1 and $B \to 1/\pi^2$. The universe is becoming flat and the frontier speed, see next section, is asymptotically approaching the speed of light.

Substituting $L = 96.656$ and $D_+ = 0.0511248$ into Equation (35) results in $\nu_B = 0.98957$, which in turn substituted into Equation (37) results in $B = 0.099219$.

The new Hubble parameter estimate is $h_0 = 2.2075 \times 10^{-18}$ 1/s ~ $H_0 = 68.12$ km/(s·Mpc).

The corrected universe age is $t_0 = 4.56 \times 10^{17}$ s = 14.46 Gyr.

4.5. Proper Distance and Light Cone Diagram

The cosmic age to proper distance (light cone) diagram is a central tool in judging the actual observable universe relative to the theoretical one. Because the expansion frontier is progressing at almost the speed of light, even near parts of our neighbourhood are disappearing.

We presume that the radius of the frontier of the expanding universe is $r_F = r/\pi$. From Equation (31) the velocity of the frontier expansion is

$$V_F = \frac{c}{\pi}\sqrt{B\ln\left(\frac{r}{r_i}\right)} = \nu c, \tag{38}$$

where the relative velocity is $\nu = V_F/c \le 1$.

The calculation of the proper distance requires the geometric representation in Figure 3. Our task is to determine the radius x as a function of the cosmic age t_x. The perimeter of a circle of x represents the proper distance d_p at $t = t_x$.

We define a time factor

$$k_x = \frac{2\pi D_+}{\sqrt{B}}, \tag{39}$$

such that $t_x = k_x r_F/c$, $t_0 = k_{0^*} r_{F0}/c$ and D_+ = Dawson integral function.

From Figure 3 we deduce

$$c^2\left(t_0 - t_x\right)^2 = r_{F0}^2 + r_F^2 - 2r_{F0}\sqrt{r_F^2 - x^2}, \tag{40}$$

where from x is solved. Let $\kappa = x/r_{F0}$ be the normalized radius of x. From Equation (40) we then have

$$\kappa^2 = a^2 - \left[\frac{1}{2}\left(1-k_{x0}^2\right) + \frac{a^2}{2}\left(1-k_x^2\right) + k_x k_{x0} a\right]^2. \tag{41}$$

The proper distance is obtained from

$$d_p = 2\kappa r_0. \tag{42}$$

The relation between the cosmic age and the proper distance is shown in Figure 4. The computed curve (green) according to Equation (42) is compared to results originally published by T. H. Davis and C. H. Lineweaver, [18], however updated with Planck 2013 satellite data, as published by N. Crichton in 2015, [19]. The shapes of the curves are almost identical, though the calculated curve shows a 5% higher maximum value.

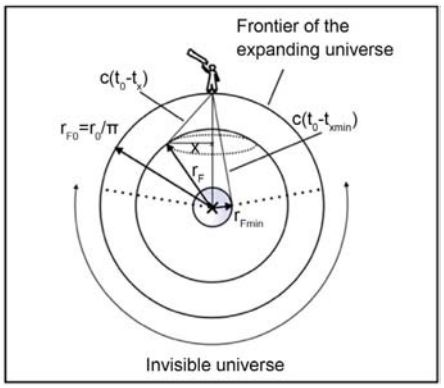

Figure 3. Geometry for the determination of the proper distance.

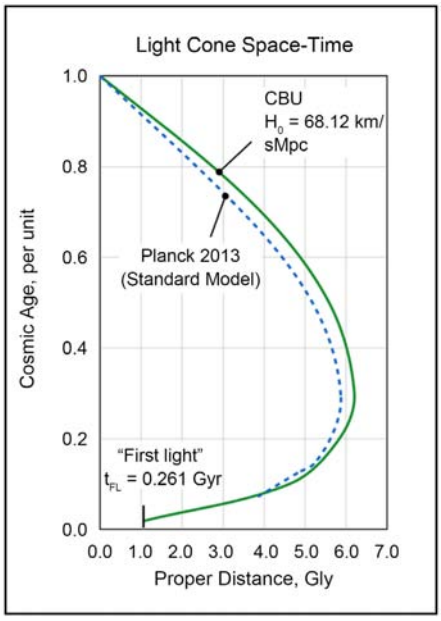

Figure 4. The light cone diagram showing the cosmic age as a function of the proper distance.

In Figure 5, the projection of the universe is shown as the surface of a cone with logarithmic scaling. The radius of the observable universe is the half-perimeter of the end circle. The real observable universe is just a small part of the surface, the fast expansion prevents light from the neighbouring areas to reach the observer. In Figure 6, the time scale is linear, the radial scale logarithmic. The projection reaches from the time of the CMB to the present. Usually, the universe is described with similar images.

4.6. Coriolis Effect on Celestial Dynamics

It was argued in Section 4.1 that the acceleration is an intrinsic 3d phenomenon that operates at any point in the universe. In rotating systems of fluids, particle clouds or star clusters, acceleration causes a Coriolis effect with a large impact

on the dynamical patterns. This is best demonstrated by satellite images of low-pressure rotation on weather maps, or of hurricanes or typhoons, Figure 7.

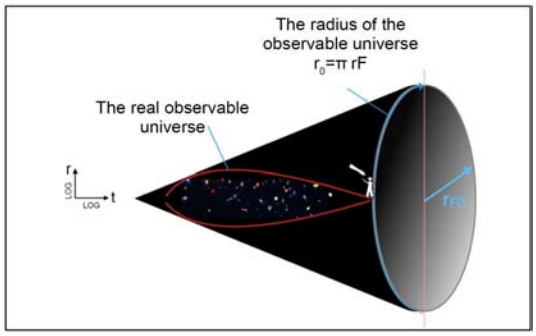

Figure 5. The 2d universe on the time-cone surface. The observable segment represents the curve of Figure 4. Due to the fast expansion light from outside the segment cannot reach an observer on the Earth.

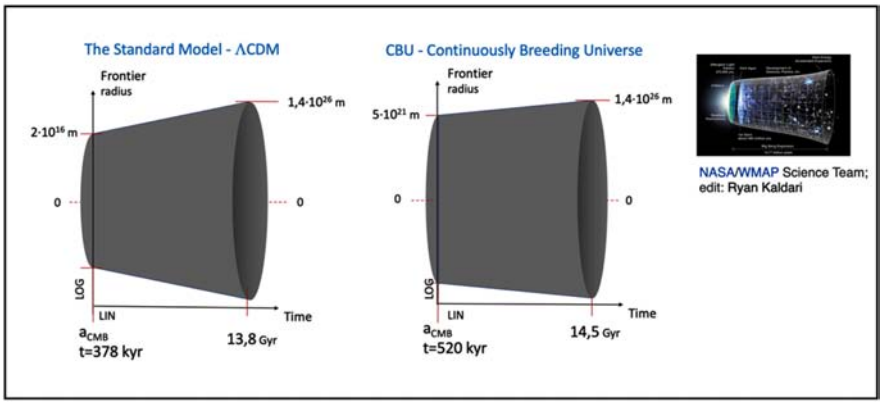

Figure 6. Comparison of the 2d projections of the standard and the CBU model along a linear time axis. The data of the CBU a_{CMB} is calculated in Chapter 7. The NASA image to the upper right is aesthetically attractive but misleading, the star sky should be a projection on the 2d surface of the cone-shaped figure.

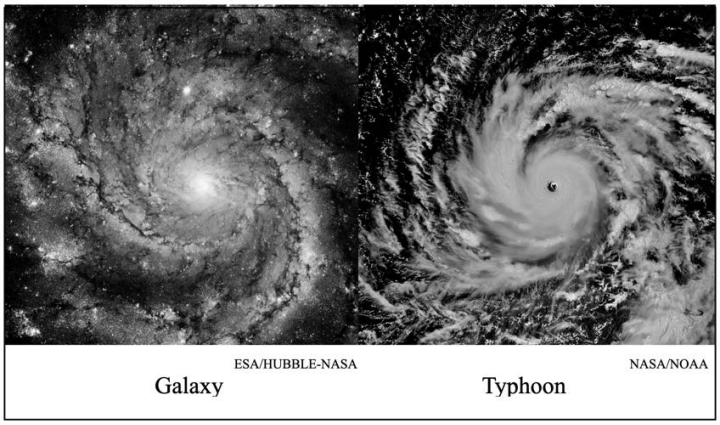

Figure 7. A comparison showing the similarity between the rotation images of a galaxy and a typhoon. It is a known fact that the spiral pattern of the latter is caused by the Coriolis effect.

Here we present a short analysis of the mathematical background of the Coriolis effect. In Figure 8 an observer is located at point O. The observer is studying the velocity relative to coordinate system A of an object at point P. The position vectors are defined as follows

$$\boldsymbol{X}_A = \sum_1^3 x_i \boldsymbol{e}_i, \tag{43}$$

and

$$\boldsymbol{X}_O = \boldsymbol{X}_{OA} + \boldsymbol{X}_A, \tag{44}$$

where $\boldsymbol{e}_i$ is the unit vector.

The observer measures the velocity

$$\frac{\mathrm{d}\boldsymbol{X}_O}{\mathrm{d}t} = \boldsymbol{V}_{OA} + \boldsymbol{V}_A + \sum_1^3 x_i \frac{\mathrm{d}\boldsymbol{e}_i}{\mathrm{d}t} = \frac{\mathrm{d}\boldsymbol{X}_{OA}}{\mathrm{d}t} + \sum_1^3 \frac{\mathrm{d}x_i}{\mathrm{d}t}\boldsymbol{e}_i + \sum_1^3 x_i \frac{\mathrm{d}\boldsymbol{e}_i}{\mathrm{d}t}, \tag{45}$$

where $\boldsymbol{V}_{OA}$ is the velocity difference between the systems, $\boldsymbol{V}_A$ is the velocity of P in A. The last term is the rate of expansion. The observer measures an acceleration g_{obs} of P according to

$$\boldsymbol{g}_{obs} = \frac{\mathrm{d}^2\boldsymbol{X}_O}{\mathrm{d}t^2} = \boldsymbol{g}_{OA} + \frac{\mathrm{d}\boldsymbol{V}_A}{\mathrm{d}t} + \sum_1^3 \frac{\mathrm{d}x_i}{\mathrm{d}t}\frac{\mathrm{d}\boldsymbol{e}_i}{\mathrm{d}t} + \sum_1^3 x_i \frac{\mathrm{d}^2\boldsymbol{e}_i}{\mathrm{d}t^2}. \tag{46}$$

The time derivative $\mathrm{d}\boldsymbol{V}_A/\mathrm{d}t$ represents the "true" (in the reference frame of A) acceleration of the body at P. By derivation of the middle term in Equation (45) we obtain

$$\boldsymbol{g}_{tru} = \frac{\mathrm{d}\boldsymbol{V}_A}{\mathrm{d}t} = \sum_1^3 \frac{\mathrm{d}x_i^2}{\mathrm{d}t^2}\boldsymbol{e}_i + \sum_1^3 \frac{\mathrm{d}x_i}{\mathrm{d}t}\frac{\mathrm{d}\boldsymbol{e}_i}{\mathrm{d}t}. \tag{47}$$

The first term in the latter part represents the Newtonian acceleration g_N. The second term is the result of expansion.

Most galaxy systems are disk-like, therefore we assume the system A being a 2-dimensional cylindrical coordinate system with x_3 coordinates set to 0. The equations of the transformation between the Cartesian and the cylindrical system are

$$x_1 = r_l \cos\theta, \tag{48}$$

$$x_2 = r_l \sin\theta, \tag{49}$$

and

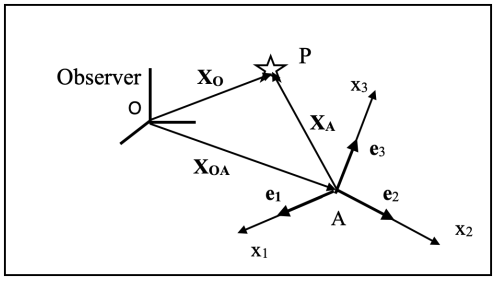

Figure 8. An observer in system O measures the velocity of an object at P in system A, [6].

$$\boldsymbol{e}_x = \cos\theta \boldsymbol{e}_r - \sin\theta \boldsymbol{e}_\theta, \tag{50}$$

$$\boldsymbol{e}_y = \sin\theta \boldsymbol{e}_r + \cos\theta \boldsymbol{e}_\theta, \tag{51}$$

Here r_l is the radial coordinate of the system A.

Next we substitute variables and unit vectors into Equations (46) and (47), and obtain

$$\begin{aligned}\boldsymbol{g}_{obs} = \frac{\mathrm{d}\boldsymbol{V}_{OA}}{\mathrm{d}t} = \boldsymbol{g}_{OA} + \boldsymbol{g}_{tru} + \left(r_l \frac{\mathrm{d}^2 e_r}{\mathrm{d}t^2} + \frac{\mathrm{d}r_l}{\mathrm{d}t}\frac{\mathrm{d}e_r}{\mathrm{d}t} \right)\boldsymbol{e}_r \\ - \left(\frac{\mathrm{d}\theta}{\mathrm{d}t}\frac{\mathrm{d}r_l}{\mathrm{d}t} + r_l \frac{\mathrm{d}^2\theta}{\mathrm{d}t^2} + r_l \frac{\mathrm{d}\theta}{\mathrm{d}t}\frac{\mathrm{d}e_\theta}{\mathrm{d}t} \right)\boldsymbol{e}_\theta,\end{aligned} \tag{52}$$

and

$$\boldsymbol{g}_{tru} = \frac{\mathrm{d}\boldsymbol{V}_A}{\mathrm{d}t} = \left(\frac{\mathrm{d}^2 r_l}{\mathrm{d}t^2} + \frac{\mathrm{d}r_l}{\mathrm{d}t}\frac{\mathrm{d}e_r}{\mathrm{d}t} \right)\boldsymbol{e}_r + \left(\frac{\mathrm{d}\theta}{\mathrm{d}t}\frac{\mathrm{d}r_l}{\mathrm{d}t} + r_l \frac{\mathrm{d}^2\theta}{\mathrm{d}t^2} + r_l \frac{\mathrm{d}\theta}{\mathrm{d}t}\frac{\mathrm{d}e_\theta}{\mathrm{d}t} \right)\boldsymbol{e}_\theta. \tag{53}$$

As the tangential centripetal velocities are of special interest, we concentrate on the radial acceleration components $\boldsymbol{g}_{obs}$ and $\boldsymbol{g}_{tru}$. We denote:

$g_N = \mathrm{d}^2 r_l / \mathrm{d}t^2$, Newtonian gravitational acceleration in radial direction,

$g_{exp} = r_l \left(\mathrm{d}^2 e_r / \mathrm{d}t^2 \right)$, intrinsic expansion acceleration,

$\mathrm{d}r_l / \mathrm{d}t = V_{r_l} = \sqrt{g_N / r_l}$,

$\mathrm{d}e_r / \mathrm{d}t = V_{exp} / r_l = \sqrt{g_{exp} / r_l}$ = increase of local space.

We then define

$$g_{kic} = \frac{\mathrm{d}r_l}{\mathrm{d}t} \cdot \frac{\mathrm{d}e_r}{\mathrm{d}t} = \frac{V_{rl} V_{exp}}{r_l} = \sqrt{g_N g_{exp}}. \tag{54}$$

The equations of the local radial accelerations are

$$g_{tru} = g_N + g_{kic} = g_N + \sqrt{g_N g_{exp}}, \tag{55}$$

$$g_{obs} = g_{tru} + g_{kic} + g_{exp}. \tag{56}$$

The velocity of an object orbiting in A obeys the law of centripetal force

$$V_{orbit} = \sqrt{r_l g}, \tag{57}$$

where g is either g_{obs} or g_{tru}.

Figure 9 shows true and observed accelerations from different published sources. The observation curves are compared with calculated functions based on Equations (55) and (56).

Results published by McGaugh *et al.*, [20] [21], indicate that for decreasing g_N the acceleration declines asymptotically towards $\hat{g} = 0.92 \times 10^{-11}$ m/s^2. The number is close to the intrinsic acceleration $g_{exp} = g_0 = 1.0533 \times 10^{-11}$ m/s^2 from Equation (28).

The MOND theory was developed by M. Milgrom early in the 1980ies, [22]. The MOND curve in Figure 9 follows almost exactly the theoretical Coriolis solution: $g_{MOND} \approx g_N + 2g_{kic}$, without the additional g_{exp} term of Equation (56).

The comparison convincingly confirms that the Coriolis approach provides a credible explanation to the dynamic behavior of the galaxies.

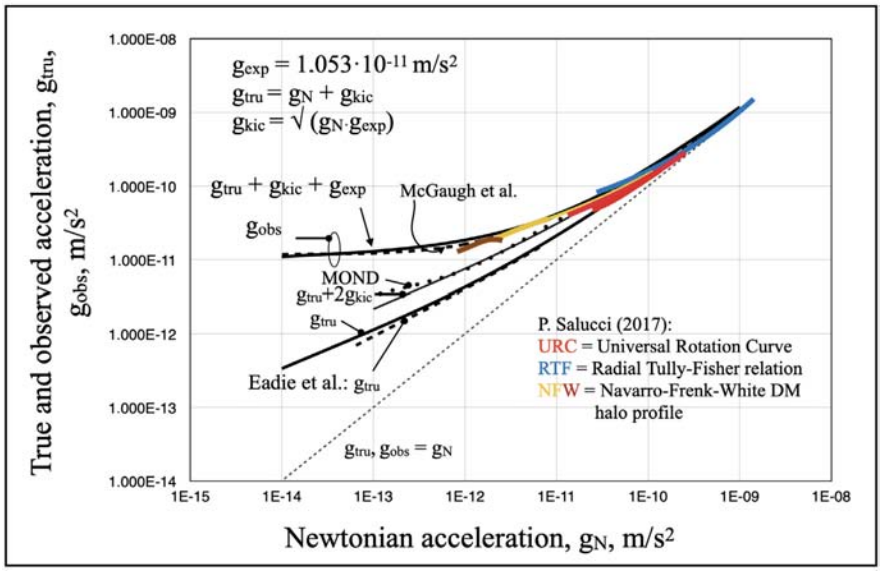

Figure 9. Observed and true acceleration versus the Newtonian acceleration. The full lines are calculated according to the CBU theory. Dashed curves show 1) the observed statistical results of McGaugh *et al.*, [20] [21], and 2) the reconstruction of the Eadie *et al.* Bayesian mass estimates of the Milky Way, [23]. The dotted curve is a calculated version of the MOND acceleration. Colored curves are based on the figure published by Paolo Salucci, [24].

In [6] the rotational velocities of the Milky Way were calculated according to the equations presented here. A spherical bulge and a thin disk, total masses $m_{MW} = 2.3 \times 10^{41}$ kg and $m_{bulge} = 0.29 \times 10^{41}$ kg, were used as a model of the galaxy. The acceleration as a function of the radius r_{MW} was obtained from gravitational potential computations. **Figure 10** shows that the calculated V_{obs} ($= \sqrt{r_i g_{obs}}$) curve follows almost perfectly an average path of Lamost measurements, [25].

5. Quantum Creation

This chapter shows how a solution to the Schrödinger equation at the initial event leads to the introduction of time-dependent Planck units, the influx of new matter and the expansion of space. The energy of the new matter is balanced by the distance extension and thus the increase in the negative gravitational potential energy.

5.1. The Schrödinger Equation

The time-dependent Schrödinger equation is

$$\nabla^2\psi + \frac{8\pi^2 m_e}{h^2}\left(E_i - U_i\right)\psi = 0, \tag{58}$$

where ψ is the quantum-mechanical wave function, E_i is the ground state energy, $U_i = 4\pi b r_i^2$ is the potential energy. The spherically symmetric form of Equation (58) is

$$\frac{\partial^2\psi}{\partial r^2} + \frac{2}{r}\frac{\partial\psi}{\partial r} + \frac{8\pi^2 m_e}{h^2}E_i\psi - \frac{32\pi^3 m_e b}{h^2}r^2\psi = 0, \tag{59}$$

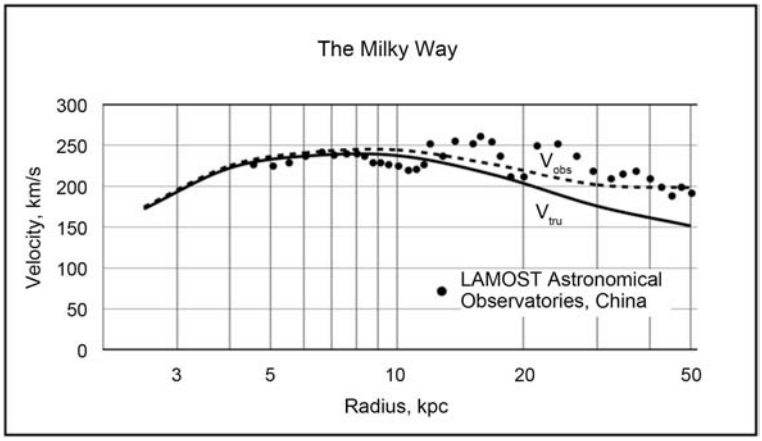

Figure 10. The rotational velocity distribution of the Milky Way. The curves are calculated according to the CBU theory, the points are from Lamost [25]. The figure from [6].

where r is the curvature radius and b the energy constant of Equation (14).

Let

$$\frac{a_1^4}{4}=\frac{h^2}{32\pi^3 m_e b}, \tag{60}$$

$$C=\frac{8\pi^2 m_e}{h^2}E_i. \tag{61}$$

The Schrödinger equation takes the form

$$\frac{\partial^2\psi}{\partial r^2}+\frac{2}{r}\frac{\partial\psi}{\partial r}+C\psi-\frac{4}{a_1^4}r^2\psi=0. \tag{62}$$

This Sturm-Liouville type differential equation has the solution

$$\psi(r)=\frac{1}{r}\mathrm{e}^{-\left(\frac{r}{a_1}\right)^2}\left\{c_1 H_n\left(\frac{r}{a_1}\right)+c_2\left|F\right|_{(a;b;x)}\left[\frac{1}{4}\left(1-Ca_1^2\right);\frac{1}{2};\left(\frac{r}{a_1}\right)^2\right]\right\}, \tag{63}$$

where H_n is the Hermite polynomial function and $\left|F\right|_{(a;b;x)}$ is the Kummer confluent hypergeometric function. c_1 and c_2 are constants of integration.

The constant a_1 is in a key position

$$a_1=\sqrt{\frac{h}{2\pi}\frac{1}{\sqrt{2\pi b m_e}}}. \tag{64}$$

By substituting b from Equation (14) we have

$$\frac{1}{\sqrt{2\pi b m_e}}=\frac{r_i}{m_e c}, \tag{65}$$

and by substituting G_i from Equation (7) we have

$$a_1=\sqrt{\frac{hG_i}{2\pi c^3}}=\ell_{Pi}. \tag{66}$$

By definition ℓ_{Pi} is the Planck length of the virgin universe. In the CBU

theory the Planck length is dependent on the radius r and time. The numerical value is $\ell_{Pi} = 1.43516 \times 10^{-14}$ m.

It can be shown that

$$\left(\frac{\ell_{Pi}}{2r_i}\right)^2 = \frac{2\pi - 1}{4\alpha_{fs}}, \tag{67}$$

where α_{fs} is the fine structure constant, 1/137.036. The result is not a coincidence, but a purely physical relation based on known physical constants. The equation emphasizes the significance of the Planck scale and the curvature radius r_i of the virgin universe. It might be seen as a proof of the connection between gravity and quantum mechanics.

Equation (67) *reflects the intuitive thought expressed by Richard Feynman in the* 1950*ies*: "137 *holds the answers to the Universe*", [26].

Here is the confirmation.

Substituting G from Equation (15) into Equation (66) we obtain a general expression for the Planck length

$$\ell_P(r) = \ell_{Pr} = \frac{1}{2\pi}\sqrt{\frac{hc}{br}}. \tag{68}$$

A simple check using $r_0 = 4.20550 \times 10^{26}$ m shows that the Planck length according to Equation (68) results in 1.61625×10^{-35} m, which exactly equals the current official value.

In analogy with the hydrogen atom the ground state energy E_{GSi} is postulated to be of the form

$$E_{GSi} = \frac{h^2}{8m_e\ell_{Pi}^2} = \frac{hc}{4\pi r_i}. \tag{69}$$

The general expression of the instantaneous ground state energy takes the form

$$E_{GS}(r) = E_{GSr} = \frac{h^2}{8m_e\ell_{Pi}\ell_{Pr}} = \frac{\pi hc\ell_{Pi}}{4\ell_{Pr}r_i} = \pi^2\frac{\ell_{Pi}}{2r_i}\sqrt{hcbr}. \tag{70}$$

The Planck energy W_P has an important bearing on the influx of new matter. By definition

$$W_{Pi} = \sqrt{\frac{hc^5}{2\pi G_i}} = \frac{\ell_{Pi}}{r_i}W_e. \tag{71}$$

At the initial event a positron and an electron are exited, from Equation (71) we deduce that the particles originate from

$$2W_e = \frac{W_{Pi}}{\ell_{Pi}/2r_i}. \tag{72}$$

The significance of $\ell_{Pi}/2r_i = 13.453499$ in the CBU theory is obvious here, if W_{Pi} is considered the virtual dark energy of the virgin universe, then the real energy is obtained by dividing it with the ratio $\ell_{Pi}/2r_i$.

The general expression for $W_P(r) = W_{Pr}$ is

$$W_{Pr} = \sqrt{hcbr}. \tag{73}$$

For $r = r_0$, W_{Pr} is 1.9560815 × 10^9 J, which is in full compliance with the official value.

A comparison of Equation (73) with Equation (70) shows the relation between the Planck and ground state energy

$$E_{GSr} = \pi^2 \frac{\ell_{Pi}}{2r_i} W_{Pr}. \tag{74}$$

5.2. Generalized Uncertainty

The temporal change of the gravity strength and the momentum has an impact on the uncertainty window, *i.e.* $\Delta p \Delta x$, which constitutes the classical Heisenberg formulation, cf. Ronald D. Adler [27]. We divide Δx into a Heisenberg component $\Delta x_H = h/(4\pi\Delta p_H)$ and a gravity component

$$\Delta x_g = \frac{h}{4\pi\Delta p_g}. \tag{75}$$

The momentum uncertainty is

$$\Delta p = \frac{\mathrm{d}p}{\mathrm{d}r} \ell_{Pr}. \tag{76}$$

We have

$$\frac{\mathrm{d}p}{\mathrm{d}r} = \frac{8\pi br}{c} \sqrt{BL} \left(1 + \frac{1}{4L}\right), \tag{77}$$

where the term containing $1/4L$ is due to the fact that L is a $\ln(r)$ function.

Presuming that the location uncertainty is $\Delta x = \ell_{Pr}/2$, we have

$$\Delta p \Delta x_H \le \frac{1}{2} \frac{\mathrm{d}p}{\mathrm{d}r} \ell_{Pr}^2 = \frac{h}{4\pi} f_r, \tag{78}$$

where $\Delta p = f_r \cdot \Delta p_H$ and

$$f_r = 4\sqrt{BL} \left(1 + \frac{1}{4L}\right). \tag{79}$$

Adler has derived an expression for the gravity component

$$\Delta x_g = \pi \frac{\Delta p \ell_{Pr}^2}{h} = \frac{h}{4\pi\Delta p} \left(\frac{2\pi\ell_{Pr}\Delta p}{h}\right)^2. \tag{80}$$

After some algebraic manipulation we arrive at the final uncertainty equation

$$\Delta p \Delta x = \Delta p \left(\Delta x_H + \Delta x_g\right) \le \frac{h}{4\pi} \left(f_r + f_r^2\right) = \frac{h}{4\pi} F_r, \tag{81}$$

where $F_r = f_r(1 + f_r)$ is the overall uncertainty factor and $\Delta p = F_r \cdot \Delta p_g$. When f_r is substituted into F_r, we obtain a proximity value to the real uncertainty factor: $F_{rU} = 4\sqrt{BL} \cdot \left(\ell_{Pi}/2r_i\right)$, which applies to the *universe BH*. A similar analysis leads to $F_{rB} = \sqrt{BL} \cdot \left(\ell_{Pi}/2r_i\right)$ for the *galaxy BH*.

We verify the validity of F_{rU} by substituting Equation (79) into $F_r = f_r(1 + f_r)$, we have

$$\frac{F_{rU}}{4\sqrt{BL}} = (1+1/4L)\left[1+4\sqrt{BL}\,(1+1/4L)\right] = 13.4539. \tag{82}$$

The result shows the resemblance with $\ell_{Pi}/2r_i = 13.4535$. It also proves that the reasoning of R.D. Adler is correct. We should consider the mathematical model as an approximation of the quantum process behind the injection of real matter particles.

A detailed analysis of the physics of *galaxy BH*s will be presented in Chapter 8.

5.3. Matter Influx

5.3.1. Universe Inside

The leading paradigm of the CBU theory says that we live inside a low-density black hole and that the expansion is explained by a continuous "creation" of matter. As our main postulate we assume that the matter influx originates from virtual dark energy. The dark energy is a state of the quantum or QED vacuum, which due to the uncertainty principle allows particles to enter the real-world space (inside the universe BH) and simultaneously increase the space. The influx rate is obtained from the virtual dark energy, W_{vDE}, time change

$$\frac{\mathrm{d}W_{vDE}}{\mathrm{d}t} = \frac{W_{Pr}}{t_P}F_{rU} = \frac{cW_{Pr}}{\ell_{Pr}}F_{rU}, \tag{83}$$

where $t_P = \ell_{Pr}/c$ is the Planck time. When the functions of W_{Pr}, ℓ_{Pr} and F_{rU} are substituted into Equation (83) we have

$$\frac{\mathrm{d}W_{vDE}}{\mathrm{d}t} = 8\pi brc\sqrt{BL}\cdot\frac{\ell_{Pi}}{2r_i}. \tag{84}$$

On the other hand, we have an increase of real matter (and radiation) according to

$$\frac{\mathrm{d}W_u}{\mathrm{d}t} = \frac{\mathrm{d}W_u}{\mathrm{d}r}\cdot\frac{\mathrm{d}r}{\mathrm{d}t} = 8\pi brc\sqrt{BL}, \tag{85}$$

meaning that

$$\frac{W_{vDE}}{W_u} = \frac{\ell_{Pi}}{2r_i} = \frac{\Omega_\Lambda}{\Omega_b}, \tag{86}$$

where Ω_Λ is the normalized dark energy density and Ω_b is the normalized baryon density, in practice the normalized real energy density. For a typical Ω_Λ= 0.68 we have Ω_b = 0.050 (officially 0.049).

Equation (86) *is an important result, because it provides a constant ratio value between the virtual dark energy density and the real energy density. The ratio is confirmed by observations. The equation also proves that the assumptions leading to the definition of the generalized uncertainty factor F_{rU} are most likely.*

There is also another route to establish Equation (86). The pressure responsible for the expansion can be linked to the energy density of the virtual dark energy as follows

$$-\frac{P_{EM}}{c^2} = -\frac{P_E}{c^2} - \frac{P_M}{c^2} = \frac{b}{4c^2 r}(1+2BL) = \frac{2}{3}\rho_{mx}(1+2BL) = \rho_{vDE}. \tag{87}$$

Here the Eulerian pressure P_E is obtained from Equation (17) and the momentum pressure is derived using the momentum force from Equation (36)

$$P_M = \frac{F_M}{A_u} = -\frac{b}{2r}BL. \tag{88}$$

From Equation (86) we have

$$\frac{W_{vDE}}{W_u} = \frac{\rho_{vDE}}{\rho_{mx}} = \frac{\ell_{Pi}}{2r_i} = \frac{2}{3}(1+2BL). \tag{89}$$

When the physical expression of $\ell_{Pi}/2r_i$ of Equation (67) is substituted into Equation (89), we obtain an exact equation for the current value of BL

$$B_0 L_0 = \frac{1}{2}\left(\frac{3}{2}\sqrt{\frac{2\pi-1}{4\alpha_{fs}}}-1\right) = 9.590125. \tag{90}$$

5.3.2. The Quantum Vacuum Energy

The ground state energy of the initial event as obtained from Equation (70) is

$$E_{GSi} = \pi^2 \frac{\ell_{Pi}}{2r_i} W_{Pi} = 2\pi^2 \left(\frac{\ell_{Pi}}{2r_i}\right)^2 \cdot W_e, \tag{91}$$

where W_e is the rest energy of the electron.

It appears that $\pi^2 \cdot \left(\frac{\ell_{Pi}}{2r_i}\right)^2 = \pi^2 \cdot (2\pi-1)/4\alpha_{fs} = 1786$ *is very close to the ratio* $W_P/W_e = 1836.15$. *This is probably not a coincidence. The electron and the proton are the most stable particles of the universe, it seems quite logical that the universe started with the emergence of a proton-antiproton pair at the outer Schwarzschild boundary and a positron-electron pair on the inner photon sphere.* We postulate that there is a B factor ν_{Bi} such that

$$\frac{W_p}{W_e} = \frac{\pi^2}{\nu_{Bi}^2}\left(\frac{2\pi-1}{4\alpha_{fs}}\right) = \frac{1}{B_i}\left(\frac{2\pi-1}{4\alpha_{fs}}\right). \tag{92}$$

For $\nu_{Bi} = 0.9863493$ we have $B_i = 0.0985739$. The result of Equation (92) is 1836.15. As we see, B varies within very small limits, $B = 0.098574$ - 0.099219 between "creation" and the present.

Next, our goal is to determine the level of the current ground state energy E_{GS0}. From Equation (70) we have that $E_{GS} = \text{constant} \cdot \sqrt{r}$. The number of electron-positron pairs is

$$N_{e^+e^-} = \left(\frac{r}{r_i}\right)^2. \tag{93}$$

The same equation is valid for the Dirac's Large Number Hypothesis (LNH). Similarly, we can calculate the number of protons and antiprotons exited on the Schwarzschild boundary

$$E_{GSr} = 2\nu_{Bi}^2 W_P \sqrt{\frac{r}{r_i}}. \tag{94}$$

In the current state of the universe E_{GS0} equals 2.597×10^{11} J, a very small number. It is not clear where these protons and antiprotons are located, but an interpretation of the ground state from the electron-positron side leads to the same equation. *In summary, the proton-antiproton pair forms the virtual quantum vacuum energy for the interior of the black hole.*

The exact value of ν_{Bi} is obtained from the equation

$$\nu_{Bi} = \sqrt{\frac{\pi^2(2\pi-1)}{4W_p\nu_{fs}} \cdot \sqrt{hcbr_i}} = 0.9863493. \tag{95}$$

6. General Relativity

6.1. The Einstein Field Equation

The most compact version of the Field Equation is

$$G_{\mu\nu} = 8\pi G T_{\mu\nu}, \tag{96}$$

where $G_{\mu\nu}$ is the Einstein tensor and $T_{\mu\nu}$ is the energy-momentum tensor. Equation (96) has an analytical solution, provided $T_{\mu\nu}$ is isotropic and homogeneous.

One objective of the study is to find a logical solution to the Field Equation without the cosmological constant Λ. We will show that incoming new matter and a variable G affect the energy density and the expansion pressure in a way making Λ unnecessary.

The Einstein tensor is divided into the Ricci curvature tensor $R_{\mu\nu}$ and the Ricci scalar R according to

$$G_{\mu\nu} = R_{\mu\nu} - \frac{1}{2}Rg_{\mu\nu}. \tag{97}$$

The components of the $R_{\mu\nu}$ tensor are obtained by using the Christoffel symbols, the procedure is found in any textbook on General Relativity, cf. Carroll [17]. The Ricci tensor is

$$R_{\mu\nu} = \begin{pmatrix} -3\frac{\ddot{a}}{a} & 0 & 0 & 0 \\ 0 & \frac{\ddot{a}}{a} + 2\left(\frac{\dot{a}}{a}\right)^2 + 2k\frac{c^2}{a^2 r_{cur}^2} & 0 & 0 \\ 0 & 0 & \frac{\ddot{a}}{a} + 2\left(\frac{\dot{a}}{a}\right)^2 + 2k\frac{c^2}{a^2 r_{cur}^2} & 0 \\ 0 & 0 & 0 & \frac{\ddot{a}}{a} + 2\left(\frac{\dot{a}}{a}\right)^2 + 2k\frac{c^2}{a^2 r_{cur}^2} \end{pmatrix}, \tag{98}$$

where r_{cur} is the curvature radius and k the curvature parameter according to the Friedmann-Robertson-Walker metrics, k cf. Equation (19).

The Ricci scalar is

$$R = -6\left[\frac{\ddot{a}}{a} + \left(\frac{\dot{a}}{a}\right)^2 + k\frac{c^2}{a^2 r_{cur}^2}\right]. \tag{99}$$

The metric tensor $g_{\mu\nu}$ is

$$g_{\mu\nu} = \begin{pmatrix} 1 & 0 & 0 & 0 \\ 0 & -1 & 0 & 0 \\ 0 & 0 & -1 & 0 \\ 0 & 0 & 0 & -1 \end{pmatrix}. \tag{100}$$

6.2. The Energy-Momentum Tensor

Based on Equations (96) and (99) the unit of the energy-momentum tensor $T_{\mu\nu}$ components are that of a mass density, kg/m^3. The tensor is defined as follows

$$T_{\mu\nu} = \begin{pmatrix} \rho_{eq} & 0 & 0 & 0 \\ 0 & \frac{P_{exp}}{c^2} & 0 & 0 \\ 0 & 0 & \frac{P_{exp}}{c^2} & 0 \\ 0 & 0 & 0 & \frac{P_{exp}}{c^2} \end{pmatrix}. \tag{101}$$

Our task is to find the equivalent density ρ_{eq} and the pressure P_{exp} that accounts for both expansion and acceleration. From Equation (87) we have

$$P_{EM} = -\frac{b}{4r}(1+2BL). \tag{102}$$

The density ρ_{eq} affects the velocity of expansion, *i.e.* the Hubble parameter. It consists of two components

$$\rho_{eq} = \rho_{mx} + \rho_{EM}, \tag{103}$$

where ρ_{EM} is caused by the momentum change, ρ_{mx} is the matter + radiation density.

According to the 1st Law of Thermodynamics we have

$$\frac{\mathrm{d}W_{exp}}{\mathrm{d}t} + P_{EM}\frac{\mathrm{d}V}{\mathrm{d}t} = 0, \tag{104}$$

where $W_{exp} = \rho_{EM}c^2 V$, the time derivative of which is

$$\frac{\mathrm{d}W_{exp}}{\mathrm{d}t} = \dot{\rho}_{EM}c^2 V + \rho_{EM}c^2\frac{\mathrm{d}V}{\mathrm{d}t}. \tag{105}$$

Here $\mathrm{d}V/\mathrm{d}t = 3V\dfrac{\dot{a}}{a}$. We approximate that

$$\dot{\rho}_{EM} \cong -\rho_{EM}\frac{\dot{a}}{a}. \tag{106}$$

From Equations (104) and (105) we now have

$$\rho_{EM} = -\frac{3}{2}\frac{P_{EM}}{c^2}. \tag{107}$$

Substituting P_{EM} from Equation (102) we have

$$\rho_{EM} = \rho_{mx}(1+2BL), \tag{108}$$

and then Equation (103) becomes

$$\rho_{eq} = \rho_{mx} + \rho_{EM} = 2\rho_{mx}(1+BL). \tag{109}$$

In order to get the total pressure P_{exp} responsible for both expansion and acceleration we need to include the gravitational parameter G into the 1st Law of Thermodynamics

$$\frac{\mathrm{d}\left(GW_{exp}\right)}{\mathrm{d}t}+GP_{exp}\frac{\mathrm{d}V}{\mathrm{d}t}=0, \tag{110}$$

where $W_{exp}=\rho_{eq}c^2V$. After some manipulations, cf. Section 4.1, we have

$$\frac{\dot{G}}{G}\rho_{eq}+\dot{\rho}_{eq}+3\rho_{eq}\frac{\dot{a}}{a}=-3\frac{P_{exp}}{c^2}\frac{\dot{a}}{a}. \tag{111}$$

From Equation (15) we conclude that $\frac{\dot{G}}{G}=-\frac{\dot{a}}{a}$. Further, we have that $\dot{\rho}_{eq}=2\rho_{mx}\left(B-BL-1\right)\frac{\dot{a}}{a}$. Finally, the pressure is obtained from

$$\frac{P_{exp}}{c^2}=-\frac{2\rho_{mx}}{3}\left(1+B+BL\right). \tag{112}$$

Now the Einstein Field Equation can be completed in a form which eliminates the need for a cosmological constant Λ

$$R_{\mu\nu}-\frac{1}{2}Rg_{\mu\nu}=8\pi GT_{\mu\nu}. \tag{113}$$

6.3. Field Equation Characteristics

All components of the energy-momentum tensor contain $2\rho_{mx}$. By substituting G from Equation (15) and ρ_{mx} from Equation (16) into Equation (113) we arrive at the following expression for the tensor

$$T_{\mu\nu}=3\left(\frac{c}{r_0}\right)^2\begin{pmatrix}\frac{1+BL}{a^2} & 0 & 0 & 0\\ 0 & -\frac{1}{3}\cdot\frac{1+B+BL}{a^2} & 0 & 0\\ 0 & 0 & -\frac{1}{3}\cdot\frac{1+B+BL}{a^2} & 0\\ 0 & 0 & 0 & -\frac{1}{3}\cdot\frac{1+B+BL}{a^2}\end{pmatrix}. \tag{114}$$

where $T_{\mu\nu}$ replaces $8\pi GT_{\mu\nu}$.

Due to substitution G has vanished, the energy-momentum tensor is independent of the gravitational parameter. Making use of the definition of the Hubble parameter in Equation (30) we can write the tensor as follows

$$T_{\mu\nu}=\begin{pmatrix}3\left(h_H^2+\frac{c^2}{a^2r_0^2}\right) & 0 & 0 & 0\\ 0 & -\left(h_H^2+\left(1+B\right)\frac{c^2}{a^2r_0^2}\right) & 0 & 0\\ 0 & 0 & -\left(h_H^2+\left(1+B\right)\frac{c^2}{a^2r_0^2}\right) & 0\\ 0 & 0 & 0 & -\left(h_H^2+\left(1+B\right)\frac{c^2}{a^2r_0^2}\right)\end{pmatrix}. \tag{115}$$

The term $1 + B$ indicates the extra pressure required for acceleration.

The Field Equation written in its most compact form is now

$$G_{\mu\nu} = R_{\mu\nu} - \frac{1}{2} R g_{\mu\nu} = T_{\mu\nu}. \tag{116}$$

The Friedmann-Robertson-Walker temporal equation, which also may be called the *Hubble expansion equation*, is

$$R_{00} - \frac{1}{2} R g_{00} = T_{00}. \tag{117a}$$

We have

$$-3\frac{\ddot{a}}{a} + 3\frac{\ddot{a}}{a} + 3\left(\frac{\dot{a}}{a}\right)^2 + 3k\frac{c^2}{a^2 r_{cur}^2} = 3h_H^2 + 3\frac{c^2}{a^2 r_0^2}. \tag{117b}$$

Further,

$$\left(\frac{\dot{a}}{a}\right)^2 + k\frac{c^2}{a^2 r_{cur}^2} \equiv h_H^2 + \frac{c^2}{a^2 r_0^2}. \tag{117c}$$

By definition $\frac{\dot{a}}{a} = h_H$. $k = 1$ means that the universe is closed. $ar_{cur} = ar_0$ proves that the average curvature radius equals the radius r of the observable universe, a circumstance emphasized by Einstein in the cosmological constant paper [5].

The *acceleration equation* is obtained from

$$R_{ij} - \frac{1}{2} R g_{ij} = T_{ij}, \tag{118}$$

where i and $j = 1, 2, 3$. After some algebraic manipulations and the substitution of Equation (117c) into the equation, we end up with

$$\ddot{a} = \frac{c^2}{2ar_0^2} B \tag{119a}$$

or

$$g = r_0 \ddot{a} = \frac{c^2}{2ar_0} B. \tag{119b}$$

For $a = 1$, $B = 0.099219$ we have $g_0 = 1.0533 \times 10^{-11}$ m/s^2.

The equation corresponds to our Ansatz in Equation (28). The acceleration g is an inherent characteristic of the expanding universe. Over a comoving distance d in the vicinity of an observer, the scale factor a in Equation (119b) equals $1 - d/r_0 \approx 1$ – extremely small influence.

The inherent acceleration g provides a Coriolis effect, which explains the rotational behaviour of the galaxies and the celestial movements at large, and thereby eliminates the need for dark matter, cf. Eriksson [6].

6.4. Energy Conservation

It is important to prove that the $T_{\mu\nu}$ tensor fulfils the temporal energy conserva-

tion condition. The general expression using Christoffel symbols Γ is, cf. Carroll [17],

$$\nabla_\mu T^\mu{}_0 = \partial_\mu T^\mu{}_0 + \Gamma^\mu_{\mu 0} T^0{}_0 - \Gamma^\lambda_{\mu 0} T^\mu{}_\lambda = -\partial_0 \rho_{eq} - 3\frac{\dot{a}}{a}\left(\rho_{eq} + \frac{P_{exp}}{c^2}\right) = 0. \tag{120a}$$

The time derivative is

$$\partial_0 \rho_{eq} = \frac{\partial}{\partial t}\left(\frac{1+BL}{a^2}\right) = -\left(\frac{2(1+BL)}{a^2} - \frac{B}{a^2}\right)\left(\frac{\dot{a}}{a}\right). \tag{120b}$$

We have

$$\frac{1}{a^2}(2+2BL-B-3-3BL+1+B+BL)\left(\frac{\dot{a}}{a}\right) = 0. \tag{120c}$$

The conservation condition is met. The result shows that the components ρ_{eq} and P_{exp}/c^2 are correctly derived.

7. Cosmic Microwave Background Radiation

7.1. Influence of Gravitation on the Redshift

The gravitational parameter G is extremely large in the initial phase, $G_i \approx 5 \times 10^{31}$ m^3/kg/s^2. The parameter decreases successively with the expansion. The photons in the cosmic microwave background (CMB) propagating faster than the expansion start from a deep gravitational well. We write the energy equation of the electromagnetic radiation as a gravitational gradient equation

$$hdf + g\frac{hf}{c^2}dr = 0, \tag{121}$$

where f is the frequency, g the gravitational acceleration along r. We obtain g from

$$g = \frac{GM}{r^2} = \frac{2c^2}{r}. \tag{122}$$

Here we make use of $M = 4\pi br^2/c^2$ and $G = c^4/2\pi br$, cf. Equations (13) and (15). Having that $f = c/\lambda$, $\mathrm{d}f = -c\mathrm{d}\lambda/\lambda^2$ and $r = r_0 a$, where a is the scale factor, we write

$$\int \frac{\mathrm{d}\lambda}{\lambda} = 2\int \frac{\mathrm{d}a}{a}. \tag{123}$$

Integration implies that λ is proportional to a^2. We deduce that

$$\frac{\lambda_0 - \lambda_s}{\lambda_s} = \left(\frac{1-a}{a}\right)^2 = z_g. \tag{124}$$

Here z_g is the gravitational redshift, λ_s and λ_0 are the wavelengths at the source and at the observer respectively.

As known, the cosmological redshift is

$$z_{cr} = \frac{1}{a} - 1. \tag{125}$$

The combined redshift is $z = z_g + z_{cr}$. We have

$$\frac{\lambda_0}{\lambda_s} = \frac{f_s}{f_0} = z + 1 = \frac{1 - a + a^2}{a^2}. \tag{126}$$

Let a_c stand for the scale factor at the CMB event. For vary small values of the scale factor the frequency of CMB photons decrease approximately according to

$$f_0 \approx a_c^2 f_c. \tag{127}$$

John Huchra at the Harvard-Smithsonian Center for Astrophysics has established the addition rule for combining multiple types of redshifts, [28].

An interesting feature of Equation (126) is that the difference between z_{cr} and z changes very slowly for scale factors close to 1. The discrepancies of the current distance estimates in the vicinity of the Milky Way are still within error limits.

Data on proper distances ($d_{p\Lambda}$, d_{pCBU}), lookback times ($t_{\Lambda z}$, $t_\Lambda(z_{cr})$ and t_{CBU}) are collected in **Table 1**. Λ refers to the standard ΛCDM model, cf. [29] and [30], and CBU to calculated numbers of the current theory.

In **Figure 11** the data of **Table 1** show the correlation between the ΛCDM and CBU models. There is a good agreement between the lookback time graphs t_{CBU} and $t_{\Lambda z}$. t_{CBU} is based on Equation (34), while $t_{\Lambda z}$ originates from the graph in [29]. z was determined from Equation (126) using the appropriate scale factor. d_{pCMB} was calculated according to a unique algorithm presented in Section 4.5, [6]. Even for the proper distances the similarity between the curves is good considering the different approaches.

The difference between the look-back times $t_\Lambda(z_{cr})$ and t_{CBU}, **Figure 12**, is interesting, because it indicates a deviation in the estimates of distant cosmic events. For instance, the most distant observed galaxy Glass-z13 has a redshift of 13, which would mean that a fully developed galaxy had evolved in about 0,35 Gyr after the Big Bang. This is an intriguing paradox; it is most uncertain that billions of stars would have developed in such a short time. According to CBU the lookback time would be 11 Gyr and, considering the age of the universe being 14.4 Gyr, the time for the galaxy to evolve would be a more plausible time of 3.4 Gyr.

Table 1. Lookback time (Gyr) and proper distance (Gly).

Scale factor a	0.1	0.2	0.4	0.6	0.8	0.9
P.u. time, τ_Λ	0.05	0.121	0.318	0.556	0.790	0.894
ΛCDM redsh. z_{cr}	6.7	3.71	1.44	0.62	0.24	0.11
Comb.redsh. z	90	20	3.75	1.11	0.313	0.123
Lookback, $t_{\Lambda z}$	13.11	12.6	9.45	6.0	2.90	1.45
Lookback, $t_\Lambda(z_{cr})$	13.8	13.5	11.9	8.1	3.43	1.56
Lookback, t_{CBU}	12.9	11.5	8.61	5.74	2.87	1.43
Proper dist. $d_{p\Lambda}$	3.58	4.91	5.82	4.75	2.75	1.42
Proper dist. d_{pCBU}	4.45	5.59	5.74	4.45	2.58	1.31

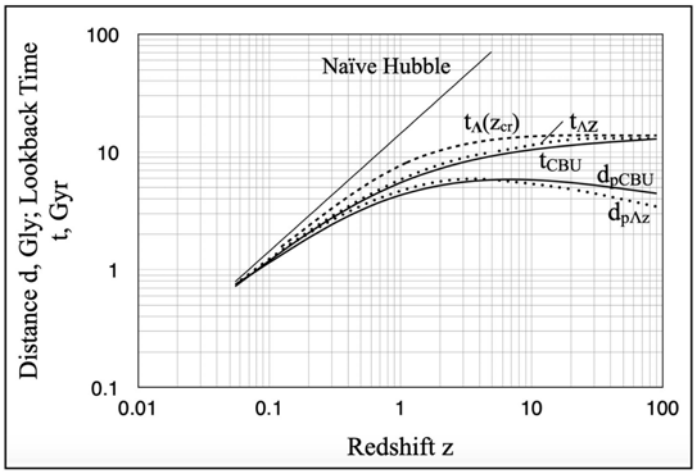

Figure 11. The lookback time and the proper distance as a function of the combined gravitational and cosmological redshift.

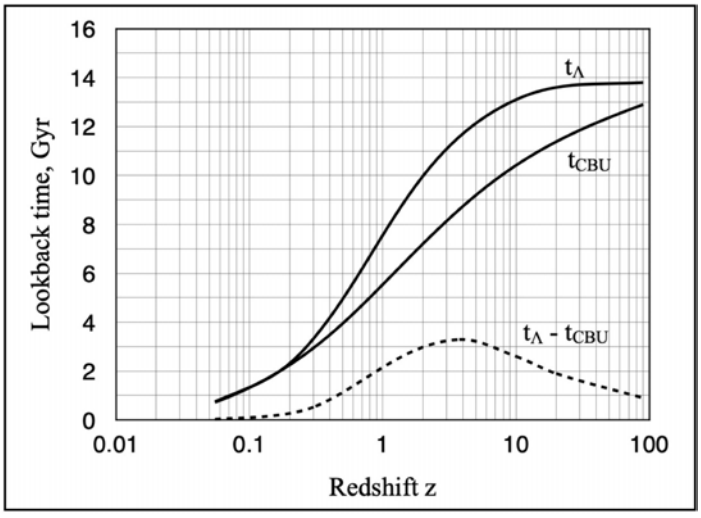

Figure 12. The lookback time as a function of the redshift according to (a) the standard model, $t_\Lambda(z_{cr})$ and (b) to the CBU theory. The deviation is at it's largest, 3.2 Gyr, around $z = 4$.

7.2. The CMB Scale Factor

We obtain the energy density w_{BB} of the black body radiation from the classical Stefani-Boltzmann equation

$$w_{BB} = \frac{8\pi^5 k_B^4}{15c^3h^3}T^4 = \alpha_B T^4. \tag{128}$$

Here $\alpha_B = 4\sigma_{SB}/c = 7.565723 \times 10^{-16}$ J/K^4·m^3 is the radiation density constant, σ_{SB} is the Stefani-Boltzmann constant, and k_B the Boltzmann constant.

The number density of the photons is obtained from, cf. Wikipedia: Photon Gas,

$$n_{ph} = 16\pi\zeta(3)\left(\frac{k_B T}{hc}\right)^3, \tag{129}$$

where $\zeta(3) = 1.202056$ is the Riemann zeta-function. By dividing Equation (128) with Equation (129) we obtain an expression for the photon energy

$$W_{ph} = \frac{\alpha_B T}{16\pi\zeta(3)}\left(\frac{hc}{k_B}\right)^3. \tag{130}$$

If we assume that the photon energy at the CMB event equals one of the two photons caused by the annihilation, we have $W_{phc} = W_e$. The current photon energy is then

$$W_{ph0} = a_c^2 W_e = \frac{\alpha_B T_0}{16\pi\zeta(3)}\left(\frac{hc}{k_B}\right)^3. \tag{131}$$

Accordingly, for $T_0 = 2.72548$ K we have

$$a_{CMB} = a_c = \sqrt{\frac{\alpha_B T_0}{16\pi\zeta(3)}\left(\frac{ch}{k_B}\right)^3 \frac{1}{W_e}} = 3.523\times10^{-5}. \tag{132}$$

Due to the square root the number is much larger than usually suggested (10^{-7} - 10^{-9}).

The current photon energy is $W_{ph0} = 1.0164 \times 10^{-22}$ J and the corresponding frequency $f_0 = W_{ph0}/h = 153.4$ GHz, slightly below the optimum frequency of the Planck black body spectrum of $f_{lmax} = 160.23$ GHz.

7.3. Origin of the CMB

7.3.1. Hypotheses

The primordial universe is the inside of a black hole, where the number of electron-positron pairs increases successively. Some of the electrons and positrons annihilate forming photons. At some point the energy of the photons is equal to the matter energy. We assume that a transition occurs, the photons fill the inner free space of the BH and the matter is concentrated in a multitude of "small" black holes. The photons are entangled in a state of superposition. They do not follow the same rules as photons from an ordinary light source, e.g. a star. We call the transition the CMB event. **Figure 13** shows the universe prior to the transition. After the CMB event, the galaxy black holes initiate an outflow of protons and antiprotons into free space, **Figure 14**.

There are divergent opinions about the destiny of the energy lost by light propagating in the expanding universe. Light waves in a gravitational field are part of the system, gaining or loosing potential energy. The CMB photons, however, are different.

It is a well-known fact that the number density of CMB photons, $n_{ph0} \approx 4 \times 10^8$ ph/m^3, is in poor conformity with a value predicted by e^+ - e^- annihilations, the number requires a boost. The state of superposition offers a novel approach. *The energy lost during the propagation of the light wave is compensated by an addition of the number of photons, which means that photons in a superposition are not a multitude of individual particles.*

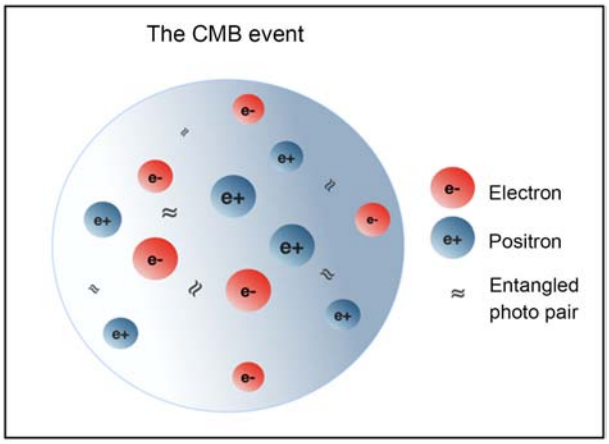

Figure 13. A schematic image of the primordial universe before the CMB transition event.

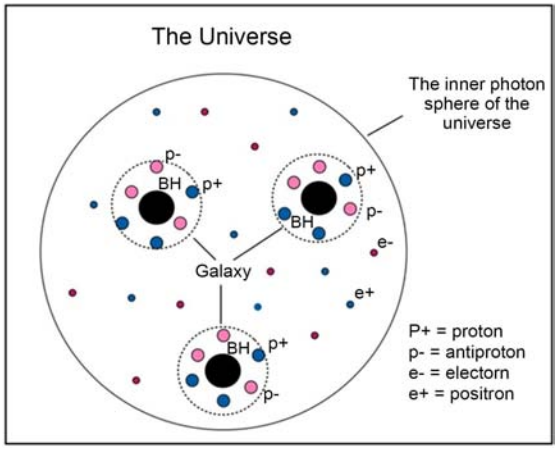

Figure 14. A schematic image of the universe after the CMB transition event.

This might sound as a strange hypothesis, but, as we will see, the numerical evidence is convincing. The standard model is incapable of explaining the current photon density. If all real energy was stored in photons at the time of the CMB, the number of photons would be 1.22×10^{84} and the density 490 ph/m^3, *i.e.* far from the previous number.

The expansion advances in all 3d directions, the number of photons increases according to

$$N'_{ph0} = \frac{N_{phc}}{a_c^3}. \tag{133}$$

When photons enter the observable universe with a scale factor of a_{fl} (first light), they so to speak, pass a single slit, a moment continuously changing with the expansion, only to be observed at the planet Earth in the Milky Way galaxy after about 14.0 Gyr. During the passage the relativistic Doppler effect, see Box below, increases the wavelength and thus lowers the photon energy. Since they are in superposition the compensation means an increase proportional to $1/a_{fl}$.

Currently the total number of CNB photons is

$$N_{ph0} = \frac{N_{phc}}{a_{fl} a_c^3}. \tag{134}$$

7.3.2. The Energy Density of the CMB

At the CMB transition, as hypothesized in Section 7.3.1, the energy splits into two components, the radiation from the CMB and the matter in the black holes. The following equation describes the transition:

$$r_{uc} = \frac{G_c W_{xc}}{c^4} + \frac{G_c M_{mc}}{c^2} \geq r_s = \frac{2G_c M_{mc}}{c^2}, \tag{135}$$

where G_c is the gravitational parameter, W_{xc} is the radiation energy and M_{mc} is the mass of all matter at a_c.

Box: Relativistic Doppler effect

The relativistic expansion velocity is a fraction v_{exp} of the speed of light, we have

$$v_{exp} = B\sqrt{L}. \tag{B1}$$

The increasing velocity causes a prolongation of the wavelength, the Doppler effect. The relativistic velocity difference is obtained from, cf. HyperPhysics/Relativistic Doppler,

$$v_{\Delta} = \frac{v_{exp0} + v_{exfl}}{1 + v_{exp0} v_{exfl}}. \tag{B2}$$

The scale factor a_{fl} is obtained from

$$a_{fl} = \sqrt{\frac{1 - v_{\Delta}}{1 + v_{\Delta}}}. \tag{B3}$$

The value obtained by iteration is $a_{fl} = 0.0173$, the same as in **Figure 4**.

At the transition we have

$$\frac{W_{xc}}{c^2} = M_{mc} = \frac{W_u(r_c)}{2c^2}. \tag{136}$$

The CMB energy is

$$W_{xc} = \frac{1}{2} W_u(r_c) = 2\pi b a_c^2 r_o^2 = 6.32 \times 10^{61} \text{ J}. \tag{137}$$

The number of photons is

$$N_{phc} = \frac{W_{xc}}{W_e} = 7.72 \times 10^{74}. \tag{138}$$

The scale factor for the "first light" moment of the observable universe was determined in [6]: $a_{fl} = 0.0173$, a value resembling $t_{fl} = 0.261$ Gyr, which is in good conformity with estimates of today.

The total number of photons is, Equation (134),

$$N_{ph0} = \frac{N_{phc}}{a_{fl} a_c^3} = 1.024 \times 10^{90}.$$

The number density is

$$n_{ph0} = \frac{N_{ph0}}{V_0} = 410 \times 10^6 \text{ m}^{-3}, \tag{139}$$

where $V_0 = 2.493 \times 10^{81}$ m^3. n_{ph0} is in good agreement with present data.

The energy density of the CMB is

$$w_{x0} = n_{ph0} W_{ph0} = 4.173 \times 10^{-14} \text{ J/m}^3. \tag{140}$$

The result is practically identical with the current Black Body density $w_{BB0} = \alpha_B T_0^4 = 4.175 \times 10^{-14}$ J/m^3, where $\alpha_B = 7.565723 \times 10^{-16}$ J/(m$^3 \cdot$K) is the Boltzmann radiation density and $T_0 = 2.7548$ K.

8. Galaxies

8.1 The Galaxy Black Hole

The black holes in the centre of the galaxies are seeds stemming from the CMB transition. During the transition, half of the energy forms the CMB radiation, while the other half is spread out in 10^{12} - 10^{13} galaxy black holes. Right after the CMB event the total energy of the BHs is $W_{Bctot} = 0.5 \times 4\pi r b r_c^2 = 6.32 \times 10^{61}$ J. There are several indications that the radius r_B of an individual BH changes very slowly, which is also shown by the outcome of this study.

We use the inner photon radius R_B as the appropriate radius instead of the Schwarzschild radius $r_s = 2 \cdot R_B$. We have

$$R_B = \frac{M_B G}{c^2}, \tag{141}$$

where M_B is the mass of the BH and G is the gravitation parameter of the universe at a given time. *With G inversely proportional to the scale factor a and R_B constant M_B becomes inversely proportional to a*, ($M_{B0} = M_{Bc}/a$). Currently the energy content of all black holes is:

$$W_{B0tot} = W_{Bctot}/a_c = 1.793 \times 10^{66} \text{ J} \quad \text{or} \quad M_{B0tot} = 2.00 \times 10^{49} \text{ kg} \quad (10^{19} \text{ suns})$$

The estimates of the number of galaxies are so far very rough, a common number is 2×10^{11} for the observable universe or 1.6×10^{12} for the whole world, cf. Mario Livio, The Universe. Space. Tech., June 2022. The average BH mass would then be 1.25×10^{37} kg or 6×10^6 solar masses. These numbers are quite usual according to observations. The black hole of the Milky Way, Sagittarius* is estimated to have a mass of 8.3×10^{36} kg.

When G from Equation (15) is substituted into Equation (141) we have

$$M_B = \frac{2\pi b R_B r}{c^2}. \tag{142}$$

The mass of an individual BH increases at the same rate as the universe itself, *i.e.* inversely proportional to *a*. Like in the universe case there is an influx of electron-positron pairs.

The time derivative is

$$\frac{\mathrm{d}M_B}{\mathrm{d}t} = \frac{2\pi b R_B \sqrt{BL}}{c}. \tag{143}$$

The equation is needed later, when we want to determine the star formation change with time as a function of the galaxy's stellar mass, cf. Figure 18.

The black hole has an inside gravitational parameter (on the surface), by applying Equation (6) we have

$$G_B = \frac{c^4}{2\pi b R_B}. \tag{144}$$

The parameter contains only constants and is accordingly a constant itself.

8.2. Instead of a Singularity

In the current study, the universe is considered to be a black hole without a singularity. The reason lies in the pressures that cause the expansion and their opposite action against gravitational contraction. The curvature of space governs electron-positron influx and thereby regulates the pace of expansion. In the *galaxy BH*s we can equally define a balance equation between expansion and contraction. Compared to the *universe BH* there is a much more moderate influx of electron-positron pairs (see next section) that causes an increase in the density without increasing the size.

The pressure driving the density increase is obtained from

$$\frac{\mathrm{d}W}{\mathrm{d}t} + P\frac{\mathrm{d}V}{\mathrm{d}t} + V\frac{\mathrm{d}P}{\mathrm{d}t} = 0. \tag{145}$$

The volume is constant along with R_B, so we are left with the equation

$$\frac{\mathrm{d}W}{\mathrm{d}t} = -V\frac{\mathrm{d}P}{\mathrm{d}t}. \tag{146}$$

The expansion pressure is

$$P_{Bexp} = -\frac{W_B}{V_B} = -\frac{3br}{2R_B^2}, \tag{147}$$

where V_B is the volume of the black hole.

The acceleration directed outwards is

$$g_{Bexp} = \frac{4\pi G_B P_{exp}}{3c^2} = -\frac{rc^2}{R_B^2}. \tag{148}$$

Alternatively, the same result is obtained by considering that $g = -\nabla\phi$, where $\phi = -G_B M_B / R_B$. For the symmetric spherical case we have

$$g_{Bexp} = \frac{\partial}{\partial R_B}\left(\frac{rc^2}{R_B}\right) = -\frac{rc^2}{R_B^2}. \tag{149}$$

The contracting acceleration due to gravitation is obtained from the familiar equation

$$g_{Bcontr} = \frac{G_B M_B}{R_B^2} = \frac{rc^2}{R_B^2}. \tag{150}$$

We end up with the balance equation

$$g_{Bexp} + g_{Bcontr} = 0. \tag{151}$$

8.3. Influx of Baryonic Matter from the Black Hole

The black hole has two boundary spheres, the inner one or the photon sphere, $r_B = 0.5 \cdot r_s$ and the outer one or the black hole event horizon at r_s. In between there is an energy gap. From these boundaries there is an influx of electron-positron pairs into the inside of the BH and proton-antiproton pairs into the space outside the BH, Figure 15. In the *galaxy BH* case the number of injected pairs, N_{pair}, is equal on the inside as on the outside, because $\sqrt{R_B/R_B} = 1$.

According to our earlier stated postulate all stellar matter of a galaxy originates from the central BH event horizon. As a result we obtain a clear-cut relation between the stellar mass, M_S, and the BH mass, M_B. The relation is

$$\frac{M_S}{M_B} = \frac{2v_{Bi}^2 m_p N_{pair}}{2m_e N_{pair}} = v_{Bi}^2 \frac{m_p}{m_e} = 1786.4. \tag{152}$$

This is a significant result. Some bold presumptions lead to a result that has a strong anchorage in current observations. The average example of Section 8.1, $M_B = 1.25 \times 10^{37}$ kg, suggests a galaxy stellar content of 2.23×10^{40} kg, which is a typical value.

During the last decade several papers have been published, wherein the mass ratio is discussed and different theories about the cause has been presented, cf. [31] [32] and [33]. The standard theory suggests that stellar matter feeds the black holes, not vice versa as the present theory (CBU) suggests.

An indication that the CBU result is the most plausible one, is shown in Figure 16. The line $M_B = \left[v_{Bi}^2 \left(m_p/m_e\right)\right]^{-1} \cdot M_S$ is shown in a chart created by Sandra Faber, [34]. There is a perfect fit with the "Small dense" galaxies. The line shows there is a linear correlation, which for the present theory means that M_B grows linearly and the assumption of R_B being constant is correct.

In Figure 17, a similar pattern as in Figure 16 is shown for galaxes of type "Active Galactic Nucleus", [31] indicating that the ratio $M_S/M_B = v_{Bi}^2 \left(m_p/m_e\right)$ results in a perfect fit. In Figure 18 the change in stellar mass $\mathrm{d}M_S/\mathrm{d}t$ is shown as a function of the mass. Here the observations are related to galaxies in a star forming phase, cf. [35]. The CBU theoretical time derivative hits into the middle of the statistical pattern.

9. Total Energy

In the original CBU model it was assumed, that the total energy was proportional to the curvature radius r squared. However, the new understanding requires the addition of a term considering the energy generated by the g*alaxy BHs*. Notice, that this is not free energy, the negative counterpart is the gravitational potential energy provided by the increasing density of the black hole. The potential acts over the gap between R_s (event horizon, equal to the Schwarzschild radius) and R_B.

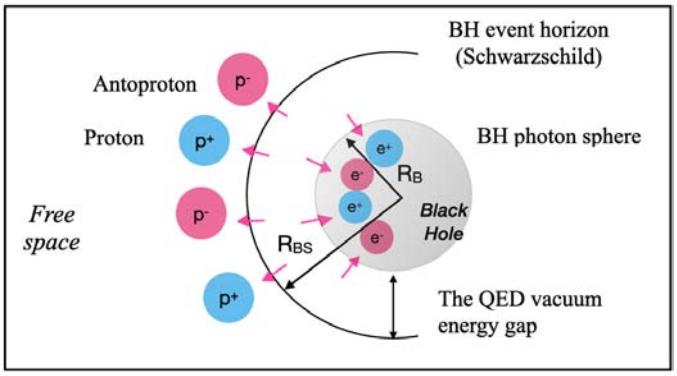

Figure 15. A schematic image of the influx of electron-positron pairs into the BH interior and proton-antiproton pairs into the BH surrounding.

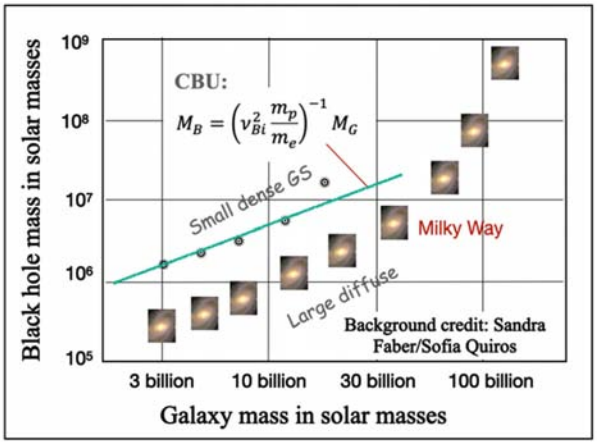

Figure 16. A wide-ranging publicly distributed chart showing the results of the relation $M_B = f(M_G)$ for numerous observed galaxies, [34]. (Here presumed that the galaxy mass M_G equals the stellar mass M_S.)

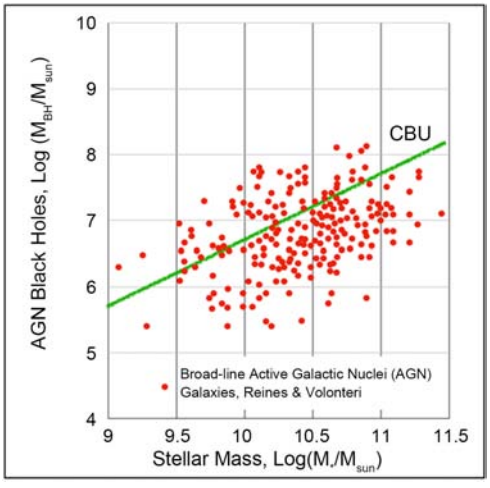

Figure 17. The CBU theory M_B-M_S relation (green line) shows good correlation with the observations of the Reines&Volonteri team, [31].

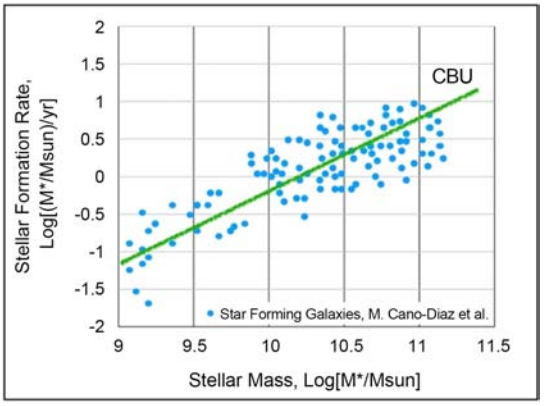

Figure 18. The time derivative of the stellar mass as a function of the mass (green line) according to the CBU theory shows good correlation with the observations of the Cano-Diaz team, [35]. ($M_S = M$).

The energy due to the electron-positron influx is

$$W_{ue^+e^-} = 4\pi br^2. \tag{153}$$

The total energy of the galaxies and the black holes is

$$W_G = W_{Su} + W_{Bu} = 2\pi br^2 a_c \left(v_{Bi}^2 \frac{m_p}{m_e} + 1 \right), \tag{154}$$

where W_{Su} and W_{Bu} are the overall energies of the stellar matter + dust + radiation and the black holes respectively.

The original estimate of the total energy (matter and radiation) was $W_{u0} = 1.018 \times 10^{71}$ J. The corrected value is $W_{u0tot} = 1.050 \times 10^{71}$ J. The increase due to the galaxies is 3.15%.

The critical density is

$$\rho_{cr} = \frac{3h_0^2}{8\pi G_0} = 8.72 \times 10^{-27} \frac{\text{kg}}{\text{m}^3}, \tag{155}$$

where $h_0 = 2.208 \times 10^{-18}$ 1/s and $G_0 = 6.67430 \times 10^{-11}$ m^3/kg/s^2. In the CBU model the critical density does not have a real meaning, because basically the universe grows eternally from the inside, there is no critical limit deciding whether the expansion will stop or continue for ever.

10. Theory Comparison, Arguments in Favour of the CBU Theory

A theory in natural sciences can only be tested by observations and measurements. In Table 2 some of the most important characteristics of the CBU and ΛCDM theories are compared with each other. The numbers are in good agreement, especially considering the different approaches. The main discrepancies relate to the interpretation of the energy content. In the standard model dark energy and dark matter are considered real, while in the CBU dark energy is a virtual ingredient, the vacuum energy from which the universe, in accordance

Table 2. CBU versus ΛCDM.

Characteristic	*CBU*	*ΛCDM*, [17]	*Diffr. %*
Radius of the obs. universe, 10^{26} m	4.206	4.396	+4.5
Age of the universe, 10^9 y	14.45	13.797	−4.7
Hubble parameter, 10^3 m/s/Mpc	68.1	67.7	−0.6
Matter + rad. density parameter, Ω_{mx}	0.05374	0.0498	−5.9
Dark energy density parameter, Ω	0.723	0.686	−5.4
Total real energy, 10^{71} J (matter + radiation)	1.050	1. 079	+2.7
CBU: Free space, 10^{71} J	1.018		
CBU: Black holes, 10^{71} J	0.000018		
CBU: Galaxies, 10^{71} J	0.0320		

with the uncertainty principle, picks up particles that accumulate as real energy. However, the virtual vacuum energy does not lead to an accumulation. Further, the CBU does not require dark matter to explain galaxy dynamics.

The CBU theory has uncovered several characteristics of the universe that seem hard to accept as coincidences. Here are the most essential ones:

1) The radius of the observable universe $r_0 = 4.206 \times 10^{26}$ m derived from the assumption that the universe is a black hole, the standard model value is 4.396×10^{26} m.

2) The ratio of the electron rest energy ($m_e c^2$) and the radius of the maiden universe (r_i) defines an energy constant b, Equation (14), that times the square of the radius r of the observable universe results in a real energy value in complete conformity with current estimates: the r^2 law, also predicted by the Dirac Large Number Hypothesis.

3) The Schrödinger solution to the virgin universe leads to an exponential constant equal to the Planck length given the Newtonian gravitational constant G is a parameter dependent on the curvature radius r.

4) The Planck length ℓ_{Pi} divided by the curvature diameter of the virgin universe, $2r_i$, equals a number consisting of fundamental constants, cf. Equation (67):

$$\frac{\ell_{Pi}}{2r_i} = \sqrt{\frac{2\pi - 1}{4\alpha_{fs}}} = 13.4535,$$

where α_{fs} is the fine structure constant. The numeral equals the ratio between virtual dark energy and total real energy, $\Omega_\Lambda/\Omega_{mx}$ (Ω_{mx} equals the standard model $\Omega_b + \Omega_r$).

5) The introduction of an acceleration factor B results into density and pressure expressions that provide a consistent solution to the Einstein Field Equation

$$G_{\mu\nu} = T_{\mu\nu}.$$

6) The hypothesis that the vacuum gap between the event horizon and the inner photon sphere of a black hole causes the excitation of electron-positron pairs

on the inside and proton-antiproton pairs on the outside of the BH is best proved correct by the graphs of Figures 16-18. The magnitude and slope of the theoretical curves follow accurately the statistical average of observational data.

11. Conclusions

Theories about the universe are based on hypotheses and educated guesses. Observations and sceptical criticality are the only tools to approach the truth. At the core of the standard model there are five central hypotheses: the Big Bang itself, inflationary expansion, dark energy, dark matter and last scattering as the CMB explanation.

In this study, we try to keep the hypotheses to a minimum and as close to known laws of physics as possible. However, there are assumptions that require scientific confirmation. Such are the black hole universe, the influx of matter from the black hole boundary spheres and the propagation of entangled photons in a superposition.

Even if the CBU theory in principle follows a plausible track, it is not perfect, many details need deeper penetration. One such area is how protons and antiprotons transforms into neutrons, electrons, neutrinos and further into atoms. The problem is similar to that of nucleosynthesis in the primordial universe of the standard model.

It is our hope that the propositions presented here will lead to new insight in the world of quantum mechanics and the understanding of the connection between gravity and the quantum world.

Conflicts of Interest

The author declares no conflicts of interest regarding the publication of this paper.

References

[1] Lemaitre, G. (1931) *Nature*, **127**, 706. https://doi.org/10.1038/127706b0

[2] Guth, A. (1997) The Inflationary Universe: The Quest for a New Theory of Cosmic Origins. Perseus Books, New York. https://doi.org/10.1063/1.881979

[3] Hubble, E. (1929) *Proceedings National Academy of Science* (*USA*), **15**, 168-173. https://doi.org/10.1073/pnas.15.3.168

[4] Einstein, A. (1916) *Annalen der Physik*, **49**, 769-822. https://doi.org/10.1002/andp.19163540702

[5] Einstein, A. (1917) Kosmologische Betrachtungen zur allgemeinen Relativitätstheorie. Sitzungsberichte der Preussischen Akad. d. Wissenschaften.

[6] Eriksson, J.-T. (2018) *International Journal of Physics*, **6**, 38-46.

[7] Eriksson, J.-T. (2019) *International Journal of Physics*, **7**, 16-20. https://doi.org/10.12691/ijp-7-1-3

[8] Eriksson, J.-T. (2021) *International Journal of Physics*, **9**, 240-244. https://doi.org/10.12691/ijp-9-5-3

[9] Eriksson, J.-T. (2020) *International Journal of Physics*, **8**, 64-70.

[10] Eriksson, J.-T. (2021) *International Journal of Physics*, **9**, 169-177. https://doi.org/10.12691/ijp-9-3-4

[11] Eriksson, J.-T. (2022) *International Journal of Physics*, **10**, 144-153. https://doi.org/10.12691/ijp-10-3-3

[12] Pathria, R.K. (1972) *Nature*, **240**, 298-299. https://doi.org/10.1038/240298a0

[13] McBryan, B. (2013) Living in a Low-Density Black Hole.

[14] Brans, C. and Dicke, R.H. (1961) *Physical Review*, **124**, 925-935. https://doi.org/10.1103/PhysRev.124.925

[15] Dirac, P.A.M. (1974) *Proceedings of the Royal Society of London. Series A*, **338**, 439-446. https://doi.org/10.1098/rspa.1974.0095

[16] Perlmutter, S. (2003) *Physics Today*, **56**, 53. https://doi.org/10.1063/1.1580050

[17] Carrol, S. (1997) Lecture Notes on General Relativity. University of Chicago, Chicago.

[18] Davis, T. and Lineweaver, C.H. (2003) Expanding Confusion: Common Misconceptions of Cosmological Horizons and the Superluminal Expansion of the Universe.

[19] Crighton, N. (2015) Make a Plot with both Redshift and Universe Age Axes Using astropy.cosmology. Ipython.display. Cosmological Calculations.

[20] McGaugh, S.S. and Lelli, F. (2016) *Physical Review Letters*, **117**, Article ID: 201101. https://doi.org/10.1103/PhysRevLett.117.201101

[21] Lelli, F., McGaugh, S.S., Schombert, J.M. and Pawlowski, M.S. (2016) *The Astrophysical Journal*, **836**, 152. https://doi.org/10.3847/1538-4357/836/2/152

[22] Milgrom, M. (2014) *Canadian Journal of Physics*, **93**, 107-118. https://doi.org/10.1139/cjp-2014-0211

[23] Eadie, M.G., Springford, A. and Harris, W.E. (2016) Bayesian Mass Estimates of the Milky Way.

[24] Salucci, P. (2017) Dark Matter Strikes Back.

[25] LAMOST Survey (2016) The Milky Way's Rotation Curve out to 100 kpc and Its Constraint on the Galactic Mass Distribution, Press Release November 18, 2016.

[26] BigThinc (2018, Oct. 31).

[27] Adler, R.J. (2010) *American Journal of Physics*, **78**, 925-932. https://doi.org/10.1119/1.3439650

[28] Huchra, J. (2018) Extragalactic Redshifts, NED, NASA/IPAC Extragalactic Database.

[29] Ringermacher, H.I. and Mead, L.R. (2015) *The Astronomical Journal*, **149**, 137. https://doi.org/10.1088/0004-6256/149/4/137

[30] Nemiroff, R. and Bonnell, J. (2013) Astronomy Picture of the Day, APOD.NASA, April 8, 2013.

[31] Reines, A.E. and Volonteri, M. (2015) *The Astrophysical Journal*, **813**, 82.

[32] Chen, Z., Faber, S.M., *et al.* (2020) *The Astrophysics Journal*, **897**, 102.

[33] Taerrazas, B.A., Bell, E.F., Pillepich, A., *et al.* (2020) *Monthly Notices of the Royal Astronomical Society, MNRAS*, **493**, 1888-1906. https://doi.org/10.1093/mnras/staa374

[34] SciTechDaily (2020) How Galaxies Die: New Insight into Galaxy Halos, Black Holes, and Quenching of Star Formation. University of California Santa Cruz, Santa Cruz.

[35] Cano-Diaz, M., *et al.* (2016) *The Astrophysical Journal Letters*, **821**, L26. https://doi.org/10.3847/2041-8205/821/2/L26

Journal of Modern Physics, 2023, 14, 501-525
https://www.scirp.org/journal/jmp
ISSN Online: 2153-120X
ISSN Print: 2153-1196

Comparative Ontology of Theories of Space and Time

Edwin Eugene Klingman

Cybernetic Micro Systems, Inc., San Gregorio, CA, USA
Email: klingman@geneman.com

How to cite this paper: Klingman, E.E. (2023) Comparative Ontology of Theories of Space and Time. *Journal of Modern Physics*, **14**, 501-525.
https://doi.org/10.4236/jmp.2023.144028

Received: February 6, 2023
Accepted: March 20, 2023
Published: March 23, 2023

Abstract

With a few exceptions, physics theories are based in a conception of time and space; our two major theories, general relativity, and quantum field theory, differ in their conceptions. Key issues herein include mathematics, logic, intuition, experiment, and ontology, with emphasis on simultaneity and dimensionality of the world. The treatment is through ontological comparison of two theories, space-time theory (special relativity) and energy-time theory (local absolute space and universal time). These two theories share many of the same equations but have different ontology.

Keywords

Spacetime Ontology, Comparative Ontology, Local Absolute Space, Relativistic Mass

1. Introduction

Ontology is singular. It is the nature of reality. A theory of physics provides mathematico-logical models of reality that assume an ontology. In fact, different theories assume different ontologies; the success of various of these different theories has caused many physicists to dismiss ontology as "unknowable". I propose that comparative ontology is of value to physics and should be part of the measure of validity of any theory. This paper presents a comparative ontology analysis of a space-time theory and an energy-time theory.

It is generally agreed that [1] "…relativity reveals the nature of time to be shockingly different from what had been taken completely for granted." Despite a century of relativity, this still gives rise to discussion and analysis. Recent papers [2] [3] [4] establish a current picture of the nature of time and space considering "the empirical success of special relativity". Despite the mathematically simple nature of the Lorentz transformation basis of special relativity, Rovelli [5]

states that "special relativity is a subtle and conceptually difficult theory." Proportional to associated ontological confusion? Per Thyssen, two debates have been central to philosophy of special relativity:

1) The debate on the conventionality of simultaneity.

2) The debate on the dimensionality of the world.

Both debates have lingered to this day without definite answers and "the link between both debates has remained largely underexplored." I herein identify this link and explore the consequences.

Thyssen states that one of the central questions in the philosophy of special relativity is "the reality question: is only the present real (presentism) or are the past and future equally real (eternalism)? …presentism is a realist thesis …the presentist thesis makes an ontological claim about the nature of time, not epistemological." I review a few recent claims about presentism before addressing issues 1 and 2 above. Golosz [6] examines the relations between presentism and his thesis concerning the existence of "the flow of time". I believe "the flow of energy" relates better to presentism. At every spatial location the present exists, but the change of location, easily measurable, provides a more ontological phenomenon. How does one measure "the flow of time"? Clocks are energy-based and hence the measurement of time is indirect at best. If we continue to observe the flow of energy (matter), it continues to be "the present", and nothing changes that fact. It is unclear ontologically what is meant by the "flow of time" as opposed to present time.

More recently [7] Golosz refutes "Brute Past Presentism" according to which the past is supposed to be both a fundamental and present aspect of reality. This ontological claim addresses the idea that true past-tense claims should not depend on any present aspect of reality. This ontology might be reformulated from "the flow of time" to the "flow of energy"-ontology:

Energy, when it crosses a threshold and effects a change of structure, records information. In essence, the flow of energy halts and the information is present in the record, right now. Information meaningfully exists only in context. For example, "One if by Land; Two if by Sea" is generally meaningless unless one has the context symbolized by Paul Revere. For another example, the context of geological information is geological theories, used to interpret the information. The point being that the past "exists" in the present only through the presence of information assumed recorded in the past and preserved in the present (plus context). This is ontologically compatible with energy-time theory without invoking the "brute past" existence.

The organization of this paper is as follows: In Section 2, we present a mathematical formalism in which two ontological classes are defined: D^{3+1} and 4D spacetime. Section 3 gives a brief overview of time and space ontology. Section 4 introduces the Lorentz transformation in the context of space-time and energy-time theories. In Section 5, both theories relate two inertial frames, primed and unprimed, containing two time entities, t' and t. Via Hestenes' geometric algebra we contrast the meaning of t' in two theories and derive the time dilation

relation for inertial clocks. Section 6 explains inertial mass in space-time physics by considering space-time physics as "slices" of energy-time physics. Section 7 uses two classes of theoretical models: empirical and conceptual, to identify our theories. Section 8 compares simultaneity definitions in space-time physics, and energy-time physics. Section 9 describes the logical error Einstein introduced in "*relativity of simultaneity*" and uncovers the source of this relativity in space-time physics—Thyssen's "largely underexplored" link between "conventionality of simultaneity" and "dimensionality of the world". Section 10 introduces the concept of ontology-dependent measurement and formulates an ontology-dependent example. Section 11 analyzes measurements in space-time specific ontology, formulating a framework that leads to the velocity addition law. Section 12 derives the velocity addition law (violated in particle colliders) with emphasis on ontologically interpreting the experiment. Section 13 discusses concepts of measurement involved in the development of the velocity addition law. Section 14 provides ontological comparison of points developed herein. Section 15 discusses alternate descriptions of ontology, while Section 16 discusses ontological understanding.

2. Does Math Determine Ontology?

Thyssen analyzes Rietdijk-Putnam, Weingard-Petkov and other arguments to the effect that "Special relativity necessitates an eternalist, four-dimensional view of reality." With key aspects still unresolved, he concludes that "special relativity leaves the debate on the dimensionality of the world underdetermined." That is, it is uncertain whether time has a unique dimension and space has three dimensions D^{3+1} or space-time is a 4D reality.

One can develop physics for a D^{3+1} universe (*presentism*) or a 4D universe (*eternalism*) in terms of Hestenes multi-vector $X=(ct+\boldsymbol{x})$ based on one's choice of basic assumptions: absolute space and time D^{3+1} or relative space-time 4D and corresponding choice of how to apply the Lorentz transformation [8]. The $X=(t+\boldsymbol{x})$ formulation is Lorentz compatible, but Lorentz-free energy-time theory based on metaphysical assumptions of absolute space and time and inertial mass yields time dilation physics; contradicting the long-held belief that the empirical fact of time dilation is proof of the theory of special relativity. Per James [9]:

> "Two or more axioms grounded in different ontologies are very likely to prove nothing real about reality, despite having met the proof hurdle within mathematics. (…) mathematics and physics need to be grounded and sorted with ontological consistency, to be able to say anything remotely definitive about reality. …you need to address the ontological landscape your mathematical or physical theory is necessarily, always within/of…"

Hestenes' employed his structure $X=(ct+\boldsymbol{x})$ to yield momentum and energy relations based on Lorentz transformation to obtain 4D special relativity; the same momentum and energy relations are derived without Lorentz transformation, using a D^{3+1} interpretation of his structure as a vehicle to introduce ener-

gy-time theory. Thus, the geometric algebra multi-vector structure $X=(ct+\boldsymbol{x})$ can represent D^{3+1} dimensional physics or 4D physics.

Either we choose metaphysics that supports Lorentz transformation on time and space, or we choose metaphysics of absolute space and time that does not support Lorentz transformation on time and space, but on mass. One choice implies paradoxes, logically unacceptable conclusions; the other choice is paradox-free. The $X=(ct+\boldsymbol{x})$ formalism does not care, physical reality cares.

Analysis of the empirical successes of relativity suggests that time dilation is probably the success most convincing to physicists; we stipulate that time dilation is an established fact, and would remain such had Einstein never existed. The question becomes how to explain time dilation in the classical world of absolute space and time. The physics of absolute space and time produces: $m=\gamma m_0$, $\gamma=\left(1-v^2/c^2\right)^{-1/2}$ and $H=\left(m_0^2c^4+c^2p^2\right)^{1/2}$. Analysis of inertial clocks shows moving clocks slowing down by factor $\mathrm{d}t'=\mathrm{d}t/\gamma$ ($\omega'=\omega_0/\gamma$), *exactly* matching relativistic time dilation. This interpretation of the fact of time dilation ontologically differs from relativity.

3. Brief Overview of Time and Space Ontology

It is the ontology of time and space that we find non-intuitive about special relativity. Historically man intuitively observed that it is always "now", independently of location in space; the present moment was assumed unconnected from space in an ultimate sense. This changed with Einstein's formulation of special relativity. The following brief metaphorical overview of special relativity ignores historical issues of Maxwell-Hertz, Michelson-Morley, and Lorentz transformation [10], in favor of a simple but accurate picture of what Einstein postulated:

> Einstein, observing that a juggler can juggle balls as easily in a uniformly moving railcar as in the railway station, created cartoon worlds to model the situation. Obviously, the laws of physics hold in both worlds else one could not juggle in both. Similarly, spatial coordinates can be mapped onto either world; at rest or moving. However, Einstein provided each world with its own absolute time and space by assigning each world its own universal time dimension, a radical break with the physics of the time. He provided absolute space for each by effectively assigning each world its own "ether", whereby light propagates with speed c in each world. In addition, space-time symmetry means there is no preferred reference frame.

Relativists always formulate their problems in terms of two or more inertial reference frames, each with its own universal time dimension, related by the Lorentz transformation—a geometric transformation in 4D space-time connecting two of Einstein's 4D cartoon worlds.

Each cartoon world in **Figure 1(a)** has its own space and time, and effectively its own ether, imposing the speed of light on local frames and a uniform relative velocity $\boldsymbol{v}$ between them; each frame has 4D dimensionality. **Figure 1(b)** shows

an alternate ontology: D^{3+1}. The big box represents all of space and a universal time dimension covering all of space right now. The two physical frames of interest, one at rest, the other in motion, each have their own spatial map but share a common time. Speed of light is with respect to local absolute space (the big box common to both frames).

4. Analysis of Lorentz in Space-Time and Energy-Time Theories

Part of Einstein's genius lay in intuiting that only if c = constant across all reference frames, can the Lorentz transformation even exist. Moving frames with arbitrary velocity are meaningless unless a universal velocity exists to which they can be compared. While this satisfies 4D geometry, it complicates the physics, essentially providing local absolute space by representing ether through which light propagates in the local frame. If one begins with the photon relation $x = \pm ct$ one can derive $c^2t^2 - x^2 - y^2 - z^2 = 0$. For another photon we have $c^2t'^2 - x'^2 - y'^2 - z'^2 = 0$. If c is constant, then we can relate the two frames in relative motion $v \neq 0$ via the Lorentz group

$$\left(x', y', z', t'\right) = L\left(v, c\right)\left(x, y, z, t\right) \tag{1}$$

and inverse transformation: $L^{-1}\left(v, c\right) = L\left(-v, c\right)$. This group symmetry is characteristic of geometry, and represented by "rotations" in the sense that rotation from $\boldsymbol{x}$ to $\boldsymbol{x}'$ can be reversed by an inverse rotation from $\boldsymbol{x}'$ to $\boldsymbol{x}$. In the same way 3D rotations mix coordinates *x*, *y*, and *z*, relativistic 4D rotations mix three-space and time:

$$x' = \gamma\left(v, c\right)\left(x - vt\right)$$
$$t' = \gamma\left(v, c\right)\left(t - vx/c^2\right) \tag{2}$$

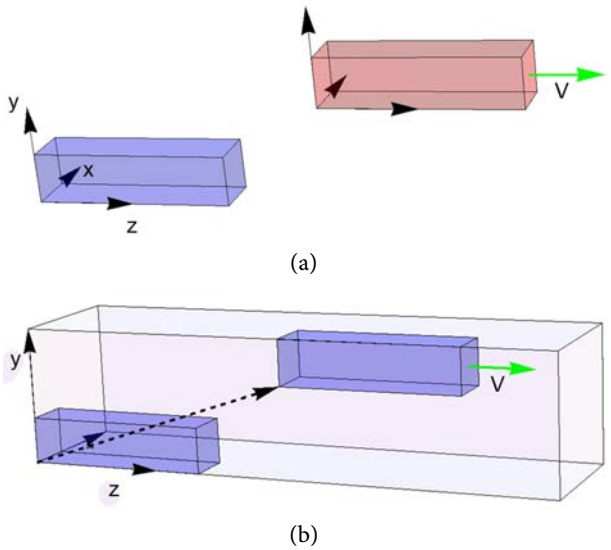

Figure 1. (a) 4D space time ontology; (b) D^{3+1}-ontology of space and time.

This mixing was immortalized by Minkowski: "only a kind of union of [time and space] will preserve an independent reality." The non-intuitive mixing of time and space in 4D is most problematic in relativity, where primed coordinates (x', t') apply in one frame: unprimed coordinates (x, t) in another. To analyze this several questions need be considered: 1) Is c = constant in all frames? 2) What is the meaning of t'? Relativity assumes c = constant in all frames. Classically, this was based on physical properties of the media through which the photon propagates, *i.e.*, the *ether*. Nevertheless, a major contributor to relativity, Rindler [11], saw that in relativity:

> "Each inertial frame now has the properties with which the ether frame had been credited."

Despite that c = constant is necessary for Lorentz to work; it still doesn't make sense. He says of Einstein's postulate: "Light propagates the same in all inertial frames…It is not for us to ask how!" If it made sense, we could ask how; Rindler is admitting that it doesn't make sense.

Ontologically, relativity banishes the medium of ether and replaces it with the proclamation that it is the local space-time coordinate frame that accomplishes the required invariance. Alternatively, energy-time theory assumes the gravitational field is present everywhere in space. Having energy, the field is material and is the medium through which electromagnetic waves and gravitomagnetic waves propagate. General relativistic problems with gravitational energy are treated elsewhere [12]. The recent discovery [13] that both waves propagate with the same speed is compatible with the assumption of an etheric medium. Propagation of light in this local medium is compatible with both Michelson-Morley experiments and Michelson-Gale experiments [14]. A consequence of propagation in local medium is the violation of Einstein's axiom of constant c in all frames and his claim that one cannot detect the speed of the local frame from within the frame.

5. The Meaning of t' in Space-Time Theory and Energy-Time Theory

The space-time ontology derived from Lorentz is based on 4D-geometry; the ability to transfer from one 4D frame (x, y, z, t) to another frame (x', y', z', t') via Equations (1) and (2). In 4D-space-time geometry basic motion is fixed by uniform velocity $\boldsymbol{v}$ between the frames. Einstein's lack of acceleration removes *force* from the picture; the transformation from an event in one frame to its corresponding event in the other frame is independent of mass, so mass does not appear in the Lorentz transformation. To understand the meaning of this we must interpret the meaning of t'.

In space-time theory t' is the time dimension in the primed frame, different from the t dimension in the unprimed frame; incompatible with physicists' intuition while the energy-time definition of t' is that of time measurement, not time dimension. To understand this, we focus on physical mass.

Hestenes, [15] presenting a new math formalism, desired complete compati-

bility with relativity:

> "The entire physical content of the relativity theory has been incorporated into our concept of space-time. It is fully expressed by the Lorentz transformation between inertial systems and the invariant interval between events. No dynamical assumptions are involved."

The curious physicist wonders: if relativistic space-time physics is derivable with no dynamical assumptions, can dynamical physics be derived without space-time assumptions? Time-dilation, the key "proof" of relativity, is derived in the ontology of absolute space and time based on Hestenes' multivector formulation: time dilation obtains; clocks do run slower when moving. We analyze this aspect of time dilation, assuming that mass is a function of velocity $m = m(v)$. Mass will thus be lowest when $v = 0$ and this would imply a preferred frame in which mass is minimized. In D^{3+1}-ontology this describes the rest frame S while 4D-ontology assigns velocity zero to *every* object at the origin of the S inertial reference frame: $m \equiv m_0$. In other words, when relativists transform (x, y, z, t) and $(x, y, z, t)'$ they reset the rest mass: $\begin{bmatrix} x = 0 \\ \dot{x} = 0 \\ m = m_0 \end{bmatrix} \Rightarrow \begin{bmatrix} x' = 0 \\ \dot{x}' = 0 \\ m' = m_0 \end{bmatrix}$.

This establishes the time-space 4D-rotation, at the expense of kinetic energy. Mass is reset to rest mass while distance is shortened, and duration is lengthened according to Lorentz transformation, while according to energy-time 3D-rotation it is inertial mass that is transformed by the inertial factor γ, but time and space are Galilean in nature.

$$\begin{array}{cc} \text{Space-time theory} & \text{Energy-time theory} \\ \left\{ \begin{array}{c} m' = m_0 \\ x' = \gamma(v)(x - vt) \\ t' = \gamma(v)(t - vx) \end{array} \right\} & \left\{ \begin{array}{c} m' = \gamma(v) m_0 \\ x' = x - vt \\ t' = t \end{array} \right\} \end{array} \tag{3}$$

Lucas and Hodgson [16] make a major point about inertial mass: "If we insist on retaining Newtonian dynamics, and the Newtonian definitions of velocity and acceleration, then we can still obtain relativistically correct results if we pay the price of allowing the mass to depend on the velocity." Checking our Hamiltonian, for inertial mass $m = \gamma m_0$, $E = mc^2$ and $\boldsymbol{p} = m\boldsymbol{v}$ we derive:

$$E = \left(m_0^2 c^4 + c^2 p^2\right)^{1/2} \Rightarrow E^2 = m_0^2 c^4 + c^2 p^2 = m_0^2 c^4 + c^2 \gamma^2 m_0^2 v^2$$

$$\Rightarrow E^2 = \gamma^2 m_0^2 c^4$$

$$\frac{E^2}{m_0^2 c^4} = 1 + \gamma^2 \frac{v^2}{c^2} \Rightarrow \gamma^2 = 1 + \gamma^2 \frac{v^2}{c^2} \Rightarrow \gamma = \frac{1}{\sqrt{1 - v^2/c^2}} \tag{4}$$

In D^{3+1}-ontology the velocity $\boldsymbol{v}$ of an object is with respect to rest frame S, local absolute space, and any change of $\boldsymbol{v}$ is via accelerating force: $m\boldsymbol{a} = \mathrm{d}\boldsymbol{p}/\mathrm{d}t = \mathrm{d}(\gamma m_0 \boldsymbol{v})/\mathrm{d}t$ while in 4D-ontology the momentum relation $\boldsymbol{p} = \gamma m_0 \boldsymbol{u}$ is applied where $\bar{u}$ is the velocity of the object in a reference frame, not the velocity of the reference frame relative to another.

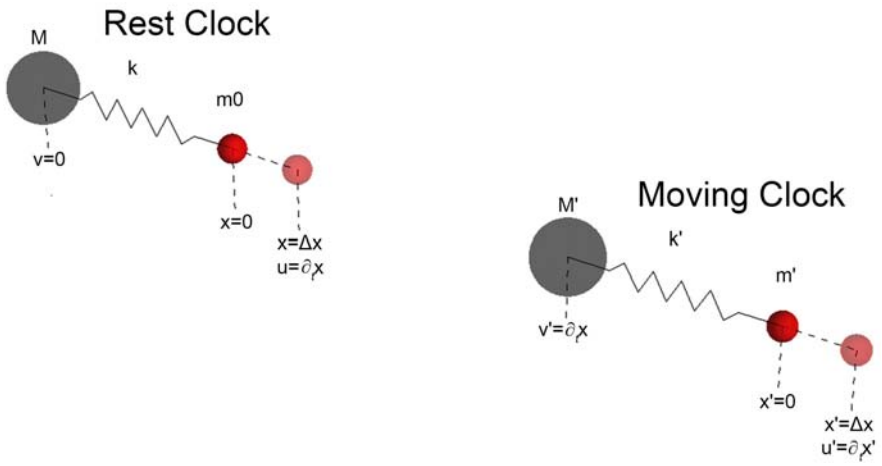

Figure 2. Diagrams with relevant parameters for rest and moving clocks.

D^{3+1}-ontology preserves the spirit of relativity, which is to preserve physics across frames, so we write the physics in S and S' frames:

$$\frac{\mathrm{d}\boldsymbol{p}}{\mathrm{d}t} = -k\boldsymbol{x}\,, \quad \frac{\mathrm{d}\boldsymbol{p}'}{\mathrm{d}t'} = -k'\boldsymbol{x}' \tag{5}$$

"Physics of clocks in absolute spacetime" derives the algebra necessary to equate these two equations in universal time:

$$\frac{\mathrm{d}p'}{\mathrm{d}t'} \Rightarrow \frac{\mathrm{d}^2x'}{\mathrm{d}t^2} + \left(\frac{\omega_0}{\gamma}\right)^2 x' = 0 \Rightarrow \ddot{x}' + \omega'^2 x' = 0 \tag{6}$$

$$\frac{\mathrm{d}p}{\mathrm{d}t} \Rightarrow \frac{\mathrm{d}^2x}{\mathrm{d}t^2} + \omega_0^2 x = 0 \Rightarrow \ddot{x} + \omega_0^2 x = 0 \tag{7}$$

In terms of universal time t, the equation of motion of the rest clock yields frequency ω_0, while the frequency of the moving clock is $\omega' = \omega_0/\gamma$, establishing time dilation for inertial clocks in relative motion in D^{3+1}-ontology. This agrees with physical intuition: increased inertial mass leads to decreased acceleration hence lower velocity; the system slows down. In the rest frame of energy-time theory inertial mass has rest mass m_0. If another frame, initially at rest in our frame, is accelerated to velocity $\boldsymbol{\upsilon}$, its associated inertial mass increases: $m = \gamma(\upsilon)m_0$. Intuition vanishes the moment special relativity is invoked; the space-time symmetry principle forbids preferred frames, so rest mass is not associated with any frame, but with every frame. An observer in the moving frame sees rest mass m_0. The time dilation derived from the physics of clocks in relative motion in D^{3+1}-ontology fails in 4D-ontology, since the no preferred frame axiom of 4D-ontology, given two inertial frames, makes it impossible to tell which is at rest or closer to rest, and therefore, to tell which mass is greater. Thus, relativistic momentum $\boldsymbol{p} = \gamma m_0 \boldsymbol{u}$ is based on $\boldsymbol{u}$ relative to an observer, to distinguish it from relative velocity $\boldsymbol{\upsilon}$ between observers. The two clock mechanisms treated in D^{3+1}-ontology (see Figure 2) are in different frames, differing by velocity $\boldsymbol{\upsilon}$.

6. Mass in Space-Time versus Energy-Time Theory

Einstein essentially invented "slices" of physical reality in which the objects of interest move with uniform velocity with respect to each other. Einstein excluded from his theory the periods of physical acceleration necessary to provide the relative velocity to objects initially at rest in a local frame and mapped 4D-ontology into "slices" of D^{3+1}-ontology as seen in **Figure 3**. The velocity curve shows constant relative velocity of relativity as shaded regions, while the acceleration portions of the curve exist only in D^{3+1}-ontology.

This automatically excludes all inter-frame kinetic energy, allowing him to, impossibly, "reset" the inertial mass of the moving objects to their rest mass by "switching" the observer from one frame to the other (conceptually easy, physically impossible). Formally, this is the result of space-time symmetry, his key postulate that there is no preferred frame, which enables geometric transformation from one frame to the other and back, but makes it is impossible to tell which inertial frame is stationary and which is moving.

The physics of two clocks in absolute space recognizes the difference in kinetic energy, hence equivalent mass; the increased mass is responsible for the moving clocks "slowing down". Time dilation in relativity is not derived from the physics of real inertial clocks operating in universal time but is conceptually tied to different time dimensions in different inertial reference frames. Recognition of the relativistic "reset" $m(\upsilon)\to m_0$ of mass as the basis of the inertial reference frame, may have caused Okun [17] to state "The terminology [relativistic mass] has no rational justification today", while Rindler and others retained it as a useful concept.

The actual nature of the relativistic mass does not change the logic of our argument. An excellent case can be made that the kinetic energy of motion is stored in the C-field circulation induced by $\boldsymbol{p}=m_0\boldsymbol{v}=\int \mathrm{d}^3x\nabla\times\boldsymbol{C}$. The force, $\boldsymbol{F}=\mathrm{d}\boldsymbol{p}/\mathrm{d}t$ ~ change in circulation that accelerates the mass between "slices" changes the momentum, and hence the kinetic energy ~ $\boldsymbol{p}^2/2m$.

7. Theoretical Models

In this paper, we compare two theories, each with its ontology: a theory of absolute time and space, derived from a structure of time and space devised by Hestenes:

> "Everything we know about physical space-time is known through its representation by some model, so when we are thinking about space-time and its properties, we're actually thinking about the model. (…) however, we attribute an independent existence to space-time which might not be accurately represented by our model (…) so we must keep the distinction clear when considering the possibility that the model is wrong."

Since Hestenes' basic structure can be developed in either ontology, we further classify theories according to Crecraft [18], who divides models into empirical and conceptual models:

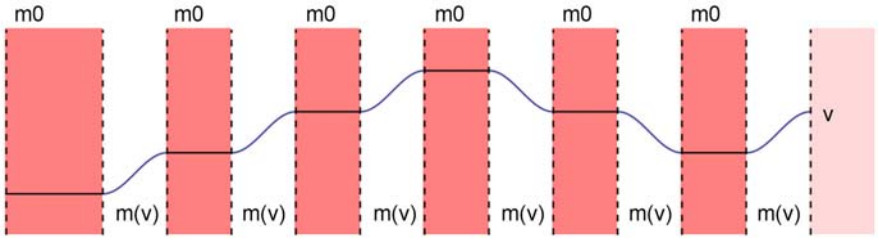

Figure 3. Map 4D-ontology onto "slices" of D^{3+1}-ontology.

"An empirical model starts with the procedure of measurement and observation…an empirical model has no rules of deduction…it uses guesswork, intuition and trial and error to deduce mathematical relationships among the system's observable properties" and lies within the domain of science.

"A conceptual model is an axiomatic system that starts with simple statements and rules of logic that we accept as self-evidently true, and from these it deduces other statements of truth. The postulates are accepted as true, without proof." Therefore, conceptual models exist within the domain of philosophy rather than science.

The space-time theory of relativity is an axiomatic model based on Einstein's relativity axioms, postulates, or principles, which are treated as truth and logic used to deduce other truths. The truths are logical, according to the axioms, but they are non-intuitive (nonsensical) in a physical ontology with acceleration forces, Thyssen declares the debates central to the philosophy of special relativity.

The energy-time theory of universal time and local absolute space is an empirical model, based on measurement and observation, limited to our real objective world. The theory treats time as the intuitive commonsense notion that it is NOW everywhere in the universe, all at once; one moment passes into the next moment; moments in time span the entire three-dimensional space, intuitively jiving with common experience. Measurements that indicate that clocks slow down when moving are compatible with kinetic energy in the empirical model with increasing inertial mass. Similar analysis applies to electromagnetic aspects of relativity. Analysis of measurement in the two theories is presented in the section dealing with velocity addition.

Where does the conceptual relativity model lead? In one example, Mermin posits two opposing trains of moving rocket ships whose various clocks have been "deliberately set out of synchronization"; but observers on the rockets are assured that clocks in other rockets are synchronized. He then contrives a situation in which "occupants of each of the two trains being firmly convinced that it is the clocks on the other train that are running slowly." Mermin concludes that "once one introduces the asynchronized clocks on each train, all the other relativistic effects follow automatically." Whatever his purpose, Mermin concludes about time:

> "…the concept of time is nothing more than a convenient…device for summarizing compactly all relationships holding between different clocks."

In a current relativity paper [19]: "Persons A and B define two distinct inertial frames of reference, corresponding to different spacetime conditions (with) different lengths of meter and durations of second…as predicted by Lorentz." and "Time dilation symmetry arose as a logical deduction of Einstein's 1905 postulates: if two clocks occupying two distinct inertial frames of reference are in relative motion, each one is expected to run slower than the other." However, the authors state that many experiments (including GPS) seem to confirm that time dilation is an asymmetric phenomenon. One might think that experimental contradiction of logical deduction from the axioms would discredit the axioms, but they conclude: "It is assumed that time and 3D space do not exist as separate features of the universe but form a 4D continuum known as spacetime."

So, spacetime theory deduces that each clock runs slower than the other one, while energy-time theory predicts that the accelerated clock will run slower than the rest frame clock. Hafele-Keating experiments resolve the issue experimentally. One can choose a paradox-free empirical theory of absolute local space and universal time with real empirical results, or a paradox-laden conceptual theory of worlds connected by a 4D "universal transformation" between worlds.

8. The Ontology of Simultaneity

Rovelli notes that there is no device that will detect "now", a concept missing from 4D-ontology. Thus, despite that in relativity the concept of simultaneity is replaced by relativity of simultaneity, there is no general means of determining distant simultaneity. Per Rovelli: "Relativity is not the discovery of a new ontology of simultaneity; it is the discovery that there is no fact of the matter, whether two distinct punctual events happen at the same time or not." Einstein chose to invent multiple time dimensions, making use of Lorentz transformation and making a metaphysical commitment, defining 4D space-time symmetry as ontology. If one commits to D^{3+1} with universal simultaneity (*now*) one commits to a metaphysics and defines an ontology—the metaphysical assumptions Thyssen claims are needed to answer the question of reality. Relativity replaces the concept of simultaneity by relativity of simultaneity yet does not present us with ontological fact; it claims that distant simultaneity is not measurable, hence not a provable ontological fact. Neither can Einstein's proposed ontology be measurably proved; we are left with ontological non-facts.

As "simultaneity" is key, we pay particular attention to how Einstein [20] defined simultaneity:

> "we must require a definition of simultaneity such that the definition supplies us with the method by means of which…(we) can decide by experiment whether or not the lightning strokes occurred simultaneously. (…) an observer should be placed at the midpoint [between lightning flashes]. …If

> the observer perceives the two flashes of lightning at the same time, then they are simultaneous."

"are two events (e.g., the two strokes of lightning A and B) which are simultaneous with reference to the railway embankment also simultaneous relatively to the train? …lightning strokes A and B are simultaneous with respect to the embankment [if] the rays of light emitted at the places A and B, where the lightning occurs, meet each other at the midpoint of the length AB…" "Let M' be the *midpoint* of the distance AB on the traveling train. Just when the flashes occur [judged from the embankment] this point M' naturally coincides with the point M, but it moves [toward the right] with the velocity v of the train."

If an observer sitting in position M' in the train did not possess this velocity (then) light rays emitted by the flashes would reach him simultaneously (…) Now in reality (…) he is hastening toward the beam of light coming from B, whilst he is riding on ahead of the beam of light coming from A. Hence the observer will see the beam of light emitted from B earlier than he will see that emitted from A. We thus arrive at the important result:

> "Events which are simultaneous with reference to the embankment are not simultaneous with respect to the train, and *vice versa* (relativity of simultaneity)."

Einstein began by requiring a definition of simultaneity capable of deciding by experiment whether both lightning strikes occurred simultaneously; he solved this problem by placing the simultaneity detector (observer) at the midpoint between the two strokes, A and B. He says:

> "There is only one demand to be made of the definition of simultaneity, namely that in every real case it must supply us with an empirical decision. (…) That my definition [of simultaneity detector] satisfies this demand is indisputable."

It is disputable if one requires a meaningful empirical decision. The detector must be at the midpoint when event detection occurs, not when the event occurred. Ideally, at both occurrences.

9. The Built-In Error: Einstein's "Simultaneity Detector"

Einstein's method is based on the simultaneity detector being exactly at the midpoint between flashes. If this is satisfied, the instrument works perfectly, but, according to him, the instrument on the train is moving away from the midpoint. As soon as the instrument moves away from the midpoint, it ceases to function as a simultaneity detector! It is effectively "broken", and any signal from the broken detector is meaningless. As the detector on the train is not midway between the two lightning strokes when it sees the light from B, it is not a properly working detector and its signal is meaningless. This logic is clear. Einstein defines the perfect instrument and then deviates from the definition. It does not

thereby become merely an imperfect instrument; it becomes an invalid instrument, and its measurements are meaningless as empirical decisions.

> Yet on this basis Einstein proposes to overturn the accepted nature of time as universal simultaneity and replace it with "the relativity of simultaneity".

Perhaps he understood that multiple time dimensions precluded meaningful simultaneity and therefore felt no need to check his logic. However, logical flow is everything in axiomatic theory, and faulty logic [failure to recognize a "broken detector" away from midpoint] appears to lead to the discovery of the "relativity of simultaneity", the hidden false assumption of relativity built into the definition of "inertial reference frame" and the formulation of relativity in at least two frames, hence at least two universal time dimensions. As noted, "there is no fact of the matter, whether the two distant punctual events happen at the same time." The truth of this statement has no bearing on the logical error of Einstein's simultaneity detector. Einstein's logical error in his simultaneity measurement experiment is independent of the dimensionality of the world; the detector is broken whatever the dimensionality. Although one must determine the midpoint of the distant events before one can measure the "simultaneity" this is in general an impossible task. In the very special case of "lightning flashes on railroad", one can substitute manmade flashes for lightning and trigger these from the midpoint; practical issues of signal distribution and timing that must be solved, but these do not correct Einstein's logic error. The unbroken stationary detector is and remains in the station midpoint between the two strikes and judges the strikes to be simultaneous. In summary: only detectors at the midpoint between two luminal events can detect simultaneity.

By defining his faulty "simultaneity detector" instrument and employing it in the station and on the railcar to detect simultaneous lightning flashes, Einstein "derives" the relativity of simultaneity using the broken instrument which moves away from the midpoint. In fact, relativity of simultaneity is not measured or derived, it is assumed, via the definition of each inertial reference frame possessing its own universal time dimension, per Rindler:

> "An inertial frame is one in which spatial relations, as determined by rigid scales at rest in the frame, are Euclidian and in which there exists a universal time…[such that Newton's laws of inertia hold.]"

A century has passed with little notice of the error of Einstein's logic. One assumes that the ontological confusion of 4D combined with empirical successes such as time dilation convinced many that his logic must hold in cartoon worlds. It does not. Relativists have argued for "two sets of lightning strokes", one in the rest frame and one in the moving frame, but Einstein clearly has both simultaneity detectors measuring the same flashes, occurring in the rest frame. Instead of a boxcar, think flatcar, open to the same sky as the rest frame observes. In relativity the moving observer believes he is at rest, so may think he remains at the midpoint, but Einstein explicitly states that he is moving toward one stroke and

away from the other. Relativity of simultaneity follows from multiple time dimensions, not from Einstein's simultaneity detector example, where it is proclaimed. This does not imply that the idea of a simultaneity detector is invalid, only Einstein's use of the detector in his derivation.

In a system where the detector is always at the midpoint of the system, his logic is valid. For example, in Figure 4(a) each frame has mirrored walls with both light source and light detector midway between the mirrors; this system will detect the simultaneity of the flash (from the LED) by registering the simultaneous arrival of the reflected rays at the detector (DET). This is easy to show for a frame at rest, as both rays will travel the same distance, and return to the center at time $t = L/c$. In fact, in energy-time theory, the simultaneity detector works in the moving frame, moving in the local ether of the rest frame. Despite that the light does not move at constant c, but at $c \pm v$, where v is the velocity of the moving frame with respect to the frame at absolute rest, the variable speed light rays (whose speed is dependent on direction) will return to the detector at the same time, $\tau = \frac{L}{c}\left(1-\frac{v^2}{c^2}\right)^{-1}$, where the time depends on velocity. A key principle of special relativity is that one cannot measure velocity v of the frame by *any* experiment performed within the frame, yet that is exactly what we have done:

$$v = \pm c\sqrt{1-\frac{L}{c\tau}}\,. \tag{8}$$

Our simultaneity detector here thus also functions as a velocity meter capable of measuring v.

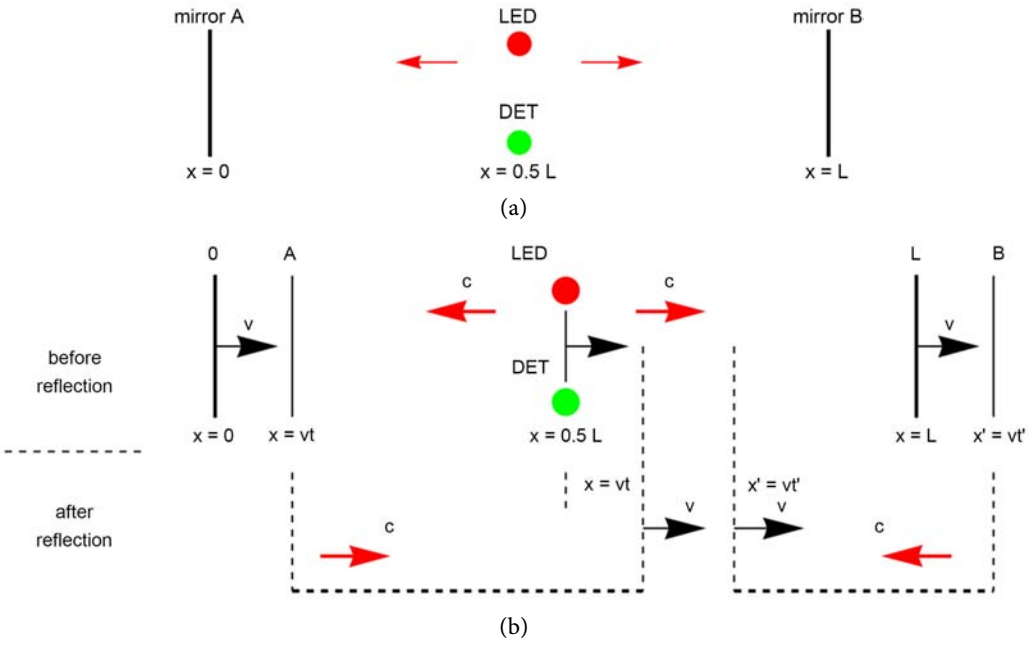

Figure 4. (a) Simultaneity detector system; (b) The system in inertial frame moving with velocity v.

Dace, in [21] argues that Einstein mis-labeled the "relativity of synchrony" as "the relativity of simultaneity" and thereby implied that "this effect concerns an actual difference in times from one frame to another, rather than merely a failure of clock synchronization across frames." From this he concludes that "special relativity fails as a theory of time on the basis of the relativity of simultaneity." Interestingly, he concludes that as a theory of length contraction and time dilation based on frames in relative motion, special relativity is the definitive interpretation of the Lorentz transformation and provides the correct explanation of relativistic phenomena. As analyzed in Sections 4 and 5, we show that "time dilation" in Energy-time theory is simply the slowing of accelerated clocks due to the equivalent mass increase associated with kinetic energy and is not properly a "relativistic phenomenon". Nor is it evident that length contraction actually exists; it has never been measured. In Section 13 we briefly introduce Jefimenko's analysis of "retardation" and "relativity", in which he concludes that relativistic length contraction does not exist.

10. Ontology-Dependent Measurement

Metaphysical assumptions underlying measurements in 4D-ontology versus measurements in D^{3+1}-ontology are ripe for analysis. Relativity excludes acceleration between frames. It has of course been mathematically extended or "continued" into non-inertial domains for reasons of necessity (for instance, the Michelson-Gale experiment), but little or no ontological analysis has been performed in this regard. In either ontology, empirical measurement of inter-frame velocity υ is accomplished using radar and returning pulses are interpreted. Apparent length contraction of the Doppler variety is found, but no Lorentz length contraction. Measuring inter-frame velocity is easy; performing physical measurements inside the moving frame from our rest frame position using meters and time clocks is impossible.

Contrast the 4D-ontology measurement procedure (to be described) with the D^{3+1}-ontology in which both frames are initially at rest in the station, where stationary observers can go inside the railcar measuring distances and durations and calibrating and syncing measurement devices. After the preparation period the railcar is accelerated to velocity v and measurements made. Empirical measurements performed in 3D-space in the stationary frame are real. They are also performed in the moving frame, which has already been measured during preparation.

The following problem illustrates the difference in measurements in 4D space-time theory versus D^{3+1} energy-time theory. A moving frame is assumed to have velocity $\upsilon = 0.9c$ as measured in the stationary frame by the radar method; compatible with both 4D-ontology and D^{3+1}-ontology. The problem is complicated by adding another inertial frame, attached to an object moving inside the moving frame. To be compatible with Leonard Susskind [22] we label the object inside the railcar a "kiddie car" and assume that a third observer exists inside the

kiddie car. The stationary frame is labeled *S*, the railcar is S' and the kiddie car is S''.

11. Measurement in Three Frames in Different Ontologies

In order to contrast energy-time ontology of absolute time and space with space-time ontology of special relativity, we formulate a problem in absolute ontology and compare it with relative ontology as follows: The railway station is located in an absolute spatial frame, *S*, and a local railcar, initially at rest in the station, is accelerated until it reaches velocity υ with respect to *S*. The frame of the moving railcar is S'. Rest frame events are labeled by $(t, \boldsymbol{x})$, but can be relabeled in frame S', now uniformly moving with respect to our absolute rest frame. That is, an x, y, z map located at the origin of the entity (railway car) is in motion with respect to absolute space. From the definition of inertial mass $m = \gamma m_0$ mass becomes infinite as $v \to c$, therefore it is impossible to accelerate any mass to the speed of light despite that how close we *can* come is a function of the energy available for accelerating. Here we assume specifically that we can accelerate the railway car to $0.9c$, 90% of the speed of light. This is certainly legitimate in a universe of absolute time and space.

We then put the kiddie car inside the moving railcar and follow Leonard Susskind's Stanford video series as seen in **Figure 5**. The kiddie car is initially at rest in the railcar, but, after acceleration of the railcar, it will have velocity $\boldsymbol{v}$ in the absolute frame of the railway station. Now we wish to accelerate the kiddie car in the railcar frame.

In our absolute frame (the station) the kiddie car is already moving at $0.9c$ when we begin acceleration relative to the railcar. We cannot increase the speed u of the kiddie car (relative to the railcar) to $0.1c$, else the kiddie car will have been accelerated to light speed in absolute space

$$\upsilon = 0.9c, u = 0.1c \Rightarrow (\upsilon + u) = c. \tag{9}$$

This is *not* the physics of relativity. In relativity, the act of placing the kiddie car inside a moving railcar switches us from D^{3+1}-ontology to 4D-ontology. Susskind says that we can accelerate the kiddie car to at least $0.9c$ relative to the railcar, which is itself moving at $0.9c$ in absolute space. That is, the observer in the relativistic railcar (with $\upsilon = 0.9c$) feels himself to be at rest and places no constraints on the velocity of objects (such as the kiddie car) in his frame. Material objects in his frame can move at any velocity, almost to the speed of light. To limit the velocity because of another "preferred" frame is to violate relativity.

12. Velocity Addition Law

Susskind, in his relativity lecture two, derives the velocity addition law for a "kiddie car" moving with velocity *u* inside a railcar moving with velocity *v* relative to the station. At ~15 minutes he asks what the velocity of the kiddie car, *w*, is with respect to the station, and, based on Lorentz,

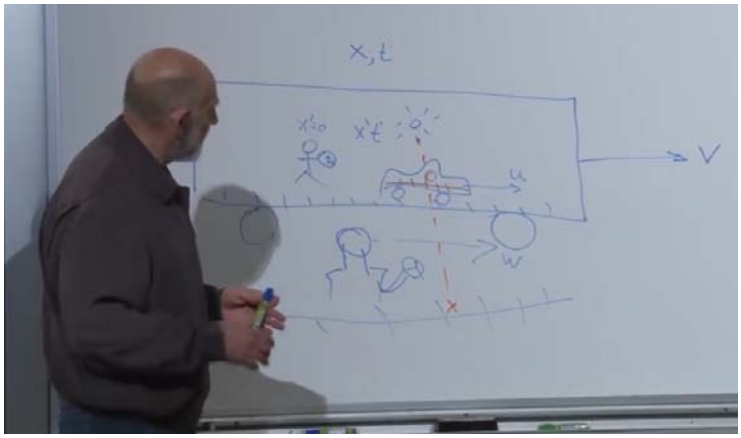

Figure 5. Susskind's formulation of velocity addition law.

$$x' = \frac{x - vt}{\sqrt{1-v^2}} \quad t' = \frac{t - vx}{\sqrt{1-v^2}} \quad c \equiv 1$$

$$x'' = \frac{x' - ut'}{\sqrt{1-u^2}} \quad t'' = \frac{t' - ux'}{\sqrt{1-u^2}}. \tag{10}$$

Plug x' into x'' in terms of t:

$$x'' = \frac{x - vt}{\sqrt{1-v^2}\sqrt{1-u^2}} - \frac{u(t - vx)}{\sqrt{1-v^2}\sqrt{1-u^2}} \Rightarrow \frac{(1+uv)x - (v+u)t}{\sqrt{}\sqrt{}}$$

If $x'' = 0$ we obtain: $x'' = 0 \Rightarrow (1+uv)x = (u+v)t \Rightarrow x = \left(\frac{u+v}{1+uv}\right)t \Rightarrow x = wt$

Thus, in relativity the stationary observer "sees" the kiddie car moving with velocity

$$w = \frac{u+v}{1+uv}.$$

Speed w is how fast the kiddie car can move as "seen from the stationary *frame*". In **Figure 6**, having just developed the law of velocity addition, Susskind shows that relativists believe that addition of velocities v and u cannot reach speed c:

$$w = \left(\frac{u+v}{1+uv/c^2}\right) \Rightarrow \frac{1.8}{1.81}c < c. \tag{11}$$

In Susskind's view, we accelerate a railcar containing a kiddie car to $0.9c$ with respect to the station, *and then* to accelerate the kiddie car to $0.9c$ with respect to the moving railcar. About 27.5 minutes into the lecture, I ask about the meaning of "seen from the stationary frame":

Klingman:

"The stationary observer sees that through the eyes of x'. What if the train had glass walls so that the stationary observer was looking at both?"

Susskind:

"If the train had…assume the train did have glass walls. I don't see how

that…

We're not talking about appearances. We're talking about what measurements of phenomena by meter sticks and by "well-designed clocks" correlate with each other. What somebody sees is much more complicated. For the simple reason that when an event happens, light has to come from the event, and it can be much more complicated what you visually see. We're not talking about which you visually see; we're talking about correlating the locations and times of events in frames of reference which are defined by meter sticks at rest relative to observers and timepieces which are also at rest relative to them.

It doesn't matter what kind of walls the car has; the transformation laws are universal.

Klingman: Consider the *glass wall* aspect of the problem. My intent is to allow us to see reality as it is, with the station, the railcar, and the kiddie car, all of which exist in objective reality. The glass wall implies it is all within our view at once. But in relativity each of the three key entities is replaced by a cartoon world, with no cartoon world preferred. We cannot perform measurements in the moving railcar or kiddie car; we can only transform event coordinates sequentially between frames: $x'' \Leftarrow x' \Leftarrow x$ where $x' = \gamma(v)(x - vt)$, $t' = \gamma(v)(t - vx)$, etc. See Figure 7.

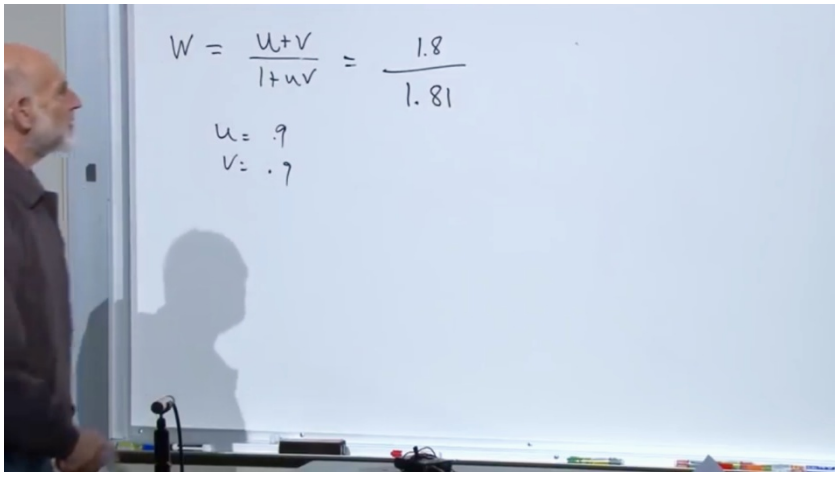

Figure 6. Lorentz summing of velocities.

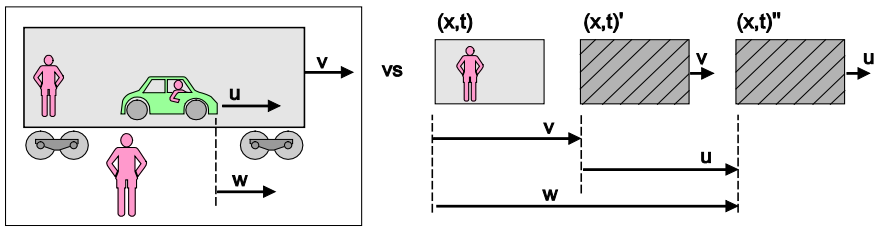

(a) (b)

Figure 7. (a) D^{3+1}-ontology representation; (b) 4D-ontology of special relativity.

My point to Susskind: "The stationary observer [x] sees the kiddie car [x''] through the eyes of x' [observing in the railcar]", whereas I, the stationary observer, want to look directly at the kiddie car with my own eyes (through glass); according to relativists, time runs differently in inertial frames in relative motion. To view, from the station, both inside the railcar and inside the kiddie car, "all at the same time" would violate "relativity of simultaneity".

Contrast the essence of special relativity with the classical idea of universal time: God sees everywhere at one instant of time; time as a one-dimensional parameter appears everywhere throughout classical mechanics, reinforced by direct experience of encompassing a wide region of space with a single glance. The moment we invoke special relativity classical real-world ontology is banished; the cartoon world ontology representing acceleration-free "slices" of the real world becomes dominant. Relativistically, in the frame of the station, we observe the railcar; we cannot observe the interior of the moving railcar. To observe the interior of the rail car we must invoke the observer in the moving railcar. Relativity sees only one frame at a time via application of the Lorentz transformation; "deeper" frames are invisible to the observer; in every cartoon world the mass can move at any speed less than c. Hence $\upsilon = 0.9c$ and $u = 0.9c$ make sense in relativistic ontology, in which one effects the critical trade-off of relativity:

Universal time and universal space $\Rightarrow$ universal transformation on cartoon worlds.

Per Susskind [23]: "Special relativity…is counter-intuitive…full of paradoxical phenomena."

> "A paradox is a statement that, despite apparently sound reasoning from true premises, leads to an apparently self-contradictory or logically unacceptable conclusion." Wikipedia

Relativists give up an absolute universe with universal time and space for a universal transformation on geometric 4D worlds. Not asking what reality looks like all at once (through glass walls) they show that one can transform from one cartoon world and back, as often as desired, and as deeply as one wishes, effectively looking "through" a sequence of nested inertial frames. Moving reference frames are not accessible by us; at best we can measure x' radar-like but we, in our own rest frame S, cannot perform measurements in moving frame S'. When compounded by the introduction of another moving frame S'' we cannot perform any measurements from S in S''; in relativity we are not even allowed to *see* S''. By transforming a real physical railcar to a cartoon world, one resets laws of physics in a way that only an extended period of training makes tolerable. Per Mermin: "some of the things…are hard to believe at first." They are eventually accepted by relativists who have learned to think in cartoon worlds. Per Smolin: [24]

> "To learn relativity is to experience a transition from one way of mentally organizing the world to another."

In contrast, there is nothing paradoxical about the energy-time perspective,

based on universal time and space, it's just that we are forbidden to look at it when we invoke relativity to solve a problem. For instance, Rindler notes that the special relativistic treatment of velocities is problematical:

> "Thus, if a light signal recedes from me and I transfer myself to ever faster moving frames in pursuit of it, I shall not alter the velocity of that light signal relative to me by one iota. This is totally irreconcilable with our classic concepts of space and time."

Thus, universal light speed enables the use of Lorentz rotations on cartoon worlds and Lorentz transformation prevents an object (or frame) from equaling or exceeding the speed of light. However, Cannoni [25] observes that the law of velocity addition is not absolute:

> "Explicitly or tacitly, in high-energy physics literature it is an accepted fact that the relative velocity of two particles can be larger than the velocity of light. …this is a macroscopic violation of the principles of relativity."

If reality violates relativity, then relativistic ontology is false. The "velocity addition law" has no problem with the Lorentz transformation *math*; the problem is ontological, *i.e.*, physical reality. Yet, believing that these procedures represent real measurements, and employing mathematical logic, relativists deduce the truth of the velocity addition law from the *axioms* and end up believing that the railcar can be given $\upsilon = 0.9c$ with respect to the station *and* that the kiddie car can exist in the railcar with velocity (relative to the railcar) $u = 0.9c$ and that kiddie car is prevented from going $w(\upsilon, u) = c$ with respect to the rail station. This view is logically perfect, and physically absurd: ($\upsilon = 0.9c$, $u = 0.9c$) instead of ($\upsilon = 0.9c$, $u < 0.1c$). In D^{3+1}-ontology we can measure the velocity of S' and S'' from absolute frame *S*. In 4D-ontology we can measure the velocity of S' from *S* but cannot measure the velocity of S'' from *S*, as there is no radar mechanism that matches the value obtained via the relativistic velocity addition law.

13. Aspects of Relativistic Ontology

Einstein's axioms provide a well-defined conceptual model that is not empirical. Why do physicists seem to view it as if it were empirical? Susskind states that we are: "correlating locations and times of events in frames of reference which are defined by meter sticks at rest relative to observers and timepieces which are also at rest relative to them."

In relativity observers in cartoon worlds make measurements via identical meter sticks and clocks in their rest frame as we have in our rest frame; measurements are correlated through Lorentz transformation effecting a 4D geometric rotation on (x, y, z, t) into $(x, y, z, t)'$ to transform our meter stick into the moving frame where it can conceptually make measurements. We cannot reach into a moving frame to measure anything, but our meter sticks measure distance differences $x_1 - x_0$ (1 meter) and time differences $t_1 - t_0$ (1 second) in our rest frame; these standard differences for measuring space and time in reali-

ty can be Lorentz transformed as coordinates into a moving cartoon frame in which moving rods become shorter, moving clocks stretch time. Relativists accept abundant evidence of time dilation as proof of relativity and assume length contraction to also be true, generally unaware that clock slowing can occur in local absolute space.

Jefimenko [26] concludes that "…as a physical phenomenon relativistic length contraction does not exist." Initially, length contraction was assumed to represent an effect on a body moving through the ether. However, while rejecting the reality of ether, Einstein accepted length contraction of moving bodies as an observable effect. But length contraction has never been measured, and, per Rindler, probably never will be. The math of Lorentz transformation suggests that to compensate for *time increasing* in a moving system, it is necessary for space to decrease, *i.e.*, length to contract. In Energy-time theory time does not increase; the measure of time, based on physical clocks slowing down, explains why "moving clocks run slower".

14. Ontological Comparison

We have two theoretical models, an empirical model based on measurements in absolute space and time and a conceptual model based on axioms that assume the existence of multiple time dimensions; acceptance of either model generally implies that the other ontology is not to be taken seriously. If we believe that $\upsilon = 0.9c$ and $u = 0.9c$ makes sense, then their sum is prevented from exceeding the speed of light in the conceptual model. If we believe that $\upsilon = 0.9c$ implies that $u \le 0.1c$ then we do not take seriously nested velocities of $\upsilon_j = 0.9c$. Nevertheless, the existence of two theories of space and time suggests F Scots Fitzgerald's remark:

> "The test of a first-rate intelligence is the ability to hold two opposed ideas in mind, at the same time, and still retain the ability to function."

concerning the ability to hold two ontologies in mind at the same time and retain the ability to function. By function we mean solve problems in either ontology, with its corresponding theory.

Relativity yields length contraction, energy-time theory does not. Relativity is space-time symmetric; energy-time theory specifies a preferred frame. The relativistic observer cannot detect his velocity from within his frame, whereas energy-time theory does allow measurement of absolute local velocity. Both theories agree on "time dilation", but the physical explanations differ.

Most significant: definitions of inertial mass, energy-momentum relations, and the Hamiltonian are the same, whether derived in the energy-time physics of absolute time and space or in Einstein's worlds governed by space-time physics of special relativity! An organized comparison in **Table 1** shows that, with some qualifications, features of reality exactly match the features of the Energy-time theory of physics, whereas only the Hamiltonian and the clock slowing of space-time theory agree with reality.

Table 1. Ontological features of theories of space and time.

Feature of theory	Space-time	Energy-time	Reality	Remarks
Relativistic mass: $m = \gamma m_0$	-	+	+	
Time dilation = f(direction)	-	+	+	Hafele-Keating experiments
Hamiltonian: $E = \left(m_0^2 c^4 + c^2 p^2\right)^{\frac{1}{2}}$	+	+	+	Derived in Hestenes' calculus
Time dilation (clock slowing)	+	+	+	All experiments
Speed $c = c'$ (in all frames)	+	-	-	Michelson-Gale experiments
Length Contraction	+	-	(-)	Unmeasured, unlikely
Time dilation (symmetric)	+	-	-	GPS experiments, etc.
Velocity Addition Law	+	-	-	Cannoni
No preferred frame	+	-	-	Michelson-Gale experiments
Past-present-future	+	-	(-)	Unmeasured, unlikely 4D
Twin paradox	+	-	-	
Barn/pole paradox	+	-	-	
Grandfather paradox	+	-	-	

Assumptions made in Table 1 concerning features of reality: if reality is unknown because unmeasured, the believed state of reality is in parentheses. All paradoxes are assumed to be unreal.

15. Alternate Descriptions of Ontology

The comparison between space-time physics (special relativity) and energy-time physics (absolute space and time) clearly contrasts major aspects of the theories but does not exhaust the possibilities. For example, consider Jefimenko's work: rather than formulate a new theory, Jefimenko simply observes that, since electric and magnetic fields propagate with finite velocity, there is always a time delay before electromagnetic conditions initiated at a point of space can produce an effect at any other point of space. The time delay is called electromagnetic retardation. Evolved from Maxwell's equations, this leads to electromagnetic relations that are customarily considered to constitute consequences of Einstein's relativistic electrodynamics.

In fact, all the fundamental equations of the theory of relativity are derived in a natural and direct way from the equations of electromagnetic retardation, without any postulates, conjectures, or hypotheses. This essentially unites Maxwellian electromagnetics, electromagnetic retardation, and the theory of relativity into a simple, clear, and harmonious theory of electromagnetic phenomena and of mechanical interaction between moving bodies and exposes certain errors in the interpretation and use of Einstein's special relativity. Jefimenko's retarded theory does not use the Lorentz contraction yet yields relativistically correct fields of the charge. He attributes this to the fact that, as a physical phenomenon, the relativistic (kinematic) Lorentz contraction does not exist. It is merely a ma-

thematical transformation between two cartoon worlds as we have shown.

16. Ontological Understanding

There is much confusion about ontology in modern physics; in the case of special relativity theory, this is understandable. Einstein essentially invented an ontology, best described as cartoon worlds, each with its own time dimension and each with an "ether equivalent" that guarantees the same speed of light in every cartoon world. Relative velocity between worlds can be any $\upsilon < c$, but this is meaningless unless there exists a velocity common to all cartoon worlds. By declaring c = constant for all worlds, Einstein made possible the factor $\gamma = \gamma(\upsilon, c)$ that allows one to correlate clocks in cartoon worlds via Lorentz, but he did so in an ontologically confusing way.

> Note that Einstein did not state an axiom to the effect that multiple time dimensions exist; nor did he clearly state this as an assumption! His key assumption is buried in the definition of inertial reference frame, and every problem in special relativity is formulated in terms of two such frames in relative motion, building in the false assumption of multiple time dimensions in a way that usually goes unnoticed. Einstein assumed the relativity of simultaneity, ostensibly based on his "simultaneity detector" but actually based on his definition of inertial reference frames as possessing separate time dimensions.

Many physicists seem not to think much about ontology; some explain non-intuitive paradoxes as: "our brains did not evolve to understand high-speed." The difference between D^{3+1} or 4D is often viewed as mathematical, rather than as physical reality. McEachern [27] comments:

> "…Planck observed a century ago, the problem is, theoretical physicists are not particularly adept at identifying that some things even are assumptions; with the result that 'self-evidently true' facts lead to long periods of stagnation, until these 'facts' are eventually shown to be just idealistic false assumptions."

Energy-time theory predictions differ from space-time theory: based on measurements, they tend to show the multiple time dimensions of cartoon worlds to be idealistic false assumptions. Energy-time theory derives clock slowing of time dilation as an energy aspect of reality, not as evidence of multiple time dimensions. Why then do particle physicists insist upon Lorentz transformation? Lorentz effectively ensures that inertial factor γ governs relativistic mass relations. By building the transformation into the Lagrangian, relativistic mass is properly handled; associated length contraction effects do not come into play. D^{3+1}-ontology physically accounts for relativistic energies without length contraction.

Einstein said of space and time and ether: "There is no such thing as empty space, *i.e.*, a space without a field. Space-time does not claim existence on its

own, but only as a structural quality of the field." Laurent Field [28] recently expressed this: "Spacetime is just an abstraction… I believed all my life that spacetime exists, but I no longer do so." Ohanian and Ruffini [29]: "The gravitational field may be regarded as the material medium sought by Newton…". In other words, the gravitational field is the medium through which electromagnetic waves and gravitomagnetic waves travel at the speed of light. As Einstein noted, the gravitational field functions as the ether, a key assumption underlying energy-time theory.

This analysis has focused on ontology, not math, and we have discussed two "ontologies". Ontology is a synonym for reality and there is only one physical reality, hence: two mathematic-based structures can co-exist for quite a while, but only one ontology exists.

Conflicts of Interest

The author declares no conflicts of interest regarding the publication of this paper.

References

[1] Mermin, D. (2005) It's about Time. Princeton University Press, Princeton. https://doi.org/10.1515/9781400830848

[2] Rovelli, C. (2019) *Foundations of Physics*, **49**, 1325-1335. https://doi.org/10.1007/s10701-019-00312-9

[3] Thyssen, P. (2019) *Foundations of Physics*, **49**, 1336-1354. https://doi.org/10.1007/s10701-019-00294-8

[4] Ben-Yami, H. (2019) *Foundations of Physics*, **49**, 1355-1364. https://doi.org/10.1007/s10701-019-00306-7

[5] Rovelli, C. (2017) Reality Is Not What It Seems. Penguin Random House, New York.

[6] Golosz, J. (2017) *Axiomathes*, **27**, 285-294. https://doi.org/10.1007/s10516-016-9305-3

[7] Golosz, J. (2021) *Axiomathes*, **31**, 211-223. https://doi.org/10.1007/s10516-020-09489-5

[8] Klingman, E. (2020) *Journal of Modern Physics*, **11**, 1950-1968. https://doi.org/10.4236/jmp.2020.1112123

[9] James, J. (2020) The Misalignment Problem. FQXi Essay. https://fqxi.org/community/forum/topic/3360

[10] Klingman, E. (2018) Everythings's Relative, or Is It? http://vixra.org/pdf/1812.0424v1.pdf

[11] Rindler, W. (1991) Introduction to Special Relativity. 2nd Edition, Oxford Science Pub., Oxford.

[12] Klingman, E. (2022) *Journal of Modern Physics*, **13**, 347-367. https://doi.org/10.4236/jmp.2022.134025

[13] Abbott, B., *et al.* (2017) *Physical Review Letters*, **119**, Article ID: 161101.

[14] Michelson, A. (1925) *The Astrophysical Journal*, **61**, 137. https://doi.org/10.1086/142878

[15] Hestenes, D. (1986) New Foundations for Classical Mechanics. 2nd Edition, Kluwer Academic Pub., Dordrecht. https://doi.org/10.1007/978-94-009-4802-0

[16] Lucas, J. and Hodgson, P. (1990) Space-Time and Electromagnetism. Clarendon Press, Oxford.

[17] Okun, L. (2008) The Concept of Mass. https://arxiv.org/pdf/hep-ph/0602037.pdf

[18] Crecraft, H. (2020) On the Decidability of Determinism…. FQXi. https://fqxi.org/community/forum/topic/3395

[19] Ferreira, R. (2022) *Journal of Modern Physics*, **13**, 1184-1196. https://doi.org/10.4236/jmp.2022.138069

[20] Einstein, A. (1951) Relativity. Crown Publishers, New York.

[21] Dace, T. (2022) *Axiomathes*, **32**, 199-213. https://doi.org/10.1007/s10516-021-09594-z

[22] Susskind, L. (2012) Relativity Lecture #2. https://www.youtube.com/watch?v=qfTJP7Soto4

[23] Susskind, L. (2017) Special Relativity and Classical Field Theory. Basic Books, New York.

[24] Smolin, L. (2014) Time Reborn. Mariner Pub., Boston.

[25] Cannoni, M. (2016) Lorentz Invariant Relative Velocity…. https://arxiv.org/pdf/1605.00569.pdf

[26] Jefimenko, O. (2004) Retardation and Relativity. Electret Scientific, Star City.

[27] McEachern, R. (2020) Comments on Hossenfelder's Essay Page.

[28] Field, L. (2021) Conversations on Quantum Gravity. Cambridge University Press, Cambridge.

[29] Ohanian, H. and Ruffini, R. (2013) Gravitation and Spacetime. 3rd Edition, Cambridge University Press, Cambridge. https://doi.org/10.1017/CBO9781139003391

Journal of Modern Physics, 2023, 14, 526-533
https://www.scirp.org/journal/jmp
ISSN Online: 2153-120X
ISSN Print: 2153-1196

Design of Four-Channel Demultiplexer Based on Whispering-Gallery Mode Resonators

Ximeng Feng, Jinsong Huang*, Hongwu Huang

School of Information Engineering, Jiangxi University of Science and Technology, Ganzhou, China
Email: *jshuangjs@126.com

How to cite this paper: Feng, X.M., Huang, J.S. and Huang, H.W. (2023) Design of Four-Channel Demultiplexer Based on Whispering-Gallery Mode Resonators. *Journal of Modern Physics*, **14**, 526-533.
https://doi.org/10.4236/jmp.2023.144029

Received: February 20, 2023
Accepted: March 21, 2023
Published: March 24, 2023

Abstract

A new four-channel demultiplexer of single photons is proposed, in which four microresonators are utilized to link the four drop waveguides and the bus waveguide. By adjusting the system parameters, the crosstalk effect of the multiple channel frequencies is suppressed, and multiple peak frequencies with high drop efficiencies in these output ports are achieved. As the 2 × 2 model is scalable, the proposed structure can provide potential applications in designing scalable optical devices.

Keywords

Optical Filtering, Scattering Theory, Optical Waveguide, Microresonator

1. Introduction

Optical drop filters are the important components in optical communication systems, as they have been employed as demultiplexers, routers, switches, etc. During the last decade, numerous researches on optical filtering has been performed in various systems, such as Bragg grating systems [1]-[6], photonic crystal structures [7]-[15], plasmonic systems [16] [17], and waveguide coupled microresonator systems [18] [19] [20] [21] [22], and so on. Specifically, whispering-gallery mode resonators as filter elements have drawn much concern due to their microscale sizes and ultra-high quality factors [23]. Using such a filter with very-low loss, the expected frequency with very-high drop efficiency can be transferred and selected from the bus waveguide to the drop waveguide.

As a scalable application of single channel filters, multi-channel filtering [24] [25] [26] [27] [28] has aroused wide attention, because the demultiplexer with multiple user ports can be used to implement multiplexing communication. However, the quality of transmission signals will be damaged by the crosstalk effect of

these signals, and thus it is of considerable interest to design a multi-channel demultiplexer with high drop efficiency and low crosstalk for a communication network.

Motivated by the above considerations, we propose a four-channel demultiplexer in which four drop waveguides are connected to a bus waveguide via intermediate coupled microresonators. By using the real-space approach, the scattering amplitudes of single photons in these output ports of drop waveguides are derived. Numerical results show that the crosstalk of the multiple central frequencies can be suppressed by increasing the inter-resonator detuning, and multiple peak frequencies with high drop efficiencies in these channels are realized by controlling the waveguide-resonator couplings. In contrast to the common schemes [7] [8] [9] requiring a reflector to reflow the forward photons and get more high drop efficiencies, the proposed structure needs no reflection feedbacks, due to the mode-direction matching between the photon and resonator modes. Moreover, the resonators are independent on their exact locations, which is helpful to save the placement spaces. The proposed compact demultiplexer as a module is easy to be extended to scalable devices, and therefore it can be applied in wavelength division multiplexing systems.

2. Theoretical Model

As displayed shown in **Figure 1**, a four-channel demultiplexer of single photons is constructed by a bus waveguide and four drop waveguides, and these waveguides are linked by four single-mode whispering-gallery resonators. These resonators are described by the creation operator $e_n^\dagger$ ($n=1,2,3,4$), with the resonance frequency ω_n. The coupling strength between four resonators and the bus waveguide is denoted as V_{an}. Similarly, V_{bn} describes the coupling strength between these resonators and these drop waveguides, respectively. When a single photon is incident from the left port of the bus waveguide, it is coupled to these resonators, and then dropped to these drop waveguides.

The total Hamiltonian via the real space approach [29] for the filtering system can be given by ($\hbar=1$)

$$\begin{aligned} H = & \sum_{n=1,2,3,4}\int \mathrm{d}x\left[-i\upsilon_g C_R^\dagger(x)\frac{\partial}{\partial x}C_R(x)+i\upsilon_g C_{Ln}^\dagger(x)\frac{\partial}{\partial x}C_{Ln}(x)\right] \\ & +\sum_{n=1,2,3,4}(\omega_n-i\gamma_n)e_n^\dagger e_n+\sum_{n=1,2}V_{an}\int \mathrm{d}x\delta(x)\left[C_R^\dagger(x)e_n+C_R(x)e_n^\dagger\right] \\ & +\sum_{m=3,4}V_{am}\int \mathrm{d}x\delta(x-d)\left[C_R^\dagger(x)e_m+C_R(x)e_m^\dagger\right] \\ & +\sum_{n=1,2}V_{bn}\int \mathrm{d}x\delta(x)\left[C_{Ln}^\dagger(x)e_n+C_{Ln}(x)e_n^\dagger\right] \\ & +\sum_{m=3,4}V_{bm}\int \mathrm{d}x\delta(x-d)\left[C_{Lm}^\dagger(x)e_m+C_{Lm}(x)e_m^\dagger\right]. \end{aligned} \tag{1}$$

Here, $C_R^\dagger(x)$ represents the generation of a right-moving photon at x in the bus waveguide, while $\left[C_{Ln}^\dagger(x)\right]$ represents the generation of a left-moving photon at x in the drop waveguide-n. υ_g denotes the group velocity of the

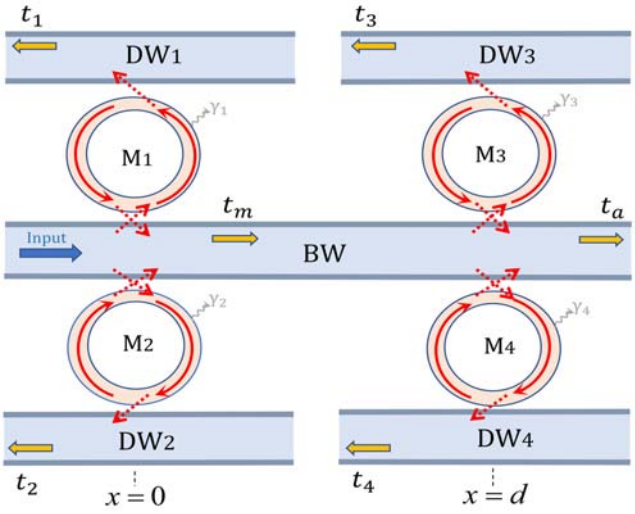

Figure 1. (Color online) Schematic view of a 2 × 2-shaped demultiplexer consisting of a bus waveguide (BW) and four drop waveguides (DWs), and four coupled single-mode whispering-gallery resonators. The input photon from the left side of the bus waveguide will be coupled to four microresonators (Mn), and transferred to four ports of these drop waveguides.

propagating photon. $\delta(x)\left[\delta(x-d)\right]$ means that the resonator-waveguide interaction occurs at $x=0(d)$. γ_n stands for the energy loss for these resonators.

The eigenstate of the Hamiltonian (1) is expressed as

$$|\psi\rangle=\int \mathrm{d}x\left[\phi_{R_a}C_{R_a}^{\dagger}+\phi_{L1}C_{L1}^{\dagger}+\phi_{L2}C_{L2}^{\dagger}+\phi_{L3}C_{L3}^{\dagger}+\phi_{L4}C_{L4}^{\dagger}\right]|\phi\rangle+\sum_{n=1,2,3,4}\xi_n e_n^{\dagger}|\phi\rangle, \quad (2)$$

$\phi_R(x)$ and $\phi_{Ln}(x)$ describe the single-photon wave functions along the right direction in the bus waveguide and the left direction in the drop waveguides, respectively. $|\phi\rangle$ describes the vacuum states of all waveguides and resonators. ξ_n represents the excitation amplitudes of these resonator modes.

The according wave functions can be described as

$$\begin{aligned}
\phi_{Ra} &= \mathrm{e}^{ikx}\left[\theta(-x)+t_m\theta(x)\theta(d-x)+t_a\theta(x-d)\right],\\
\phi_{L1} &= \mathrm{e}^{-ikx}t_1\theta(-x),\\
\phi_{L2} &= \mathrm{e}^{-ikx}t_2\theta(-x),\\
\phi_{L3} &= \mathrm{e}^{-ikx}t_3\theta(d-x),\\
\phi_{L4} &= \mathrm{e}^{-ikx}t_4\theta(d-x),
\end{aligned} \quad (3)$$

where, t_n represents the transmission amplitudes for four ports in these drop waveguides, and t_m and t_a represent the transmission amplitudes behind $x=0$ and $x=d$ in the bus waveguide, respectively. $\theta(x)$ denotes the Heaviside step function, with $\theta(0)=1/2$.

Suppose that a single photon is incoming from the left side of the bus waveguide with the energy $E_k=\omega$. By solving the eigen-equation $H|\psi\rangle=E_k|\psi\rangle$, these transmission amplitudes can be obtained as follows:

$$
\begin{aligned}
t_m &= 1-\frac{2iQ_2\Gamma_{a1}+2iQ_1\Gamma_{a2}+4\Gamma_{a1}\Gamma_{a2}}{Q_1Q_2+\Gamma_{a1}\Gamma_{a2}},\\
t_a &= t_m\left(1-\frac{2iQ_4\Gamma_{a3}+2iQ_3\Gamma_{a4}+4\Gamma_{a3}\Gamma_{a4}}{Q_3Q_4+\Gamma_{a3}\Gamma_{a4}}\right),\\
t_1 &= -\frac{2i\sqrt{\Gamma_{a1}\Gamma_{b1}}\left(Q_2-i\Gamma_{a2}\right)}{Q_1Q_2+\Gamma_{a1}\Gamma_{a2}},\\
t_2 &= -\frac{2i\sqrt{\Gamma_{a2}\Gamma_{b2}}\left(Q_1-i\Gamma_{a1}\right)}{Q_1Q_2+\Gamma_{a1}\Gamma_{a2}},\\
t_3 &= -\mathrm{e}^{2ikd}t_m\frac{2i\sqrt{\Gamma_{a3}\Gamma_{b3}}\left(Q_4-i\Gamma_{a4}\right)}{Q_3Q_4+\Gamma_{a3}\Gamma_{a4}},\\
t_4 &= -\mathrm{e}^{2ikd}t_m\frac{2i\sqrt{\Gamma_{a4}\Gamma_{b4}}\left(Q_3-i\Gamma_{a3}\right)}{Q_3Q_4+\Gamma_{a3}\Gamma_{a4}},
\end{aligned}
\tag{4}
$$

Here, $Q_n=\Delta\omega_n+i\gamma_n+i\Gamma_{an}+i\Gamma_{bn}$, $\Gamma_{an}=V_{an}^2/\left(2\upsilon_g\right)$, and $\Gamma_{bn}=V_{bn}^2/\left(2\upsilon_g\right)$. Generally, the transition frequencies of these resonators are different. Thus, we introduce these detunings as $\Delta\omega=\omega-\omega_{c1}$, which is the frequency detuning between the incident photon and the resonator-1, and $\Delta\omega_{1n}=\omega_1-\omega_n$, which is the frequency detuning between the resonator-1 and resonator-n. Then, $Q_n=\Delta\omega+\Delta\omega_{1n}+i\gamma_n+i\Gamma_{an}+i\Gamma_{bn}$ is rewritten for the sake of simplification.

3. Filtering Properties of Single Photons in the Coupled System

To characterize the filtering properties of the proposed system, we will investigate the transmission in the coupled system, which is denoted as $T_{a(1,2,3,4)}=\left|t_{a(1,2,3,4)}\right|^2$. As a contrast, we first consider the single-resonator case that only the drop waveguide-1 is coupled to the bus waveguide. When a single photon is incident from the left side of the bus waveguide, it will pass through the bus waveguide, or transmits to the left port of the drop waveguide-1 under the mode-direction matching condition between the resonator and waveguide modes.

Figure 2 displays the filtering spectra of single photons for different waveguide-resonator couplings when no dissipations are assumed. As shown from the green straight line, the total photon flow relation $T_a+T_1=1$ for two ports remains unchanged for any input frequencies. Moreover, a single drop peak for T_1 with maximal drop efficiency of 1 is represented at the resonance point $\Delta\omega=0$, for the equal waveguide-resonator couplings $\Gamma_{b1}=\Gamma_{a1}$. This means that the resonator behaves as a perfect mirror, and the moving photon along the bus waveguide is completely reflected on resonance, as investigated in Ref. [18]. To further examine the dependence of the drop efficiency on the couplings, the ratio $R=\Gamma_{b1}/\Gamma_{a1}$ is used to show their relationship in **Figure 2(d)**. It can be found that T_1 can get the maximum drop efficiency of unity only for $R=1$, arising from the fact that two same coupled routes between the resonators and waveguides are formed for two equal couplings, and thus the whole transfer over the two routes can be achieved.

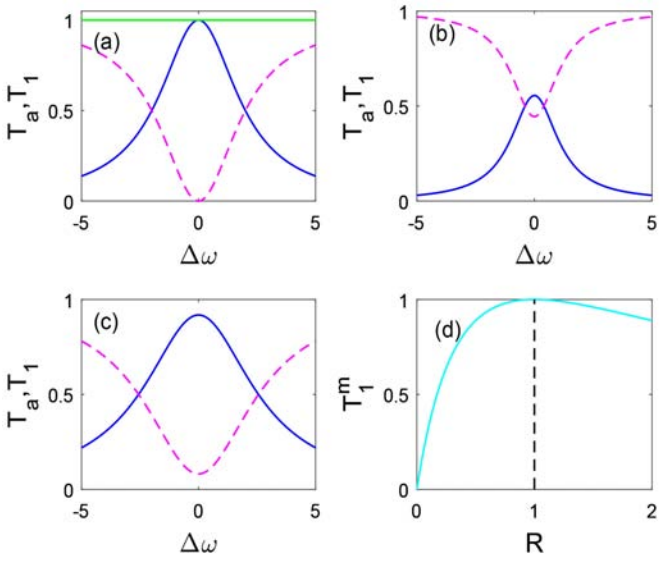

Figure 2. (Color online) The transmission T_a (pink dashed lines) and the drop efficiency T_1 (blue solid lines) for different coupling ratios: (a) $P=1$, (b) $P=0.2$, and (c) $P=1.8$. (d) The maximal drop efficiency T_1^m as a function of the coupling ratio *R*. Zero dissipation ($\gamma_1=0$) is assumed. For convenience, all the parameters are in units of Γ_{a1}.

When more waveguides are coupled to the bus waveguide through the coupled resonator, more transmission channels are generated. Consequently, the crosstalk emerges owing to the quantum interference from different transmission signals, which reduces the drop efficiencies of the filtering waves. The optical spectra in two output ports for the detuning $\Delta\omega$ are shown in **Figure 3(a)**, where two drop peaks with the central frequencies of $\Delta\omega_1$ and $\Delta\omega_2$ are presented. When tuning the inter-resonator detuning $\Delta\omega_{12}$ to broaden the resonance frequency interval, the crosstalk induced by quantum interference of two channel signals is reduced, and therefore the drop efficiencies of two channels are improved. Similarly, **Figure 3(b)** shows four drop peaks with unities for the appropriate detunings $\Delta\omega_{12}=\Delta\omega_{23}=\Delta\omega_{34}=20$, where the signal crosstalk from four channel signals can be suppressed by controlling the inter-resonator detunings. **Figure 3(c)** further displays the effect of the resonator-waveguide couplings on four drop peaks. For simplification, $R=\Gamma_{bn}/\Gamma_{an}$ is here taken as the coupling ratio and assumed to be same. As seen, four drop peaks in these channels emerge for four equal resonator-waveguide couplings, and a white straight line with $R=1$ passes through these crimson regions, since these symmetrical coupling paths among these waveguides results in the full transfers of these signals, as mentioned previously.

Note that these channel filterings are independent of the determined locations of these resonators, as indicated in Equation (4). In addition, compared with the previous schemes requiring the reflectors to reflow the forward photons to enhance the drop efficiencies [7] [8] [9], no reflection feedbacks are needed here due to the per-

fect transfers under the mode-direction matching condition. Thus, the 2×2 demultiplexer can scale up as a fixed module, for example, eight channel filtering $T_m\left(m=1,2,\cdots,8\right)$ with the drop efficiencies of unities are exhibited in Figure 3(d), which has potential in wavelength division multiplexing communication.

Notice that the dissipations are not considered in the above investigations. In fact, the practical system inevitably suffers loss like the photon leakage from the waveguides and resonators. In contrast to the filtering spectra without dissipations, all of four drop efficiencies decrease with the increase of dissipations, as plotted in Figure 4. For a high-quality resonator with very low losses, however, high drop efficiencies are still obtainable, such as the desired result around 0.95 of T_n for $\gamma=0.05$. Here, equal dissipations $\gamma_n=\gamma$ are assumed.

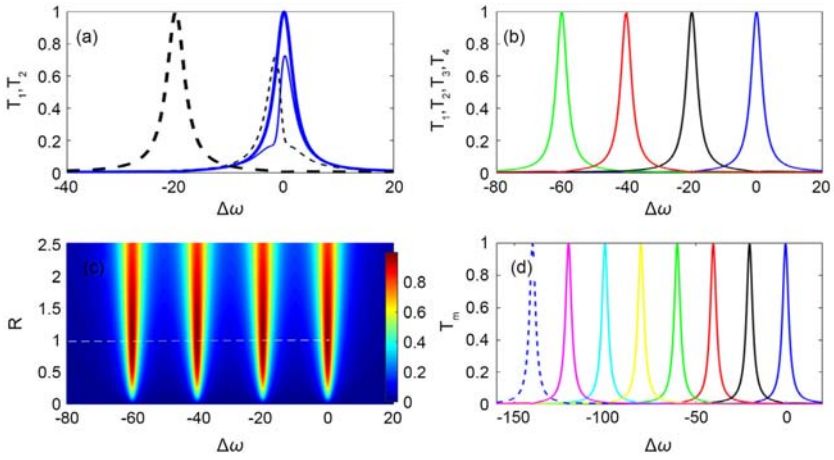

Figure 3. (Color online) (a) The drop transmission T_1 (blue solid lines) and T_2 (black dashed line) for different inter-resonator detunings: $\Delta\omega_{12}=1.5$ (thin lines) and $\Delta\omega_{12}=20$ (thick lines). (b) T_1, T_2, T_3, and T_4 (from the right to left) versus $\Delta\omega$. (c) T_1, T_2, T_3, and T_4 (from the right to left) as a function of $\Delta\omega$ and R. (d) Eight channel transmission T_m versus $\Delta\omega$. Other parameters are set as: $\Gamma_{bn}=\Gamma_{an}=1$, $\gamma_n=0$.

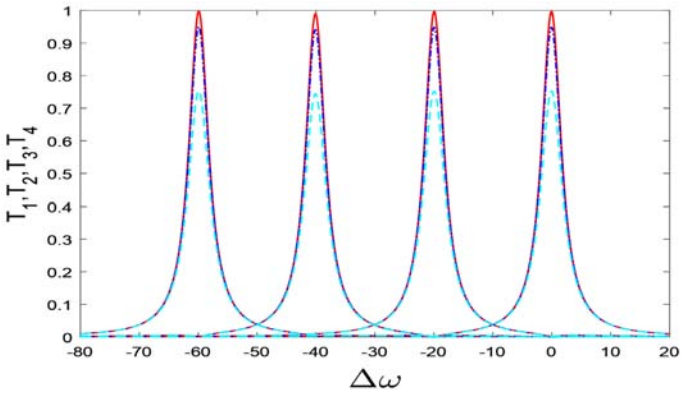

Figure 4. (Color online) T_1, T_2, T_3, and T_4 (from the right to left) for different dissipations: $\gamma=0, 0.05, 0.3$ (solid curves, dash dotted curves, dashed curves). Other parameters are the same as in Figure 3.

4. Conclusion

In summary, we have proposed a novel four-channel quantum demultiplexer of single photons in a coupled waveguide system. Our numeric results indicate that four drop peaks with high drop efficiencies within such a demultiplexer can be obtained in the scattering spectra, by tuning the inter-resonator frequency detunings and the resonator-waveguide couplings. In addition, as a fixed module, the compact demultiplexer is easy to scale up, which can be exploited in optical quantum communication.

Fund

This work was supported by Natural Science Foundation of Jiangxi Province (Grant No. 20212BAB201014).

Conflicts of Interest

The authors declare no conflicts of interest regarding the publication of this paper.

References

[1] Bilodeau, F., Johnson, D.C., Theriault S., Malo B., Albert, J. and Hill, K.O. (1995) *IEEE Photonics Technology Letters*, **7**, 388. https://doi.org/10.1109/68.376811

[2] Riziotis, C. and Zervas, M.N. (2001) *Journal of Lightwave Technology*, **19**, 92-104. https://doi.org/10.1109/50.914490

[3] Hamarsheh, M.M.N., Falah, A.A.S. and Mokhtar, M.R. (2015) *Optical Engineering*, **54**, Article ID: 016105. https://doi.org/10.1117/1.OE.54.1.016105

[4] Yun, B., Hu, G., Zhang, R. and Cui, Y. (2015) *Optics Communications*, **336**, 30-33. https://doi.org/10.1016/j.optcom.2014.09.048

[5] Zhang, Z.X., Mou, C.B., Yan, Z.J, Wang, Y.J., Zhou, K.M. and Zhang, L. (2015) *Optics Express*, **23**, 1353-1360. https://doi.org/10.1364/OE.23.001353

[6] Yang, J.J., Fan, J., Zou, Y.G., Wang, H.Z. and Ma, X.H. (2022) *Chinese Physics B*, **31**, Article ID: 084203. https://doi.org/10.1088/1674-1056/ac5391

[7] Kim, S., Park, I., Lim, H. and Kee, C.S. (2004) *Optics Express*, **12**, 5518. https://doi.org/10.1364/OPEX.12.005518

[8] Ren, H.L., Chun, J., Hu, W.S., Gao, M.Y. and Wang, J.Y. (2006) *Optics Express*, **14**, 2446. https://doi.org/10.1364/OE.14.002446

[9] Ren, H.L., Zhang, J.H., Qin, Y.L., Li, J., Guo, S.Q., Hu, W.S., Jiang, C. and Jin, Y.H. (2013) *Optik*, **124**, 1787-1791. https://doi.org/10.1016/j.ijleo.2012.05.017

[10] Qiang, Z.X., Zhou, W.D. and Soref, R.A. (2007) *Optics Express*, **15**, 1823-1831. https://doi.org/10.1364/OE.15.001823

[11] Monifi, F., Ghaffari, A., Djavid, M. and Abrishamian, M.S. (2003) *Applied Optics*, **48**, 804-809. https://doi.org/10.1364/AO.48.000804

[12] Barati, M. and Aghajamali, A. (2016) *Physica E*, **79**, 20-25. https://doi.org/10.1016/j.physe.2015.12.012

[13] Kumar, A., Suthar, B., Kumar, V., Bhargava, A., Singh, K.S. and Ojha, S.P. (2013) *Optik*, **124**, 2504-2506. https://doi.org/10.1016/j.ijleo.2012.08.030

[14] Wang, H.T., Timofeev, I.V., Chang, K., Zyryanov, V.Y. and Lee, W. (2014) *Optics*

Express, **22**, 15097. https://doi.org/10.1364/OE.22.015097

[15] Zhao, X.D., Yang, Y.B., Wen, J.H., Chen, Z.H., Zhang, M.D., Fei, H.M. and Hao, Y.Y. (2017) *Applied Optics*, **56**, 5463. https://doi.org/10.1364/AO.56.005463

[16] Khani, S., Danaie, M. and Rezaei, P. (2018) *Optical Engineering*, **57**, Article ID: 107102. https://doi.org/10.1117/1.OE.57.10.107102

[17] Geng, X.M., Wang, T.J., Yang, D.Q., He, L.Y. and Wang, C. (2016) *IEEE Photonics Journal*, **8**, Article ID: 4801908. https://doi.org/10.1109/JPHOT.2016.2573041

[18] Monifi, F., Friedlein, J., Özdemir, S.K. and Yang, L. (2012) *Journal of Lightwave Technology*, **30**, 3306. https://doi.org/10.1109/JLT.2012.2214026

[19] Monifi, F., Özdemir, S.K. and Yang, L. (2013) *Applied Physics Letters*, **103**, Article ID: 181103. https://doi.org/10.1063/1.4827637

[20] Zhou, Z.H., Chen, Y., Shen, Z., Zou, C.L., Guo, G.C. and Dong, C.H. (2018) *IEEE Photonics Journal*, **10**, Article ID: 7101607. https://doi.org/10.1109/JPHOT.2017.2764071

[21] Yin Y.H., Niu, Y.X., Dai, L.L. and Ding, M. (2018) *IEEE Photonics Journal*, **10**, Article ID: 7103810. https://doi.org/10.1109/JPHOT.2018.2849976

[22] Deng, L., Li, D.Z., Liu, Z.L., Meng, Y.H., Guo, X.N. and Tian, Y.H. (2017) *Chinese Physics B*, **26**, Article ID: 024209. https://doi.org/10.1088/1674-1056/26/2/024209

[23] Vahala, K.J. (2003) *Nature*, **424**, 839-846. https://doi.org/10.1038/nature01939

[24] Soma, S., Sonth, M.V. and Gowre, S.C. (2019) *Journal of Electronic Materials*, **48**, 7460-7464. https://doi.org/10.1007/s11664-019-07572-1

[25] Zhan, W.L., Xu, J.X., Zhao, X.L., Hu, B.J. and Zhang, X.Y. (2020) *IEEE Transactions on Circuits and Systems*, **67**, 2858-2862. https://doi.org/10.1109/TCSII.2020.2982409

[26] Zhou, K., Sun, X.X., Ma, H.Y. and Zhong, X.X. (2023) *IEEE Sensors Journal*, **23**, 3567-3572. https://doi.org/10.1109/JSEN.2023.3234544

[27] Huang, J.S. and Feng, X.M. (2023) *Journal of Modern Physics*, **14**, 101-110. https://doi.org/10.4236/jmp.2023.142007

[28] Huang, J.S. and Peng, H.Q. (2023) *International Journal of Theoretical Physics*, **62**, 42. https://doi.org/10.1007/s10773-023-05306-y

[29] Shen, J.T. and Fan, S.H. (2009) *Physical Review A*, **79**, Article ID: 023838. https://doi.org/10.1103/PhysRevA.79.039904

Journal of Modern Physics, 2023, 14, 534-551
https://www.scirp.org/journal/jmp
ISSN Online: 2153-120X
ISSN Print: 2153-1196

The Origin of Cosmic Microwave Background Radiation

Zhenglong Xu

Wuzhen High School, Tongxiang, China
Email: zhl-xu@126.com

How to cite this paper: Xu, Z.L. (2023) The Origin of Cosmic Microwave Background Radiation. *Journal of Modern Physics*, **14**, 534-551.
https://doi.org/10.4236/jmp.2023.144030

Received: February 9, 2023
Accepted: March 26, 2023
Published: March 29, 2023

Abstract

This paper explains the Olbers paradox and the origin of cosmic microwave background radiation (CMBR) from the viewpoint of the quantum redshift effect. The derived formula dispels the Olbers paradox, confirming that the CMBR originates from the superposition of light radiated by stars in the whole universe, not the relic of the Big Bang. The dark-night sky and CMBR are all caused by Hubble redshift—the physical mechanism is the quantum redshift of the photon rather than cosmic expansion. So this theory supports the infinite and steady cosmology.

Keywords

Olbers Paradox, Cosmic Microwave Background Radiation (CMBR), Big Bang Theory, Hubble Redshift, Quantum Redshift Effect of Photon, Stefan-Boltzmann Law, Blackbody Radiation

1. Introduction

Long before the Big Bang theory, the mystery of the luminosity of the night sky appeared, that is, why the night sky is dark instead of bright. After a long debate among many astronomers, in 1826, H. Wilhelm M. Olbers summed it up as the luminosity paradox called the Olbers paradox later by the astronomical community. Historically, there have been explanations for solving this paradox, such as Olbers' belief that cosmic space dust obscures the light of distant stars. The flaw in this explanation is that dust absorption, so where does that light energy go? Moreover, dust not only absorption but also confuses the sky, making it no longer transparent. It still does not explain the paradox. In these explanations, the mainstream is the Big Bang theory. The Big Bang theory states that the universe is expanding and the lifespan of stars is finite.

In the 1920s, Edwin Hubble discovered the spectral redshift of extra-galactic galaxies, which provided observational evidence for solving the Olbers paradox. However, to establish the Big Bang theory, the Big Bang cosmologists explained the Hubble redshift as the Doppler effect produced by the light emitted by the stars when the extra-galactic galaxies are far away from the Earth and regarded Hubble redshift as evidence of the expansion of the universe.

The non-Big Bang theory has proposed many explanations for Hubble redshift, among which more famous ones are the tired-light theory, Compton scattering redshift theory, photon aging theory, elementary particle mass change theory, intrinsic redshift theory, gravitational redshift theory, new tired-light theory, and so on. These theories all have a similar problem using hypothesis to explain redshift. For example, the tired-light—Compton scattering—new tired-light does not solve the problem of the direction change of light during scattering. The photon aging theory violates the existing laws of physics—the lifespan of a photon is infinite. The elementary particle mass change—intrinsic redshift cannot find a theoretical and experimental basis for physics. Gravitational redshift theory can explain the redshift phenomenon that occurs when photons escape the gravitational pull of massive objects, but it cannot explain cosmological redshift. Therefore, the previous non-Big Bang theory failed to explain the physical mechanism of the origin of redshift.

Arno Penzias and R. W. Wilson discovered CMBR in 1965. This discovery should have been the evidence to solve the Olbers paradox and Hubble redshift. However, the Big Bang theorists took it as a relic of the Big Bang.

The non-Big Bang theory has made a variety of explanations for CMBR, the more typical of which is the cosmic dust occlusion theory. The thermodynamic theory believes that the light emitted by stars in the entire universe is absorbed and scattered by the dust of the interstellar and intergalactic medium during propagation so that the radiation and the medium reach thermodynamic equilibrium, and Planck blackbody radiation occurs in the medium, which is the CMBR. Opponents argue that if the stellar radiation and the medium reach thermodynamic equilibrium, the temperature of the medium will rise to the temperature of the star's surface. Thus, the thermodynamic interpretation leads to another new paradox similar to Olbers'. The problem with this interpretation is that it treats CMBR as the black body radiation of the medium and does not use the redshift effect of photons to explain how the visible light of stars converts into microwaves.

The previous non-Big Bang theory did not correctly explain the Olbers paradox, Hubble redshift, and CMBR, thus allowing the Big Bang theory to dominate the interpretation of these three phenomena.

So, what is the relationship between the three physical phenomena—Olbers paradox, Hubble redshift, and CMBR? How exactly do Olbers paradox and CMBR come about? Can they be explained by applying the quantum redshift effect of photons?

2. Derivation of Olbers Paradox

In 1826, German astronomer H.W.M. Olbers pointed out that a static infinite universe model with uniformly distributed stars would draw the following conclusion: the background radiant emittance of all parts of the universe is equal to the emittance of the star's surface. But the night sky is dark. This contradiction between theory and observation is called Olbers paradox by later generations [1].

2.1. The First Type of Expression

According to the cosmological principle, the universe is uniform and isotropic on a large scale in space. Assuming that if the universe is infinite, the luminous stars uniformly distribute in the universe, and the number of stars in the unit volume of the universe is certain. Suppose that the number density of luminous stars (actually, it is not uniform, but understand it as the mean density) is n_L, and the radiant power of all the luminous stars in the universe is the same (can understand it as the mean radiant power), and suppose that the value is P_0, then the irradiance on the plane at the arbitrarily selected point O of all stars in the universe with radius R is

$$I = \int_0^{2\pi}\int_0^{\frac{\pi}{2}}\int_0^{R} \frac{P_0}{4\pi r^2} n_L r^2 \sin\theta\cos\theta \mathrm{d}r\mathrm{d}\theta\mathrm{d}\varphi \tag{1-a}$$

$$= \frac{P_0}{4\pi} n_L R \int_0^{2\pi}\int_0^{\frac{\pi}{2}} \sin\theta\cos\theta \mathrm{d}\theta\mathrm{d}\varphi \tag{1-b}$$

$$= \frac{P_0}{4\pi} n_L R \cdot \frac{1}{2}\int_0^{2\pi} \mathrm{d}\varphi \tag{1-c}$$

$$= \frac{1}{4} n_L P_0 R \tag{1-d}$$

Here r, θ, and φ are shown in Figure 1.

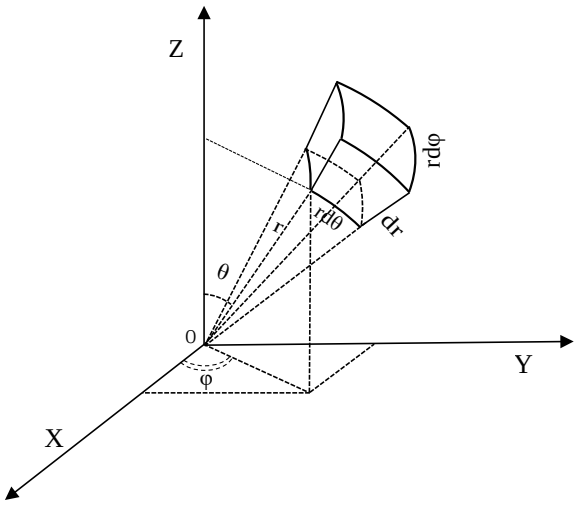

Figure 1. This diagram shows the integral calculation of the irradiance on the plane OXY from stars in the upper half of space.

If the radius of the universe is infinite, that is, $R=\infty$, then the result of the above integral is infinite, that is

$$I=\lim_{r\to\infty}\left(\frac{1}{4}n_L P_0 R\right)=\infty \tag{1-e}$$

This result means that the irradiance anywhere in space is infinite. Therefore, under the condition that the universe is infinite, the calculated value of irradiance does not conform to reality. In the 16th century, Thomas Digges, a British astronomer, first proposed this paradox.

As for this paradox, Diggs thought the above statement was inaccurate and gave a new explanation. He believed that the night sky is dark because nearby stars block the light of distant stars. J. Kepler and E. Halley also pondered this question, but neither gave a satisfactory answer.

2.2. The Second Type of Expression

According to the cosmological principle, assume that the universe is infinite and cosmic matter uniformly distributes. Suppose that the mean density of luminous stars is n_L; The total number density of the stars (including luminous and non-luminous) is n_s. Each luminous star has the same radiant power, P_0. (The above assumptions can interpret as statistical averages). With the radius R and the arbitrarily selected point O as the center of the sphere, the irradiance on the plane at point O is different from that described in Equation (1) because stars close to the observer block the light radiated by distant stars.

A star is usually a sphere, so its luminous area is spherical. If the radius of a star's sphere is r_0, the spherical area is S_L. As the nearby stars block the light of the distant stars, the blocking area is the largest cross-sectional area of the sphere, S_0, so the two expressions are as follows

$$\begin{cases} S_L=4\pi r_0^2 & \text{(2-1)} \\ S_0=\pi r_0^2 & \text{(2-2)} \end{cases}$$

Let the surface radiant emittance of the star,that is, the radiant power per unit area of a luminous star, be R_e, and the radiant power of the star is given by

$$P_0=S_L R_e=4\pi r_0^2 R_e \tag{3}$$

If distant stars emit N_0 photons, the number of photons, N, varies in the propagation abiding by the following equation:

$$\begin{cases} \dfrac{\mathrm{d}N}{\mathrm{d}t}+cn_s S_0 N=0 & \text{(4)} \\ N_{t=0}=N_0 & \text{(5)} \end{cases}$$

The solution is given by

$$N=N_0\mathrm{e}^{-cn_s S_0 t}=N_0\mathrm{e}^{-n_s S_0 r} \tag{6}$$

where c is the speed of light, t is the time for light to travel on the way, and $r=ct$ is the distance the light travels. Equation (6) shows that the photon number N attenuates negatively exponentially with propagation time t or dis-

tance *r*.

The irradiance passing through the unit area at any point O in the universe is

$$I = \int_0^{2\pi}\int_0^{\frac{\pi}{2}}\int_0^R \frac{P_0}{4\pi r^2} \mathrm{e}^{-n_s S_0 r} n_L r^2 \sin\theta\cos\theta \mathrm{d}r\mathrm{d}\theta\mathrm{d}\varphi \tag{7-a}$$

$$= \frac{n_L P_0}{4}\int_0^R \mathrm{e}^{-n_s S_0 r}\mathrm{d}r \tag{7-b}$$

$$= \frac{n_L P_0}{4n_s S_0}\left(1-\mathrm{e}^{-n_s S_0 R}\right) \tag{7-c}$$

This formula shows that if the universe is infinite, $R\to\infty$, then $\lim_{R\to\infty} \mathrm{e}^{-n_s S_0 R} = 0$. Applying Equations (2-1) (2-2) and (3), the above formula becomes

$$I = \frac{n_L P_0}{4n_s S_0} = \frac{n_L}{n_s} R_e \tag{8}$$

where n_L/n_s is the ratio of the number density of luminous stars to the total number density of stars. Because there are always stars that don't emit light or are dim, that is $n_L/n_s \le 1$. Suppose that $n_L = n_s$, then $n_L/n_s = 1$, the Equation (8) becomes

$$I = R_e \tag{9}$$

Equation (9) means: For whatever direction we look in the sky, our line of sight eventually intercepts a star, and the whole sky should therefore be ablaze with light as bright as the Sun [2]. But the sky at night is dark. This disagreement between theoretical inference and observation is now called the Olbers paradox.

Although known that stars do not uniformly distribute in space, from the Mach principle, if galaxies or galaxy clusters replace stars, this conclusion can remain unchanged.

The two expressions of the Olbers paradox imply that: 1) If the universe is infinite, without considering the light blocking of the stars, the irradiance anywhere in the universe is infinite; 2) If the universe is infinite, with considering the light blocking of the stars, the irradiance anywhere in the universe does not exceed the radiant emittance of the surface of the stars.

In both cases, the light energy absorbed by the stars' surface balances with the light energy radiated. Either way of expression is unrealistic since the night sky is dark. The problem is to find out what is wrong with these logical calculations.

3. The Resolution to Olbers Paradox

3.1. Debates about the Olbers Paradox in History

In history, there has been a long-term debate on the Olbers paradox. Many explanations emerged. Now, summarizing them can get four controversial conclusions [2] [3]:

1) Stars don't shine long enough: Stars don't shine long enough, so the light from distant stars is still on the way to the Earth, and the observers on the Earth can only receive the light from stars in a finite range. (It implies that the night

sky will brighten as time goes on.)

2) The universe is expanding: Because the universe is expanding and the stars are moving away from the Earth, the Doppler effect causes the photon to redshift, which reduces the frequency of light and makes part of the light observable by the human eye invisible.

3) The light energy density of stars is too scarce: The total energy density of light radiated by stars in the observable range (due to the product $n_L P_0$) is too little to reach the irradiance perceived by human eyes.

4) There is a medium in space: Space is not an absolute vacuum, but a medium exists which can absorb and block light.

In the above four conclusions, in the author's opinion, point 1) involves the theory of the finite universe, and point 2) involves the theory of the expanding universe. The two points have low reliability. Point 3) is flawed but does not involve whether the universe is finite. Point 4) indicates that there is a medium in space, and there is no doubt that the medium can absorb and block light.

All the existing explanations of the Olbers paradox can only explain one phenomenon, and there are loopholes, mainly because they are not coherent theories.

3.2. A New Explanation of the Olbers Paradox

This paper accepts the two points: 3) and 4) in 3.1. The following explains the Olbers paradox mathematically.

On the one hand, due to the block of stars, the number of photons attenuates negatively exponentially with distance. Equation (6) expresses this relation. On the other hand, as pointed out in the paper "*The Quantum Redshift Effect of Photon*" [4], due to the existence of a medium in intergalactic space, the main component of the medium is atomic hydrogen. When photons propagate in the medium, the quantum redshift effect occurs, and the frequency of each photon attenuates negatively exponentially with the propagation time t or distance r. The following formula can express this relation:

$$\nu = \nu_0 \mathrm{e}^{-H_0 t} = \nu_0 \mathrm{e}^{-\frac{H_0}{c} r} \tag{10}$$

The wavelength increases exponentially with the propagation time t or distance r. The following formula can express this relation:

$$\lambda = \lambda_0 \mathrm{e}^{H_0 t} = \lambda_0 \mathrm{e}^{\frac{H_0}{c} r} \tag{11}$$

So, a beam of light with energy E_0 emitted from the stars, its energy E attenuates in a negatively exponential law with the propagation distance r. When it reaches the observer, it becomes

$$E = E_0 \mathrm{e}^{-\left(n_s S_0 + \frac{H_0}{c}\right) r} \tag{12}$$

If the universe is infinite, the energy limit above is given by

$$E_\infty = E_0 \lim_{r \to \infty} \mathrm{e}^{-\left(n_s S_0 + \frac{H_0}{c}\right) r} = 0 \tag{13}$$

Thus, as the propagation distance increases, the number of photons decreases and finally tends to zero, as stars continuously block photons. At the same time, the frequency of photons gradually decreases and eventually equals zero. Both work at the same time. When the propagation distance of a beam of light tends to infinity, its light energy tends to zero. It means that space gradually converts to a black body from a transparent body. Therefore, the infinite universe is a three-dimensional blackbody, which differs from the familiar surface blackbody.

It is speculated from Equation (12) that the irradiance at any point in the space of the universe changes from Equation (1) to

$$I = \int_0^{2\pi}\int_0^{\frac{\pi}{2}}\int_0^R \frac{P_0}{4\pi r^2} \mathrm{e}^{-\left(n_s S_0 + \frac{H_0}{c}\right)r} n_L r^2 \sin\theta\cos\theta \mathrm{d}r\mathrm{d}\theta\mathrm{d}\varphi \tag{14-a}$$

$$= \frac{n_L P_0}{4\left(n_s S_0 + \frac{H_0}{c}\right)}\left[1 - \mathrm{e}^{-\left(n_s S_0 + \frac{H_0}{c}\right)R}\right] \tag{14-b}$$

The derivation of Equations (14-a) and (14-b) implies that if the distance traveled by light in space is small enough, that is, $R \ll 1\Big/\left(n_s S_0 + \frac{H_0}{c}\right)$, there is $\mathrm{e}^{-\left(n_s S_0 + \frac{H_0}{c}\right)R} \approx 1 - \left(n_s S_0 + \frac{H_0}{c}\right)R$. Thus

$$I \approx \frac{1}{4} n_L P_0 R \tag{15}$$

It is the same as (1-d). It suggests that light travels through space at a distance short enough to see space as a transparent body and that the blocking effect of stars and media does not work. In other words, if the universe is finite, the space can regard as a three-dimensional transparency body.

Equation (14-b) means that no matter whether the universe is finite or infinite, the irradiance of any point in space cannot be infinite. Assuming that the universe is infinite, then $R \to \infty$ in Equation (14-b), thus $\lim_{R\to\infty} \mathrm{e}^{-\left(n_s S_0 + \frac{H_0}{c}\right)R} = 0$, and Equation (14-b) becomes

$$I = I_{\max} = \frac{n_L P_0}{4\left(n_s S_0 + \frac{H_0}{c}\right)} = \frac{c n_L P_0}{4\left(c n_s S_0 + H_0\right)} \tag{16}$$

It means that if the universe is infinite, the irradiance of any point in space is finite. In other words, the irradiance of starlight on the ground is not infinitive.

Equation (16) means that if there is no factor H_0/c, or if there is no redshift effect, only the light-blocking of the stars exists, then Equation (16) returns to Equation (8). Equation (8) shows that if there is no medium in space, the irradiance of any point is close to the radiant emittance of the star's surface.

Comparing Equation (16) with (1-d) can see that $c\big/\left(H_0 + c n_0 S_0\right)$ in Equation (16) plays the role of "cosmic radius" R in Equation (1-d).

Ignoring $c n_s S_0$ in Equation (16), the factor c/H_0 acts as the radius of the

universe. It is the so-called Hubble Radius, which is finite.

According to the paper *the Quantum Redshift Effect of Photon* [4], the Hubble constant should take as

$$H_0 = \frac{3\pi}{8\alpha} c\sigma_T n_e \tag{17-a}$$

$$= 2.27\times10^{-18}/\mathrm{s} = 70\ \mathrm{km/s\cdot Mpc} \tag{17-b}$$

where α is the fine structure constant, $\sigma_T = 8\pi r_e^2/3$ is the Thomson scattering cross-sectional area of the electron, and $n_e \approx 0.7/\mathrm{m}^3$ is the electron density bound in the atom in the intergalactic medium.

According to reference [5] and **Table 1**, if the mean light-blocking radius of the star is $r_0 = 4.0\times10^8$ m, take the approximation $n_s \approx n_L$, then the light-blocking area of a star is given by

$$S_0 = \pi r_0^2 = 5.03\times10^{17}\ \mathrm{m}^2 \tag{18}$$

Hence

$$cn_sS_0 \approx cn_LS_0 = 3\times10^8\ \mathrm{m/s}\times 2.17\times10^{-58}/\mathrm{m}^3\times 5.03\times10^{17}/\mathrm{m}^2 \tag{19-a}$$

$$= 3.27\times10^{-32}/\mathrm{s} \tag{19-b}$$

Comparing the two factors in Equation (17) and Equation (19) in the denominator of Equation (16) can obtain a relationship

$$cn_sS_0/H_0 = \left(3.27\times10^{-32}\right)/\left(2.27\times10^{-18}\right) = 1.44\times10^{-14} \tag{20}$$

Because $cn_sS_0 \ll H_0$ in the denominator in Equation (16), cn_sS_0 is negligible. So Equation (16) becomes

$$I = I_{\max} = \frac{cn_LP_0}{4H_0} \tag{21}$$

This formula shows that the irradiance at any point in the universe is finite, and the value is inversely proportional to the Hubble constant.

Equations (8) and (9) show that stars in the universe emit enough light to make any point as bright as the surface of the Sun. However, according to Equation (21), the irradiance at any point in the universe is little. Moreover, from Equation (20) can know that $cn_sS_0/H_0 = 1.44\times10^{-14}$ so that $I \ll R_e$, that is, the irradiance of the night sky is 14 orders of magnitude lower than the radiant emittance of the star's surface. By comparing Equations (21) and (8) can know in the two factors of the star's light-blocking effect and the redshift effect, the former is negligible while the latter plays a dominant role. The redshift is the main reason why the night sky is so dark.

Even if the universe is infinite, due to the redshift effect of photons propagating in the medium of the universe, the irradiance of light radiated by all stars in the whole universe is very dim at any point, so the Olbers paradox does not exist. The infinite universe becomes a three-dimensional black body.

Table 1. Cosmic stellar parameters.

The radiant power of a star	$\overline{P}_0 = 6.35\times10^{26}$ W
The number density of stars	$\overline{n}_L = 2.17\times10^{-58}/\mathrm{m}^3$
The light-blocking radius of a star	$\overline{r}_0 = 4\times10^8$ m
The radiant emittance of the star's surface	$\overline{R}_e = 3.16\times10^8\ \mathrm{W}/\mathrm{m}^2$
The temperature of the star's surface	$\overline{T}_0 = 8640$ K

4. The Origin of CMBR

4.1. Discovery and Explanation of CMBR

In 1964, engineers A.A. Penzias and R.W. Wilson of Bell Laboratory stumbled upon the presence of microwave radiation with a wavelength of 7.35 cm in space during an experiment to test the noise performance of the antenna and that the radiation is isotropic. This radiation has neither diurnal nor seasonal changes. This additional radiation is the CMBR, which corresponds to the black body radiation of about 3 K in space. They published this result in 1965 [6]. CMBR is one of the significant discoveries in astrophysics in the 1960s.

In history, astronomers have long predicted the temperature of interstellar space and intergalactic space [7]. As early as 1926, astronomer A.S. Eddington predicted 3.2 K; In 1933, E. Regener predicted 2.8 K; In 1937, W. Ernst predicted 2.8 K; In 1941, Stephen G. Brush estimated 2.3 K; in 1954, E. Finlay Freundlich predicted a temperature of $1.9\ \mathrm{K} \le T \le 6.0\ \mathrm{K}$. These numerical predictions of temperature did not base on the Big Bang. The temperatures predicted by these non-Big Bang theorists are close to the currently recognized value of 2.725 K.

In 1948, George Gamow put forward the Big Bang theory. The theory points out that the Big Bang sent out intense light at the moment, but at the beginning of the Big Bang, the whole universe was hot and dense, just like the core of a star, and the universe was opaque to electromagnetic waves. The temperature dropped to 3100 K about 380,000 years after the Big Bang. The electrons and atomic nuclei began to combine to form atoms. Then atoms repeatedly scattered the photons. This period, known as final scattering, was long before the formation of galaxies (the formation of galaxies was about 1 billion years after the explosion). Because galaxies have not yet formed, the universe is a homogeneous and highly bright cluster. During this period, the intense light radiation made the whole universe bright. The light radiation during the "final scattering" period has been redshifted due to the expanding of the universe, and these ancient light waves have now been redshifted to the microwave wavelength range. They are no longer visible light and cannot illuminate the night sky. The redshift effect not only converts light waves during "final scattering" into microwave background radiation but also shifts all spectral lines propagating from distant galaxies to Earth toward the lower-frequency, enhancing the effect of night dark.

Since the standard model of the universe created in the Big Bang theory has become mainstream, the theorists naturally connect the discovery by A.A. Pen-

zias and R. W. Wilson to Gamow's hypothesis. The 3K microwave background radiation became evidence of the Big Bang.

Several Big Bang theorists have predicted the temperature of space [7]. In 1949, Ralph A. Alpher and Robert C. Herman predicted $T \geq 5\,\mathrm{K}$. In 1953, G. Gamow predicted 7 K; In 1961, G. Gamow predicted 50 K. The predicted data of Big Bang theorists vary widely, proving that Big Bang predictions are far less accurate than those of non-Big Bang theories.

As for the CMBR, though Big Bang theorists can't predict its exact value, they certainly need it as evidence for the Big Bang.

4.2. A Unified Explanation of Three Phenomena

Leaving aside the Big Bang theory explanation of CMBR, this section unifies the Hubble redshift (the law of attenuation of photon frequencies) and the CMBR phenomenon in the infinite and steady-state universe.

Equation (21) represents the superposition of the light radiated by stars on the plane of any point after redshift. The selected point, whether it is the vacuum or the location of the medium, is unnecessary to be the surface of the black body.

That is to say, the radiation at any point is not the sudden transformation of the light emitted by the star through the surface of the black body, but because the light of stars is originally blackbody radiation, which has conformed to the Planck blackbody radiation formula. On the way of propagation, the frequency of each photon attenuates and shifts to the band of microwave frequency. Therefore, CMBR must be black body radiation.

Universe space is almost close to a vacuum, and there is no temperature. To describe the temperature of molecular motion can find the wavelength corresponding to the peak intensity of blackbody radiation. Applying this wavelength can calculate the temperature of molecular motion in space according to the Stefan-Boltzmann formula. Thus, the radiation emitted at any point in space equals the radiation received by this point. Both conform to the blackbody radiation spectrum and obey the Planck blackbody radiation formula, which differential form is given by

$$\rho_{\lambda'}\mathrm{d}\lambda' = \frac{8\pi}{c^3\lambda'^5}\frac{h}{\mathrm{e}^{\frac{hc}{\lambda' kT'}}-1}\mathrm{d}\lambda' \tag{22}$$

Since the irradiance is the superposition of photons of various wavelengths, as the wavelength of each photon increases according to Equation (11), the wavelength corresponding to the peak also increases. According to Wien's law of displacement

$$\lambda_m' T' = \lambda_m T \tag{23}$$

redshift lowers the temperature of the radiant emittance in space. Here an increase in λ_m' means a decrease in T'. The radiation temperature T' here plays the role of space temperature in the universe, corresponding to the wavelength of the peak of radiant emittance, λ_m'.

Here T' may be misinterpreted as the thermal radiation temperature of the thermal motion of molecules when the medium of space reaches thermal equilibrium with radiation. In fact that it represents the superposition of the radiation of all celestial bodies in the universe at the investigation point. It is not molecular thermal radiation in space, so the temperature T' does not represent the intensity of the thermal movement of molecules. Therefore, no matter how long the exposure time is, the temperature at the investigation point will not rise.

The radiant emittance on a plane at any point in space is given by

$$R'_e = \frac{c}{4}\int_0^\infty \rho_{\nu'} \mathrm{d}\nu' = \int_0^\infty \frac{2\pi}{c^2} \frac{h\nu'^3}{\mathrm{e}^{\frac{h\nu'}{kT}} - 1} \mathrm{d}\nu' \tag{24}$$

where h is Planck constant , $k = 1.380649 \times 10^{-23}\ \mathrm{J/K}$ is the Boltzmann constant.

The result of the integral above is the Stefan-Boltzmann law of blackbody radiation

$$R'_e = \sigma T'^4 \tag{25}$$

where σ is the Stefan-Boltzmann constant, whose value is given by

$$\sigma = \frac{2\pi^5 k^4}{15c^2 h^3} = 5.67 \times 10^{-8}\ \mathrm{W/m^2 \cdot K^4} \tag{26}$$

The point arbitrarily selected in space is not a luminous body or a blackbody surface, so this point does not produce radiation. Its radiation is from a superposition of that emitted by luminous celestial bodies throughout the universe.

As shown in Figure 2, a plane at the location of an arbitrarily selected point O in space, and the radiant emittance of this point towards the upper half-space angle 2π range is equal to the irradiance from the lower half-space angle 2π range.

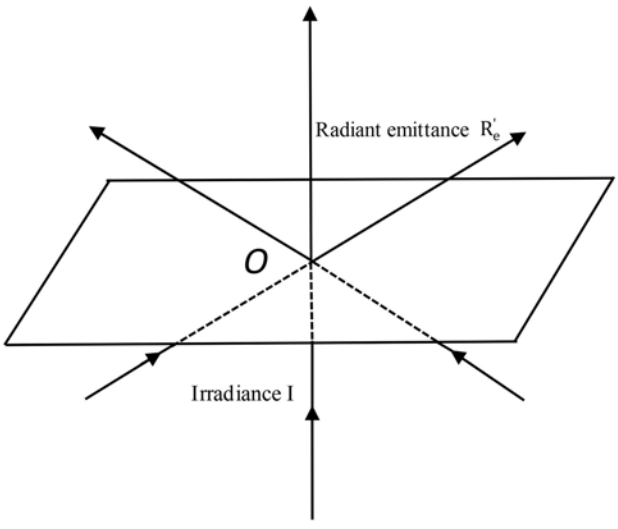

Figure 2. At an arbitrarily selected point O in cosmic space, the radiant emittance toward the upper half-space of the plane at point O is equal to the irradiance of all luminous objects from the lower half-space of this plane.

Vice versa, the emittance towards the lower half-space angle 2π equals the irradiance from the upper half-space angle 2π. (As shown in **Figure 2**, reverse the direction of the arrow. Illustration omitted.)

It implies that R_e' in Equation (25) equals I in Equation (21), *i.e.*, $R_e' = I$. Combining (21) and (25) can obtain

$$R_e' = I = \frac{cn_L P_0}{4H_0} = \sigma T'^4 \tag{27}$$

Solving it can obtain

$$T' = \left(\frac{cn_L P_0}{4\sigma H_0}\right)^{\frac{1}{4}} \tag{28}$$

Applying Equation (28) can find the temperature T' corresponding to the CMBR under the known conditions n_L, P_0, and H_0.It implies that as long as the parameters n_L, P_0, and H_0 are stable, the temperature T' at any point in space will not change with time.

The radiant power P_0 of a star can express as the product of the radiance R_e per unit area of the star's surface and the area S_L of the star's surface, as shown in Equation (3).

Since the surface radiation of a star is blackbody radiation, the radiant emittance R_e can express as Stephan-Boltzmann's law

$$R_e = \frac{c}{4}\int_0^\infty \rho_\nu \mathrm{d}\nu \tag{29-a}$$

$$= \frac{c}{4}\int_0^\infty \frac{8\pi h}{c^3}\frac{\nu^3}{\mathrm{e}^{\frac{h\nu}{kT}}-1}\mathrm{d}\nu \tag{29-b}$$

$$= \sigma T^4 \tag{29-c}$$

Substituting (3) and (29) into (27) obtain

$$\sigma T'^4 = \frac{\pi c n_L r_0^2}{H_0}\sigma T^4 \tag{30}$$

Solving it can obtain

$$T' = \left(\frac{\pi c n_L r_0^2}{H_0}\right)^{\frac{1}{4}} T \tag{31}$$

Using the Hubble constant Equation (17-a) and Thomson's electron cross-sectional area $\sigma_T = 8\pi r_e^2/3$, Equation (31) can express as

$$T' = \left(\frac{\alpha}{\pi}\cdot\frac{n_L}{n_e}\cdot\frac{r_0^2}{r_e^2}\right)^{\frac{1}{4}} T \tag{32}$$

This formula establishes the relationship between the radiation temperature at any point in the universe and the mean surface temperature of stars.

4.3. Verification by Numerical Calculations

The distribution of luminous stars in the universe is non-uniform. So, n_L varies

everywhere; Stars vary in radius r_0, and surface temperature T. According to the rough statistical estimation of the Chinese scholar G. Pan [5] can obtain three parameters in Equations (28) (31) for stars in the universe: 1) The mean radiant power of stars in the universe, $\overline{P}_0$; 2) The mean number density of stars in the universe, $\overline{n}_L$; 3) The mean light-blocking radius of stars in the universe, $\overline{r}_0$. Using this set of data and according to Equations (3) and (29) can calculate 4) The mean radiant emittance of the surface of stars in the universe, R_e; 5) The mean temperature of the surface of a luminous star in the space, $\overline{T}_0$. In this way can obtain Table 1.

Using the Hubble constant Equation (17-a) and replacing n_L, r_0, and T in Equation (28) with $\overline{n}_L$, $\overline{r}_0$, and $\overline{T}_0$ can obtain

$$T' = \left(\frac{\pi c \overline{n}_L \overline{r}_0^2}{H_0}\right)^{\frac{1}{4}} \overline{T}_0 \tag{33-a}$$

$$= \left[\frac{\pi \times 3\times 10^8 \text{ m/s} \times 2.17\times 10^{-58}/\text{m}^3 \times \left(4\times 10^8 \text{ m}\right)^2}{2.27\times 10^{-18}/\text{s}}\right]^{\frac{1}{4}} \times 8640 \text{ K} \tag{33-b}$$

$$= 2.994 \text{ K} \tag{33-c}$$

This result is 0.269 K or 9.87% higher than the accepted CMBR temperature of 2.725 K.

The Sun is a medium star among the stars. The total radiant power of the Sun is P_s, the radius of the Sun is r_s, the mean radiant emittance of the surface of the Sun is R_s, and the surface temperature of the Sun is T_s [8]. In this way can obtain Table 2.

The number density of stars in the universe is still $\overline{n}_L$, and the Hubble constant is Equation (17-a). Substituting them into Equation (31) can obtain

$$T_s' = \left(\frac{\pi c n_L r_s^2}{H_0}\right)^{\frac{1}{4}} T_s \tag{34-a}$$

$$= \left[\frac{\pi \times 3\times 10^8 \text{ m/s} \times 2.17\times 10^{-58}/\text{m}^3 \times \left(6.96\times 10^8 \text{ m}\right)^2}{2.27\times 10^{-18}/\text{s}}\right]^{\frac{1}{4}} \times 5800 \text{ K} \tag{34-b}$$

$$= 2.651 \text{ K} \tag{34-c}$$

This result is 0.074 K or 2.71% lower than the accepted CMBR temperature of 2.725 K.

Table 2. Solar parameters.

The radiant power of the sun	$P_s = 3.83\times 10^{26}$ W
The radius of the sun	$r_s = 6.96\times 10^8$ m
The radiant emittance of the sun's surface	$R_s = 6.29\times 10^7$ W/m^2
The temperature of the sun's surface	$T_s = 5800$ K

Although obtained different calculated values using various data, these values deviate very little from acceptable measurements. How can the cosmic background temperature, which spans such orders of magnitude and is composed of so many physical quantities, coincidentally makes up such a precise physical quantity?

The deviation can attribute to four factors: the density n_L of luminous stars in the universe, the mean radius r_0 of stars, the mean temperature T of stars, and the Hubble constant H_0. Any deviation between any one factor and the actual value will cause the calculation result to deviate from the actual one, not to mention that T' is affected by a combination of 4 factors.

Since the stars' radiation conforms to the blackbody radiation spectrum, the quantity expressed by Equation (21) is the superposition of light of various frequencies radiated by all celestial bodies on the plane of any point after redshift. Thus, Equation (21) expresses the intensity of blackbody radiation without the blackbody surface.

Equation (28) contains the mean radiant power P_0 of stars and the Hubble constant. It proves that CMBR is the light radiated by luminous stars that undergoes redshift. In other words, CMBR is not a relic of the Big Bang. Thus, both the night sky darkness and CMBR originate from the quantum redshift of photons.

The above calculations show that the radiation of luminous stars, through quantum redshift, is converted into CMBR.

5. Discussion

5.1. The Explanations Required for the Big Bang Theory

The Big Bang theory explains the Olbers paradox as the age of the stars, the finite space-time of the universe, the expansion of space, and the sparseness of the luminescent energy density of stars. It regards the CMBR as the relic of the Big Bang and Hubble redshift as the Doppler effect of photons caused by the galaxies' recession.

Proponents of the Big Bang theory believe that if the medium absorbs the energy of the light can cause the temperature of the medium to continue to rise so that it can emit visible light and the entire sky is bright. It is one reason for Big Bang theorists to oppose the idea that the medium causes darkness in the night sky.

The Big Bang Theory explains Hubble redshift, Olbers paradox, and CMBR as the following:

1) Attribute Hubble redshift to the Doppler effect caused by the expanding universe.

2) Attribute the Olbers paradox to the finite age of stars in the universe, the energy radiated by all-stars too scarce, and the expanding universe.

3) Attribute CMBR to the relic of the Big Bang.

In a word, attribute all three phenomena to the finite universe and the expan-

sion of the universe.

5.2. Explanations Based on the Quantum Redshift Effect

Through theoretical derivation and numerical calculations can affirm that the energy radiated by stars throughout space is converted into CMBR, making the sky dark, and the Olbers paradox is solved together with the CMBR.

The quantum redshift effect theory explains Hubble redshift, Olbers paradox, and CMBR as the following:

1) Attribute Hubble redshift to the quantum redshift effect of photons caused by the cosmic medium.

2) Attribute the Olbers paradox to the fact that the energy radiated by stars is too scarce, and the photons collide with atoms of the medium, which causes photons to undergo quantum redshift, reducing the brightness of the sky and frequency of photons.

3) Attribute the CMBR to the quantum redshift of photons of light radiated by the stars colliding with atoms of the medium, making the light become blackbody radiation of the temperature of 3 K.

In a word, unify all three phenomena by the quantum redshift effect of photons.

The energy of CMBR converts from luminous stars in the universe. The photons emitted by stars collide with the atoms of cosmic medium and undergo a quantum redshift. This effect makes the photon frequency lower and the light intensity weaker. The light becomes invisible and makes the night sky dark. After the stellar radiation is redshifted, it is superimposed at any point in space to become CMBR. The CMBR originates from stellar blackbody radiation, so the CMBR presents a blackbody spectrum.

5.3. Distinction in Observation

As can be seen from Equations (21) and (31), both the sky irradiance and CMBR temperature depend on the Hubble constant. So, the key to explaining the Olbers paradox and CMBR is the Hubble constant, which relates to the origin of photon redshift.

There are different explanations of the origin of photon redshift in the Big Bang theory and non-Big Bang theory:

In the 1920s, E. Hubble discovered a systematic redshift in the spectrum of extragalactic galaxies. Interpreting it as the Doppler effect by luminous stars moving away from Earth with galaxies, the photon frequency decreases according to the following formula:

$$\nu = \nu_0 \sqrt{\frac{1-\frac{V}{c}}{1+\frac{V}{c}}} \tag{35}$$

where ν_0 is the initial frequency of the photon, and V is the receding velocity

of the luminous celestial body.

Redshift z is defined by

$$z = \frac{\lambda - \lambda_0}{\lambda_0} = \frac{\nu_0 - \nu}{\nu} \tag{36}$$

Hubble found that the redshift z is proportional to the distance r, so substituting Equation (35) to Equation (36) gives the approximate formula:

$$V = H_0 r \tag{37}$$

where H_0 is the Hubble constant.

Equation (37) is Hubble's Law, which expresses the relationship between the receding speed and distance of the celestial bodies. Therefore, the Hubble redshift becomes the direct evidence of the Big Bang.

In history, astronomers have never independently measured the receding speed of distant galaxies. Its calculation is dependent on the photon redshift. Therefore, Hubble's law is very dubious.

The physical meaning of the Hubble constant in the paper "*The Quantum Redshift Effect of Photon*" is well defined.

In the process of photon propagation in space, energy loses due to collision with the atoms in the medium. On average, the lost portion every time it collides with a bound electron is given by

$$\Delta\varepsilon = \frac{\pi^2}{4}\frac{(h\nu)^3}{(m_e c^2)^2} = \frac{3\pi}{8\alpha}\frac{\sigma_T}{\sigma_p}\cdot h\nu \tag{38}$$

In Equation (38), α is the fine structure constant, σ_T is the classical electron cross-sectional area—Thomson electron cross-sectional area, and $\sigma_p = \alpha\lambda^2/\pi^2$ is the photon cross-sectional area.

Photons propagate in space, causing frequency reductions such as in Equation (10) or wavelength elongation as in Equation (11). The Hubble constant H_0 is the damping coefficient of photon motion. It is also the attenuation rate of photon frequency, which is proportional to the density of bound electrons in space, as in Equation (17-a). Therefore, the theory of the quantum redshift effect of the photon negates that of cosmic expansion.

So, is there any distinction in the aspect of observation between the cosmic expansion and the quantum redshift effect?

The redshift caused by the Doppler effect does not produce secondary waves, while the quantum redshift effect necessarily generates secondary waves. In the quantum redshift effect, each time a photon collides with a hydrogen atom, it loses energy, as in Equation (38). The atom can't always absorb energy, but it has to store the gained energy and radiate it into space after the collision to maintain the stability of the atom.

The radiated energy corresponding to Equation (38) is an electromagnetic wave lower than that of microwaves. Therefore, radio radiation necessarily occurs after the quantum redshift effect. So, it is hard to observe secondary pho-

tons due to the low frequency and weak intensity of secondary waves after a single collision. But if the hydrogen atom density is high and the radiance of the incident light is powerful, photons will collide with atoms frequently. In this way, the secondary waves will be strong, and it will be possible to observe with instruments. It is how the radio phenomenon of certain quasars arises.

As Max Born famously predicted in 1954, "The redshift is linked to radio astronomy." [7]

In addition, the quantum redshift effect of photons accompanies phenomena such as 21 cm hydrogen lines, Lyα, and Lyβ forests.

6. Conclusion

The light radiated by stars in the universe is collided by the atoms in the medium to produce a quantum redshift effect, which is the physical mechanism of Hubble redshift. It causes the frequency of photons to attenuate negatively exponentially with the propagation distance. It unifies the explanation of two seemingly unrelated phenomena. On the one hand, the irradiance of the night sky becomes very low, showing darkness. On the other hand, the light emitted by the stars becomes CMBR. The quantum redshift effect generates radio background radiation. This effect explains where the light energy radiated by stars in the universe goes and dispels the Olbers paradox. It explains the origin of CMBR at the same time. The Hubble redshift, Olbers paradox, and CMBR are all caused by the quantum redshift effect of photons and cannot use to be the basis for the Big Bang theory.

Acknowledgements

Thanks my family for supporting my scientific research!

Conflicts of Interest

The author declares no conflicts of interest regarding the publication of this paper.

References

[1] Harrison, E.R. (1965) *Monthly Notices of the Royal Astronomical Society*, **131**, 1-12. https://doi.org/10.1093/mnras/131.1.1

[2] Harrison, E.R. (1974) *Physics Today*, **27**, 30-36. https://doi.org/10.1063/1.3128443

[3] Assis, A.K.T. (1992) *Apeiron*, **12**, 10-16.

[4] Xu, Z.L. (2021) *Journal of Modern Physics*, **12**, 2003-2030. https://doi.org/10.4236/jmp.2021.1214115

[5] Pan, G. (1988) *Chinese Astronomy and Astrophysics*, **12**, 191-196. https://doi.org/10.1016/0275-1062(88)90046-X

[6] Penzias, A.A. (1965) *Astrophysical Journal*, **142**, 419-421. https://doi.org/10.1086/148307

[7] Assis, A.K.T. and Neves, M.C.D. (1995) *Astrophysics and Space Science*, **227**, 13-24.

https://doi.org/10.1007/978-94-011-0405-0_2

[8] He, X.T. (2007) Observational Cosmology, Postgraduate Textbook of New Century Colleges and Universities. Beijing Normal University Press, Beijing.

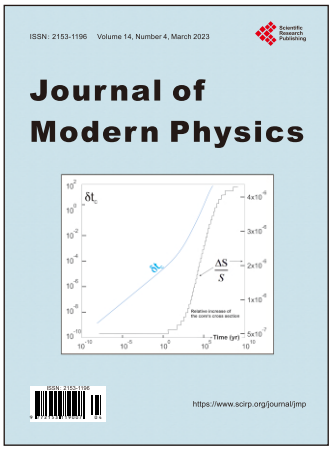

Call for Papers

Journal of Modern Physics

ISSN: 2153-1196 (Print) ISSN: 2153-120X (Online)
https://www.scirp.org/journal/jmp

Journal of Modern Physics **(JMP)** is an international journal dedicated to the latest advancement of modern physics. The goal of this journal is to provide a platform for scientists and academicians all over the world to promote, share, and discuss various new issues and developments in different areas of modern physics.

Subject Coverage

Journal of Modern Physics publishes original papers including but not limited to the following fields:

Biophysics and Medical Physics
Complex Systems Physics
Computational Physics
Condensed Matter Physics
Cosmology and Early Universe
Earth and Planetary Sciences
General Relativity
High Energy Astrophysics
High Energy/Accelerator Physics
Instrumentation and Measurement
Interdisciplinary Physics
Materials Sciences and Technology
Mathematical Physics
Mechanical Response of Solids and Structures
New Materials: Micro and Nano-Mechanics and Homogeneization
Non-Equilibrium Thermodynamics and Statistical Mechanics
Nuclear Science and Engineering
Optics
Physics of Nanostructures
Plasma Physics
Quantum Mechanical Developments
Quantum Theory
Relativistic Astrophysics
String Theory
Superconducting Physics
Theoretical High Energy Physics
Thermology

We are also interested in: 1) Short Reports—2-5 page papers where an author can either present an idea with theoretical background but has not yet completed the research needed for a complete paper or preliminary data; 2) Book Reviews—Comments and critiques.

Notes for Intending Authors

Submitted papers should not have been previously published nor be currently under consideration for publication elsewhere. Paper submission will be handled electronically through the website. All papers are refereed through a peer review process. For more details about the submissions, please access the website.

Website and E-Mail

https://www.scirp.org/journal/jmp **E-mail: jmp@scirp.org**

What is SCIRP?

Scientific Research Publishing (SCIRP) is one of the largest Open Access journal publishers. It is currently publishing more than 200 open access, online, peer-reviewed journals covering a wide range of academic disciplines. SCIRP serves the worldwide academic communities and contributes to the progress and application of science with its publication.

What is Open Access?

All original research papers published by SCIRP are made freely and permanently accessible online immediately upon publication. To be able to provide open access journals, SCIRP defrays operation costs from authors and subscription charges only for its printed version. Open access publishing allows an immediate, worldwide, barrier-free, open access to the full text of research papers, which is in the best interests of the scientific community.

- High visibility for maximum global exposure with open access publishing model
- Rigorous peer review of research papers
- Prompt faster publication with less cost
- Guaranteed targeted, multidisciplinary audience

Scientific Research Publishing

Website: https://www.scirp.org

Subscription: sub@scirp.org

Advertisement: service@scirp.org